Optimization and control of heat exchanger network under uncertainty

by

Chaitanya Manchikatla

A thesis submitted in partial fulfillment of the requirements for the degree of

Master of Science

in

PROCESS CONTROL

Department of Chemical and Materials Engineering
University of Alberta

Abstract

The dynamic control of heat exchanger network is important for developing energy efficient and safe industrial processes. In Chapter 3 of this work, the uncertainty is considered in inlet temperature of hot stream. The cold stream is bypassed around the heat exchanger. This work aims to track the setpoint temperature of the mixed stream by manipulating the bypass fraction of the cold stream around the heat exchanger. The implemented control is in Nonlinear Model Predictive Control (NMPC) framework. The uncertain optimal control problem (OCP) is dealt by using scenario tree based approximation along with an affine policy based method. The first principles model of shell and tube heat exchanger is used. The orthogonal collocation technique is applied to discretize the first principles model into the system of algebraic equations. The results show that for possible scenarios of uncertainty, the controlled variable efficiently tracks setpoint. In comparison, considering the same scenarios of uncertainty used, the deterministic optimization approach shows significant deviation of the controlled variable from the setpoint as time passes.

Fouling is a concerning problem for heat exchange in industries. It is the deposition of unwanted materials on heat exchanger surfaces which offers extra resistance for heat transfer. Generally, chemical cleaning and flowrate distribution are used to mitigate fouling. In Chapter 4 of this work, the optimal cleaning scheduling and bypass control problems are formulated simultaneously considering disturbances in inlet temperature of cold stream. This integrated problem is formulated as a MINLP problem. The cleaning scheduling variables are binary decision variables, and the bypass

fractions are continuous decision variables. A axially lumped and radially distributed model of HEN is considered in this chapter. The uncertain OCP is made tractable using an affine policy based methods and scenario tree based approximations. The performance of the proposed uncertain optimization problem is demonstrated using various case studies which include PHT of crude. This is because fouling is a relevant and most evident in PHT due to presence of impurities in crude. In this uncertain optimization, the value of objective function which represents the additional cost occurred because of fouling as compared to ideal clean conditions is reduced by 44% as compared to deterministic optimization.

Acknowledgements

Firstly, I would like to thank Dr. Biao Huang and Dr. Zukui Li for their continuous support in completing my thesis. I express my heartfelt gratitude to both of them as without them it's impossible to complete this thesis. I would like to thank Dr. Li for the frequent discussions and his guidance at each step of my thesis. I really appreciate your patience. A special thanks to Dr. Li for encouraging me to learn optimization, and giving me an oppurtunity to work as grader. I wholeheartedly thank Dr. Huang for giving me an opportunity to explore my research interests. I express my sincere gratitude to Dr. Huang for making me conscious about the deadlines, and for motivating me about the next steps of my research work. I appreciate your persistence in guiding all your students.

I would like to thank my parents for their continuous encouragement. Those late night calls kept me uplifted to do my work. I thank my sister for her frank feedbacks all the time.

I would like to thank all the research group members of Dr. Li and the CPC group under Dr Huang. The weekly group meetings and presentations have helped me immensely to improve my knowledge in the field of process control and data science. I would like to thank Sanjula for her continuous help which made me understand the concepts and helped me to the solve the issues I had in my research work. I also thank my friends Krishna, Kiran, Alireza, Dr. Santhosh, Sarupa, and Yousef for keeping me engaged and charged all the time.

I thank my friends Surya, Karthik, Rakshith, and Sai Meghana for giving me constant

support. Thanks for entertaining me when I'm low. Working from home wouldn't be possible without you people. My gratitude for those positive words which gave me enough strength to finish this thesis.

Contents

1 Introduction **1**

1.1 Motivation 1

1.2 Literature survey on control of HEN 3

1.3 Literature survey on integrated optimal cleaning and control of HEN 3

1.4 Optimization under uncertainty 4

1.5 Thesis structure 5

2 Optimization under uncertainty **7**

2.1 Illustration Problem 7

2.2 Static robust optimization 9

2.3 Scenario-based method 11

2.4 Affine policy based method 14

2.5 Conclusion 18

3 MPC of HEN under uncertainty **19**

3.1 Problem statement 19

3.2 Deterministic MPC for single HE 20

3.2.1 Dynamic model 21

3.2.2 Spatial Discretization 23

3.2.3 Objective function 24

3.2.4 Results of single heat exchanger case 25

3.3 Deterministic MPC For HEN 26

3.3.1 Results 27

3.4 MPC of single heat exchanger and HEN under uncertainty 34

3.4.1 Discretization of ODEs 35

3.4.2 Affine policy based method 36

3.4.3 Results 40
3.5 Conclusion 51

4 Integrated optimal cleaning and control problem 52
4.1 Introduction 52
4.2 Heat exhanger model, fouling dynamics, and additional constraints . 53
4.3 Objective function 57
4.4 Results 57
4.5 Integrated problem under uncertainty 62
4.5.1 Tractable problem formulation 65
4.5.2 Results 70
4.5.3 Industrial preheat train for a crude oil distillation column . . . 78
4.6 Conclusion 83

5 Conclusions and prospective work 85
5.1 Conclusions 85
5.2 Prospective work 86

List of Tables

3.1 Results of uncertain MPC for single HE 45
3.2 Results of uncertain MPC for HEN 51

4.1 Results of uncertain integrated problem for single HE 74
4.2 Results of uncertain integrated problem for 2HE parallel 77
4.3 Results of uncertain integrated problem for PHT 83

List of Figures

1.1 Fouling resistance vs time [1] 2
1.2 General uncertain optimization methods 5

2.1 The plot on the left shows the plot for inputs of products over time, while the plot on the right shows the stock of the product over time [39] 9
2.2 The plot on the left shows the plot for inputs of products over time while the plot on the right shows the stock of the product over time . 11
2.3 Scenario tree describing the deviation from nominal values in each one of the scenarios. Each scenario has the same probability of occurrence and hence a probability of 0.25 is assigned to each of the scenarios . . 12
2.4 The plot on the left shows the plot for inputs of products over time while the plot on the right shows the stock of the product over time . 13
2.5 Results obtained from simulating 1200 scenarios and applying scenario tree based method [39] 14
2.6 The plot on the left shows the plot for inputs of products over time, while the plot on the right shows the stock of the product over time . 16
2.7 The figure summarizes the results obtained from simulating 1200 scenarios and applying affine policy based method [41] 17

3.1 Bypass control of heat exchanger 20
3.2 Shell and tube heat exchanger with unit element 21
3.3 prediction horizon divided into n equal intervals 24
3.4 The plot on the left shows the plot for input over time, while the plot on the right shows the controlled variable(T_2^{out}) over time 25
3.5 The plot on the left shows the plot for controlled variable (T_2^{out}) in step change in setpoint, while the plot on the right shows optimized input (u) step change in setpoint case 25

3.6 The plot on the left shows the plot optimized input (u) disturbance rejection case, while the plot on the right shows controlled variable (T_2^{out}) in case of disturbance rejection 26
3.7 heat exchanger network 26
3.8 Optimized input (u_1) 28
3.9 Optimized input (u_2) 28
3.10 Optimized input (u_3) 29
3.11 The plot on the left shows the plot controlled variable (T_{H1}^{out}), while the plot on the right shows controlled variable (T_{C2}^{out}) 29
3.12 Optimized input (u_1) setpoint tracking case 30
3.13 Optimized input (u_2) setpoint tracking case 30
3.14 Optimized input (u_3) setpoint tracking case 31
3.15 The plot on the left shows the plot controlled variable((T_{H1}^{out}), while the plot on the right shows controlled variable ((T_{C2}^{out}) with step change in setpoint 31
3.16 Optimized input (u_1) disturbance rejection case 32
3.17 Optimized input (u_2) disturbance rejection case 32
3.18 Optimized input (u_3) disturbance rejection case 33
3.19 The plot on the left shows the plot controlled variable((T_{H1}^{out}), while the plot on the right shows controlled variable ((T_{C2}^{out}) in disturbance rejection case 33
3.20 Steps to convert intractable problem to tractable 34
3.21 Polynomial approximation of state profile across finite element with 3 collocation points 35
3.22 T_1^{in} considering 4 scenariors used in optimization 41
3.23 $T_{2,n,k}^{out}$ considering 4 scenarios used in optimization 42
3.24 u_n for 4 scenarios used in optimization 42
3.25 T_1^{in} considering 4 random scenariors 43
3.26 $T_{2,n,k}^{out}$ considering 4 random scenariors 44
3.27 $T_{2,n,k}^{out}$ using the deterministic input considering 4 scenariors 44
3.28 T_{H1}^{in} considering 4 scenariors used in optimization 46
3.29 $T_{C2,n,k}^{out}$ considering 4 scenarios used in optimization 47
3.30 u_1 for four scenarios used in optimization 47
3.31 u_2 considering four random scenariors 48

3.32 u_3 considering four scenarios used in optimization 48
3.33 T^{in}_{H1} considering 4 random scenariors 49
3.34 $T^{out}_{C2,n,k}$ considering 4 random scenariors 50
3.35 $T^{out}_{C2,n,k}$ using the deterministic input considering 4 scenariors 50

4.1 Multiple layer representation for the heat transfer between the shell-side fluid and the tube-side fluid [20] 53
4.2 Optimal cleaning schedule for single HE 58
4.3 The optimal bypass fraction 58
4.4 Furnace duty 59
4.5 Mixed stream temperature 59
4.6 optimal cleaning schedule for 2HE 60
4.7 The optimal bypass fraction of cold stream through HE 2 60
4.8 The optimal bypass fraction of hot stream through HE 2 61
4.9 Furnace duty 61
4.10 mixed stream temperature 62
4.11 The optimal bypass fraction of cold stream 71
4.12 Furnace duty 72
4.13 Mixed stream temperature 72
4.14 Optimal cleaning schedule for 1HE 73
4.15 CIT using deterministic input 73
4.16 2 parallel HEN 74
4.17 Optimal cleaning schedule for 2HE 74
4.18 The optimal bypass fraction of cold stream through HE 2 75
4.19 The optimal bypass fraction of hot stream through HE 2 75
4.20 Furnace duty 76
4.21 Mixed stream temperature (controlled variable) 76
4.22 Mixed stream temperature (controlled variable) using deterministic input for different scenarios of uncertainty 77
4.23 Grid diagram of the preheat train for a crude oil distillation column . 78
4.24 optimal cleaning schedule for PHT 79
4.25 Bypass fraction 1 80
4.26 Bypass fraction 2 80
4.27 Bypass fraction 3 81
4.28 Bypass fraction 4 81

4.29 Mixed stream temperature (controlled variable) 82
4.30 Mixed stream temperature (controlled variable) using deterministic input for different scenarios of uncertainty 82
4.31 Furnace duty 83

Nomenclature

To avoid confusion the nomeclature uniform throughout the thesis is given here. The nomenclature specific to a section is given in that section.

Abbreviations

MPC Model Predictive Control

CDU Crude Distillation Unit

CIT Coil Inlet Temperature

HEN Heat Exchanger Network

$MINLP$ Mixed Integer Nonlinear Problem

MSE Mean Square Error

$NMPC$ Nonlinear Model Predictive Control

OCP Optimal Control Problem

PHT PreHeat Train

Parameters and variables

α	Weighing term for economic term in objective function
ΔT_m	Mean temperature difference
λ	Thermal conductivity of wall
C_p^w	Specific heat capacity of wall of Heat Exchanger
C_{p_1}	Specific heat capacity of hot stream

C_{p_1}	Specific heat capacity of hot stream
C_{p_2}	Specific heat capacity of cold stream
d^{in}	Tube inner diameter
d^{out}	Tube outer diameter
K	Overall heat transfer coefficient
K^{in}	Heat transfer coefficient at inner wall
K^{out}	Heat transfer coefficient at outer wall
M^{w}	Mass of wall of heat exchanger
M_1	Unit mass flow rate of hot stream
m_1	Mass flow rate of hot stream
M_2	Unit mass flow rate of cold stream
m_2	Mass flow rate of cold stream
n	Control horizon
Q	Heat transfer rate
R^{in}	Fouling resistance of inner wall of heat exchanger
r^{in}	Tube inner radius
R^{out}	Fouling resistance of outer wall of heat exchanger
r^{out}	Tube outer radius
t	Time coordinate
T'^{out}_{2}	Temperature of cold stream at outlet of heat exchanger
T_1^{in}	Temperature of hot stream at inlet of heat exchanger
T_2^{in}	Temperature of cold stream at inlet of heat exchanger
T_1^{out}	Temperature of hot stream at outlet of heat exchanger

T_2^{out} Temperature of mixed stream

T^{wi} Temperature of inner wall of heat exchanger

T^{wo} Temperature of outer wall of heat exchanger

t_p Prediction horizon

T_{st} Setpoint of temperature of mixed stream

u Bypass fraction

$u^{opt,past}$ Optimal bypass fraction obtained in previous iteration

x Spatial coordinate

x_{length} Spatial discretization points

Sets and superscripts

in inlet

i heat exchanger

j collocation point

len length

n control interval

out outlet

past previous time step

s scenario

w wall

wi inner wall

wo outer wall

Chapter 1

Introduction

1.1 Motivation

In industries, nearly 80% of the total energy consumption is related to heat transfer [1]. For energy intensified processes, dynamic control of the HEN plays an important role [3]. Generally, the outlet temperatures are controlled by manipulating flow rates. However, when the flow rates are determined by process requirements in HEN, bypass control is adopted widely [6]. Bypass control provides tight temperature control since the dynamics of blending a hot stream (stream through the heat exchanger) and a cold stream (bypassed stream) is fast.
But, the control problem of heat exchanger is considerably difficult because of the reasons like following [1]:

1. Nonlinear dynamics
2. Disturbances in inlet temperatures of streams and uncertainties like leakages
3. Temperature dependent flow properties and contact resistance.
4. Time varying properties like fouling resistance.

So in this work, using bypass control, an attempt is made to track the temperature setpoint considering disturbances in inlet temperature of hot stream as described in chapter 3.

Fouling is the deposition of unwanted material over the surface of process equipment, which reduces the performance of heat transfer operations. It is a phenomenon that is not yet fully understood, but it is known that fouling can be caused by the presence of impurities in the process streams, the crystallization of salts, biological reactions, deposition of suspended particles, thermal decomposition of certain components, and corrosion [9]. The causes of fouling vary among different processes. Some are process-specific, such as the biological fouling caused by the thermal degradation of proteins in milk pasteurization processes [10] and the crystallization of salts in water treatment applications [11]. In other areas, such as refining applications, fouling can be caused by more than one mechanism at the same time [9]. Its consequences on the operation of chemical processes are of major concern.

In heat exchanger units, fouling reduces both thermal and hydraulic performance. The deposited material generates an additional thermal resistance that reduces the heat-transfer rate and the potential to recover high amounts of energy in heat exchangers. Figure 1.1 is taken from [1]. For example, the fouling resistance with respect to time is given by Figure 1.1. Generally, these are the curves used to represent fouling resistance with respect to time time [1].

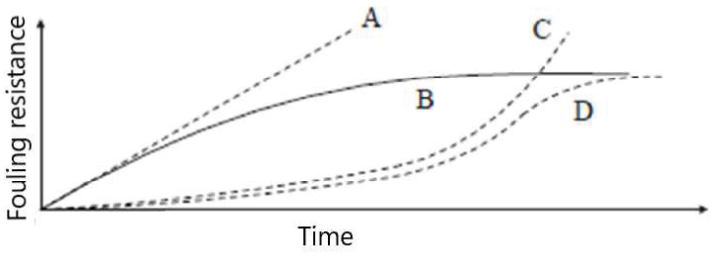

Figure 1.1: Fouling resistance vs time [1]

In addition, the deposit reduces the hydraulic radius, which increases the pressure drop, and in extreme cases, it causes a complete blockage of the unit [12]. These factors increase the operational cost, the risk of operation during cleanings, and the environmental impact. The consequences of fouling are of major concern in refinery operations where large HENs are used in the energy integration of the process. This is most evident in the PHT of the CDU, which processes all the crude oil that comes into the refinery under extreme conditions, such as high temperature, varying range

of composition, and high amounts of contaminants [9]. In this case, the extra thermal resistance in the heat exchangers reduces the CIT to the furnace, more furnace fuel is burned, increasing the amount of carbon emissions and the operational cost.
So, in chapter 4, considering fouling, the integrated optimal cleaning scheduling and control problem of HEN is described.

1.2 Literature survey on control of HEN

Temperatures and/or flow rates of incoming streams may introduce disturbances to a HEN owing to uncontrolled upsets in upstream process units and affect target streams, and hence, the operations in downstream process units. Thus, temperatures of target streams of a HEN should be tightly controlled for the safety of downstream operations. In practice, it is necessary to place bypasses for satisfying the degrees of freedom required to achieve control objectives [14]. Few researchers have looked at the controllability or bypass selection for control of HENs. Nisenfeld introduced the use of then relative gain array (at steady-state) to evaluate control of a HEN [15], but in this case the control scheme for the HEN had already been designed. Beautyman and Cornish [16] observed that the proper placement of bypass lines around heat exchangers affects the dimensions of the operability region, but they did not offer any systematic suggestions as to where to put the bypass lines such that certain design objectives are achieved. Calandranis and Stephanopoulos [17] addressed flexibility and controllability and discussed the dynamics of HEN briefly.
McMillam and Toarmina [18] and Riggs and Karim [19] discuss a number of piping and control configurations, including bypassing, and point out some of the advantages of manipulating the bypass configuration.

1.3 Literature survey on integrated optimal cleaning and control of HEN

[20] presents an efficient and general formulation for solving a optimal cleaning scheduling problem and the optimal control problem of HENs under fouling. A model and a formulation are presented that are versatile, in the sense that some variables can be fixed to examine only one or both of the scheduling or control problems, or include

just some aspects of both. Some fouling mitigation alternatives are cleaning in place (chemical cleaning), mechanical cleaning, the use of antifouling agents, and changing the operation conditions [21], [9]. The cleaning options have been proven to be an effective way to recover the thermal and hydraulic efficiency [23]. However, it is not easy to decide which heat exchanger to clean and when the operational cost is minimum. These decisions are often made using heuristic criteria but quantitative, model-based mathematical programming approaches have also been used. Even with highly simplified models,the large size of the problems and their combinatorial nature make it hard to solve [20]. Furthermore, in the case of MINLP formulations, only a local minimum can be guaranteed. Solution approaches have been proposed, such as simulated annealing [24] or greedy algorithms [25] that produce a rapid solution, but give no guarantee that this solution is optimal, and they have problems with constraints.

Operationally, a practical alternative for fouling mitigation is to manipulate the flow rate distribution in the network over time, through use of bypasses of individual units and control of flow splits between parallel branches in the HEN. Optimizing such flow distribution profiles has also been formulated as a mathematical programming problem with the objective of minimizing the operational cost [26].

These are two mitigation alternatives. The first one is to tackle the problem as an optimal scheduling problem, in which the main decision variables are binary variables associated with the operating states of the units (cleaning or operating) and the timing and sequencing of the task. The optimal cleaning scheduling problem is combinatorial in nature, and it is typically addressed using steady-state models. The second one involves the optimization of the HEN flow rate distribution over time. This is a dynamic, optimal control problem that involves differential-algebraic equations. Most of the literature on the fouling mitigation of HENs addresses the two alternatives individually, and most of it only focuses on the scheduling problem [21].On the other hand, some works tackle the second problem only from a dynamic optimization perspective, ignoring the cleaning scheduling [27].

1.4 Optimization under uncertainty

Optimization under uncertainty refers to the branch of optimization where uncertainties are associated with parameters or states used in the model. This uncertainty in

parameters or states makes the mathematical model uncertain, presenting us with a class of optimization problems commonly called Stochastic Programming (SP). Stochastic programming requires the knowledge of probability distribution of uncertain parameters or states. The probability distribution of uncertainty is considered to be known or can be estimated [13]. Another method to deal with uncertainty involves finding an optimal solution that is optimal at the worst-case of uncertainty realized for the considered set. Robust optimization requires the programmer to assume or have the knowledge of the uncertainty set for the considered problem. Figure 1.2 represents the summary of methods used for optimization under uncertainty, the literature survey for optimization under uncertainty with the formulations and tutorials are given in chapter 2.

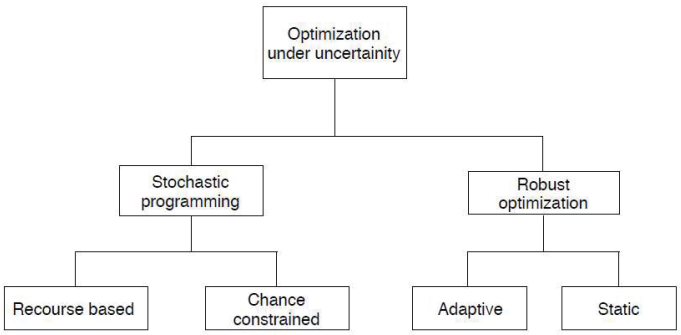

Figure 1.2: General uncertain optimization methods

1.5 Thesis structure

In this thesis, the scenario tree based method and affine policy based method will be applied to solve the uncertain optimization problem. In Chapter 2, these methods are explained using a simple example of the optimization problem. Chapter 3 shows the problem statement, formulation and results of MPC of HEN. At first, the control problem is formulated in the deterministic sense, and the uncertainty is later introduced. The continuous system of ODEs which describe the first principles model of HEN is discretized using orthogonal collocation technique. Chapter 3 also describes this discretization technique. Chapter 4 shows the integrated optimal cleaning scheduling and control of HEN. In this chapter, the decision variables also include the binary variables which describe the optimal cleaning scheduling. Chapter

5 gives the summary of the work done along with possible future work along similar lines to the work presented in the thesis.

Chapter 2

Optimization under uncertainty

This chapter explains various uncertain optimization techniques using an illustration example. The formulation of the problem and solutions are taken from [40] and [39]. It is presented here to give basic knowledge of uncertain optimization techniques, which are needed to understand the subsequent chapters of this thesis.

2.1 Illustration Problem

The simple case of supply chain management has been considered to implement stochastic optimization techniques. The problem considers the supply-chain components that involve ordering costs, inventory handling costs and external order costs. The problem is solved over a finite time horizon, given as T. The objective of the problem is to minimize the costs of operation while satisfying demand. To derive an analogy between supply chain management problem and linear MPC, we can look at the following highlights of the analogy:

- The stock level of a certain product is analogous to the measured state in MPC. It is represented by the variable $x(k)$, stock level of product at time k
- The product bought at a certain time k is analogous to the control input given to a system at time k, in the case of MPC. The input is represented by $u(k)$ for time k
- The demand for a product is analogous to the demand of a certain product

produced from the system under MPC control. The demand at time k is represented by $w(k)$

The mathematical representation for a supply chain model with one good and time period T is given below :
The stock level of the good at time $k+1$ is given as:

$$x(k+1) = x(k) + u(k) - w(k),\ k = 0, 1, ..., T-1$$

Here, $x(0) = x_0$ is the initial stock of the goods in the inventory. The current level of stock is, thus the sum of level at the previous time instant and the products ordered in, while removing the stock that is sold to meet the demand $w(k)$. The holding cost for inventory is denoted by h, and the costs of meeting demand from external buying, and of buying the good are denoted by p and c, respectively. The cost objective to be minimized is given as:

$$cu(k) + max(hx(k+1), -px(k+1))$$

When the stock is positive, the holding cost $hx(k+1)$ is incurred. When the stock is negative, the stock has to be bought from an external supplier thus incurring an external cost of $-px(k+1)$. Considering an upper bound M on size of order, the T-stage optimization problem can be written as:

$$\begin{aligned} &\min_{u(0),..,u(T-1)} \sum_{k=0}^{T-1} cu(k) + max\left(hx(k+1), -px(k+1)\right) \\ &s.t. \quad 0 \leq u(k) \leq M, \quad k = 0, 1, ..., T-1 \end{aligned}$$

where, $x(k) = x_0 + \sum_{i=0}^{k-1}(u(i) - w(i)), \quad k = 1, ..., T$. Introducing slack variables, the max operator in the objective function can be removed. The formulation now can be represented as:

$$\min_{u(0),..,u(T-1),y(0),...,y(T-1)} \sum_{k=0}^{T-1} y(k) \tag{2.1}$$

$$s.t. \quad cu(k) + hx(k+1) \leq y(k) \quad k = 0, ..., T-1 \tag{2.2}$$

$$cu(k) - px(k+1) \leq y(k) \quad k = 0, ..., T-1 \tag{2.3}$$

$$0 \leq u(k) \leq M, \quad k = 0, ..., T-1 \tag{2.4}$$

Solving the above deterministic problem, we get the ordering schedule and stock levels as shown below:

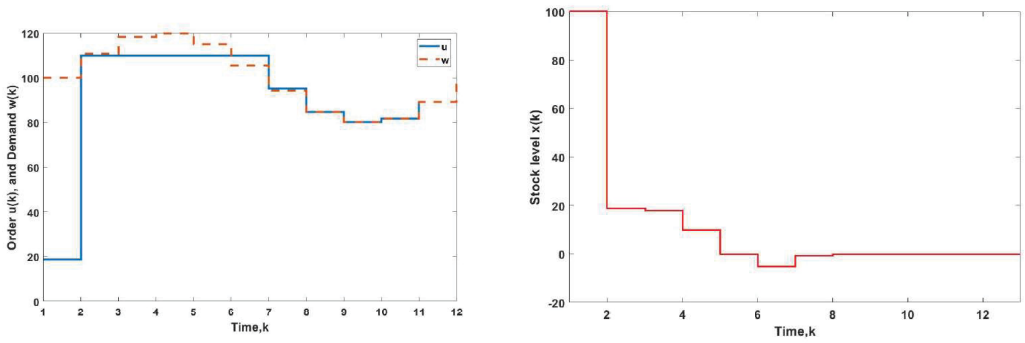

Figure 2.1: The plot on the left shows the plot for inputs of products over time, while the plot on the right shows the stock of the product over time [39]

Figure 2.1 is taken from [39]. Since the demand of a given product is not certain, we assume there is a deviation of 15% on the upper and lower bounds of nominal demand. The lower and upper limit on the demand can be written as:

$$w_{lb} = (1-\rho)\hat{w}(k)$$
$$w_{ub} = (1+\rho)\hat{w}(k)$$

where, ρ can be defined as the assumed degree of deviation from the nominal case. The nominal case of demand can be defined by a sinusoidal function given as:

$$\hat{w}(k) = 100 + 20sin\left(2\pi\frac{k}{T-1}\right), \quad k = 0, .., T-1$$

The uncertainty in the model is solved using the methods discussed as follows:

2.2 Static robust optimization

The static robust method utilizes the worst-case limits on the uncertain parameters in order to convert the uncertainty problem into a deterministic problem that is solved at the extreme limits of the uncertain parameter.

Two new variables x_1 and x_2 are defined in order to get the correct stock for the case of extreme lower bound and extreme upper bound respectively. The formulation of the static robust problem is shown below:

$$\min_{u(0),..,u(T-1),y(0),...,y(T-1)} \sum_{k=0}^{T-1} y(k) \tag{2.5}$$

$$s.t.\ x_1(k) = x_1(0) + \sum_{i=0}^{k-1} (u(i) - w_{lb}(i)) \quad \forall k = 1, ..T-1 \tag{2.6}$$

$$x_2(k) = x_2(0) + \sum_{i=0}^{k-1} (u(i) - w_{ub}(i)) \quad \forall k = 1, ..T-1 \tag{2.7}$$

$$cu(k) + hx_1(k+1) \leq y(k) \quad k = 0, ..., T-1 \tag{2.8}$$

$$cu(k) - px_2(k+1) \leq y(k) \quad k = 0, ..., T-1 \tag{2.9}$$

$$0 \leq u(k) \leq M, \quad k = 0, ..., T-1 \tag{2.10}$$

Since each element of w belongs to an interval, Equation 2.2, $cu(k) + hx(k) \leq y$ will only be satisfied iff,

$$cu(k) + h(x_1(0) + \sum_{i=0}^{k-1} (u(i) - w_{lb}(i))) \leq y$$

Equation 2.3, $cu(k) - px(k) \leq y$ is satisfied iff,

$$cu(k) - p(x_2(0) + \sum_{i=0}^{k-1} (u(i) - w_{ub}(i))) \leq y(k),$$

thus giving rise to the equations 2.6 to 2.9. The solution thus obtained will be based on the extreme limits of the demand, thus making the solution very conservative. The results obtained by static robust method is given below.

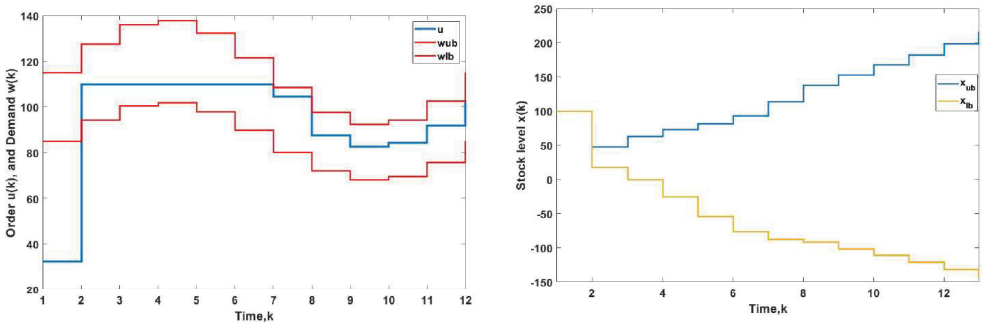

Figure 2.2: The plot on the left shows the plot for inputs of products over time while the plot on the right shows the stock of the product over time

Figure 2.2 is taken from [41].

2.3 Scenario-based method

The scenario-method was used to solve the uncertain model problem using robust horizon of 1 i.e. to make the problem simple, only one control interval is considered. These scenarios represent the possible values that primitive uncertainty can take. It is assumed that these finite number of scenarios are sufficient to formulate the problem. The scenario trees used to describe the demand parameter are shown below.

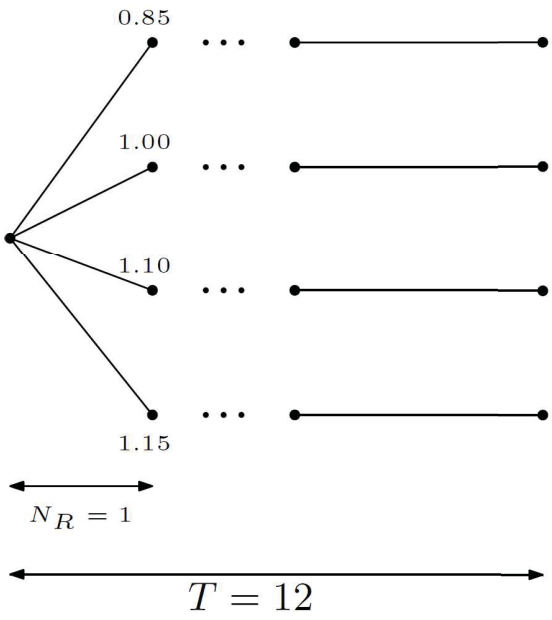

Figure 2.3: Scenario tree describing the deviation from nominal values in each one of the scenarios. Each scenario has the same probability of occurrence and hence a probability of 0.25 is assigned to each of the scenarios

The formulation for the scenario based method can be derived from the deterministic formulation such that a new index s is added in order to provide an input and a stock level for each occurrence of a scenario. The formulation is given below:

$$\min_{u(0,s),..,u(T-1,s),y(0,s),...,y(T-1,s)} \sum_{s=1}^{S} \omega(s) \sum_{k=0}^{T-1} y(k,s) \tag{2.11}$$

$$s.t.\ x(k) = x(0,s) + Uu - Uw \tag{2.12}$$

$$cu(k) + hx_1(k+1) \leq y(k) \quad k = 0, ..., T-1 \tag{2.13}$$

$$cu(k) - px_2(k+1) \leq y(k) \quad k = 0, ..., T-1 \tag{2.14}$$

$$0 \leq u(k) \leq M, \quad k = 0, ..., T-1 \tag{2.15}$$

$$u(0,1) = u(0,2) = u(0,3) = u(0,4) \tag{2.16}$$

The U matrix here is defined as:

$$U = \begin{bmatrix} 1 & 0 & 0 & \cdots & 0 \\ 1 & 1 & 0 & \cdots & 0 \\ \vdots & \vdots & \ddots & \ddots & \vdots \\ 1 & 1 & 1 & \cdots & 1 \end{bmatrix}$$

The solution to the scenario tree problem can be given as:

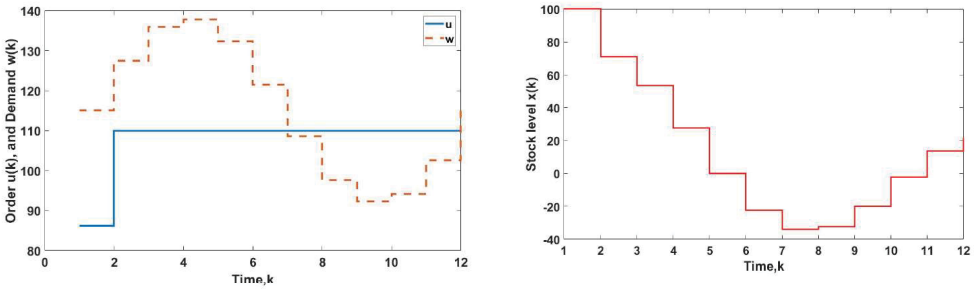

Figure 2.4: The plot on the left shows the plot for inputs of products over time while the plot on the right shows the stock of the product over time

Figure 2.4 is taken from [39]. The profit obtained using the scenario tree in terms of the expectation values of the objective function is \$7959.8. The above figure shows only one scenario, and the performance of the methods can be compared only when they are being tested for a statistically significant number of generated scenarios. There were 1200 scenarios generated such that they have a mean that is the same as nominal demand, while the variance of the scenarios is increased with increase in time, and is given as:

$$\sigma_k^2 = (1+k)\bar{\sigma}^2, \quad k = 0, ..., T-1$$

where, $\bar{\sigma}^2 = 1$ Figure 2.5 summarizes the results obtained from utilizing scenario tree method for 1200 scenarios.

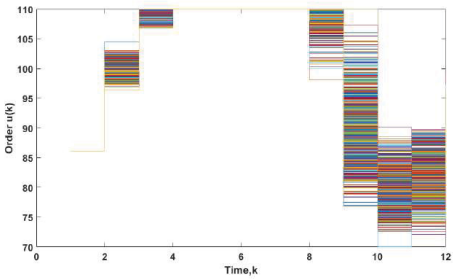

(a) Input for 1200 scenarios

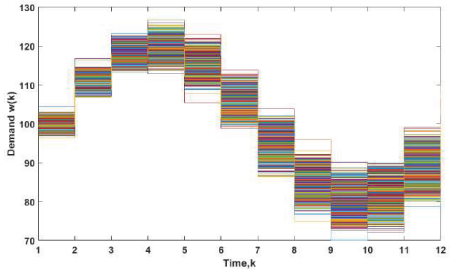

(b) Demand simulated for 1200 scenarios

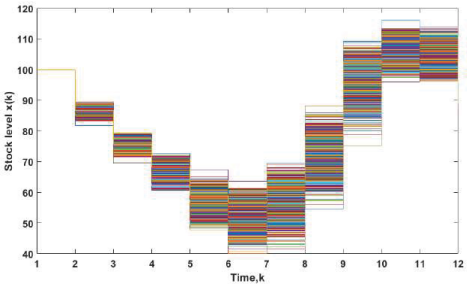

(c) Stock level for 1200 scenarios

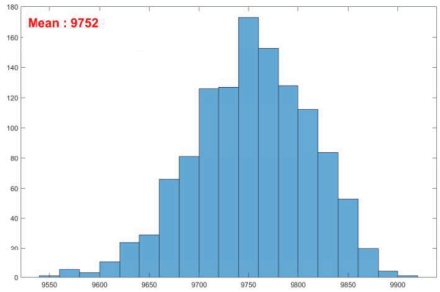

(d) Cost distribution for 1200 scenarios

(d) Cost distribution for 1200 scenarios

Figure 2.5: Results obtained from simulating 1200 scenarios and applying scenario tree based method [39]

2.4 Affine policy based method

Affine policy based method utilizes a closed-loop approach to address uncertainty. The input is parametrized with respect to uncertainty. The first stage decision is taken with no knowledge of uncertainty, while at consequent stages over the realization of uncertainty, the function output with respect to uncertainty gives the input at the current stage of optimization. Writing input as a function of uncertainty in demand, we have $u = \bar{u} + A(w - \hat{w})$, where $\bar{u}$ represents the decision taken at current time, A represents the coefficients to be optimized, and the term $w - \hat{w}$ represents the

deviation of actual demand from the nominal case.

$$A = \begin{bmatrix} 0 & 0 & \cdots & 0 \\ \alpha_{1,0} & 0 & \cdots & 0 \\ \alpha_{2,0} & \alpha_{2,1} & \cdots & 0 \\ \vdots & \vdots & \ddots & \vdots \\ \alpha_{T-1,0} & \cdots & \alpha_{T-1,T-2} & 0 \end{bmatrix}$$

Representing the demand deviation by $\tilde{w}$, we have $\tilde{w} = w - \hat{w}$, which lies in the interval:

$$-\bar{w} \leq \tilde{w} \leq \bar{w}; \quad \bar{w} = \frac{\rho}{100}\hat{w} \geq 0$$

Substituting the parametrized input in place of u, we have the formulation as given below:

$$\min_{\bar{u},y,A} 1^\top y \tag{2.17}$$

$$s.t \quad (c\bar{u} + cA\tilde{w}) + h(x_0 + U(\bar{u} + A\tilde{w}) - Uw) \leq y, \ \forall w \in W \tag{2.18}$$

$$(c\bar{u} + cA\tilde{w}) - p(x_0 + U(\bar{u} + A\tilde{w}) - Uw) \leq y, \ \forall w \in W \tag{2.19}$$

$$0 \leq \bar{u} + A\tilde{w} \leq M, \ \forall w \in W \tag{2.20}$$

Observe that, if ν is a vector, and $\bar{w} \geq 0$, the robust limits can be explained by:

$$\max_{-\bar{w} \leq \tilde{w} \leq \bar{w}} \nu^\top \tilde{w} = |\nu|^\top \bar{w}$$

$$\min_{-\bar{w} \leq \tilde{w} \leq \bar{w}} \nu^\top \tilde{w} = -|\nu|^\top \bar{w}$$

Applying the robust limits to Equations 2.18 and 2.19, we can reformulate the affine formulation as:

$$\min_{\bar{u},y,A} 1^\top y \tag{2.21}$$

$$s.t \quad c\bar{u} + hU\bar{u} + hx_0 - hU\hat{w} + |cA + hUA - hU|\,\bar{w} \leq y, \tag{2.22}$$

$$c\bar{u} - pU\bar{u} - px_0 + hU\hat{w} + |cA - pUA + pU|\,\bar{w} \leq y \tag{2.23}$$

$$\bar{u} + |A|\bar{w} \leq M, \tag{2.24}$$

$$\bar{u} - |A|\bar{w} \geq 0 \tag{2.25}$$

The above formulation is no longer defined on the deviation $\tilde{w}$ which is the uncertainty considered in our problem. The robust counterpart, thus, lets us consider the extreme limits of the uncertainty set $\tilde{w}$, removing the uncertain parameter $\tilde{w}$. The above problem is now simplified using slack variables, Z_1, Z_2 and Z_3.

$$\min_{\bar{u},y,A} 1^\top y \tag{2.26}$$

$$s.t \quad c\bar{u} + hU\bar{u} + hx_0 - hU\hat{w} + Z_1\bar{w} \leq y, \tag{2.27}$$

$$c\bar{u} - pU\bar{u} - px_0 + hU\hat{w} + Z_2\bar{w} \leq y \tag{2.28}$$

$$\bar{u} + Z_3\bar{w} \leq M, \tag{2.29}$$

$$\bar{u} - Z_3\bar{w} \geq 0, \tag{2.30}$$

$$|cA + hUA - hU| \leq Z_1, \tag{2.31}$$

$$|cA - pUA + pU| \leq Z_2, \tag{2.32}$$

$$|A| \leq Z_3 \tag{2.33}$$

The results obtained for 15% uncertainty is shown in Figure 2.6.

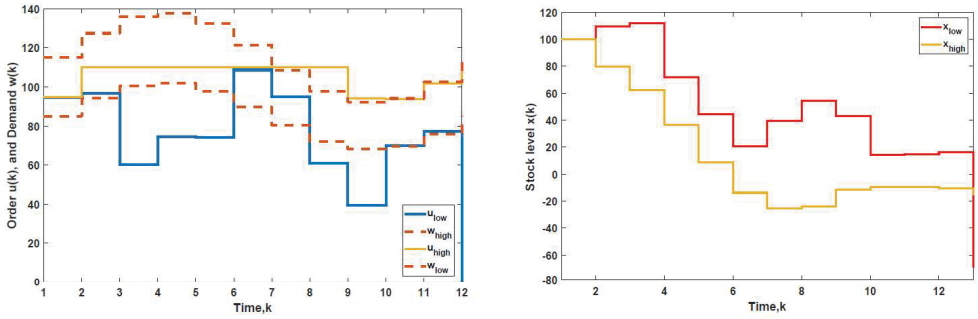

Figure 2.6: The plot on the left shows the plot for inputs of products over time, while the plot on the right shows the stock of the product over time

The ordering policy and stock can be derived as:

$$u = \bar{u} + A\tilde{w}$$

$$x = x_0 + U(\bar{u} - \hat{w}) + (UA - U)\tilde{w}$$

The above formulations give the right ordering policy as uncertainty is realized. The value of $\tilde{w}$ can be calculated at each stage to find the appropriate policy. The upper

and lower limits for the orders and stock are derived as:

$$
\begin{aligned}
u_{lb} &= \bar{u} - |A|\bar{w}, \\
u_{ub} &= \bar{u} + |A|\bar{w}, \\
x_{lb} &= x_0 + U(\bar{u} - \hat{w}) - |UA - U|\bar{w}, \\
x_{lb} &= x_0 + U(\bar{u} - \hat{w}) + |UA - U|\bar{w}
\end{aligned}
$$

The limits are plotted in Figure 2.6. The above figure shows only one scenario, and the performance of the methods can be compared only when it is being tested for a statistically significant number of generated scenarios. Applying the method to the same 1200 scenarios generated for scenario tree method, we have the results summarized in Figure 2.7.

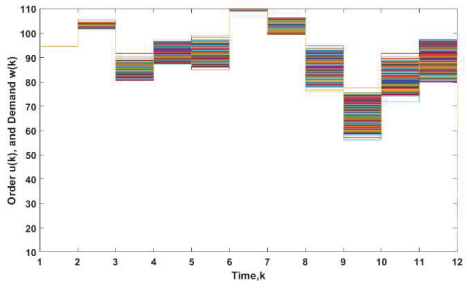

(a) Input for 1200 scenarios

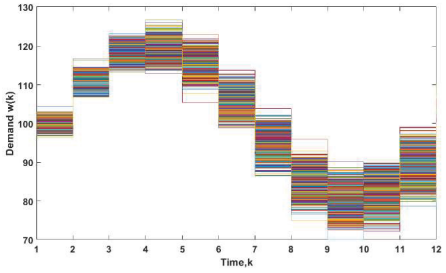

(b) Demand simulated for 1200 scenarios

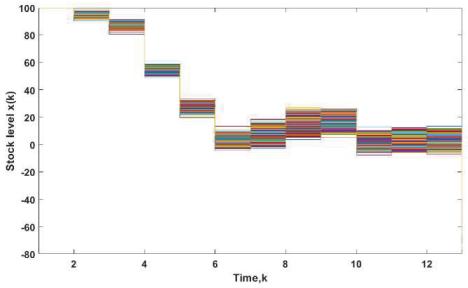

(c) Stock level for 1200 scenarios

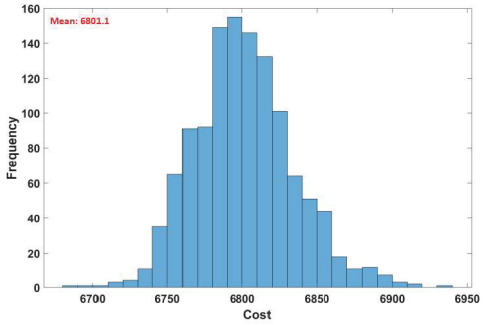

(d) Cost distribution for 1200 scenarios

Figure 2.7: The figure summarizes the results obtained from simulating 1200 scenarios and applying affine policy based method [41]

The profiles were generated for the case where uncertainty was assumed to be $0.15\hat{w}$.

2.5 Conclusion

In this chapter a simple uncertain optimization problem is considered as a background for the following chapters. Various techniques like static robust optimization, scenario-based method, and affine policy based method are demonstrated using this example.

Chapter 3

MPC of HEN under uncertainty

In this chapter, the MPC problem of HEN is formulated and implemented. Initially the deterministic problem is presented, and later, uncertainty is introduced. The formulated control problem is demonstrated using several case studies.

3.1 Problem statement

Bypass control is used for efficient heat integration. For instance, in many oil reservoirs, steam is used to extract oil. Along with hot utility, the high temperature of extracted oil can be used to generate this steam from water.
Consider Figure 3.1, the red color represents is hot stream consisting of oil and steam. Blue represents cold stream, namely water, which is bypassed around the heat exchanger. u is fraction that is bypassed. $m_2(1-u)$ is the mass flowrate of cold stream through heat exchanger.

The steady state equations for the process are given by,

$$Q = KA\Delta T_m \tag{3.1}$$

$$Q = (1-u)m_2 C_{p_2}(T_2'^{out} - T_2^{in}) \tag{3.2}$$

$$\Delta T_m = \frac{1}{2}((T_1^{out} - T_2^{in}) + (T_1^{in} - T_2'^{out})) \tag{3.3}$$

where, Eq. 3.1 denotes Fourier's law. Eq. 3.2 denotes energy conservation of cold stream. K is heat transfer coefficient, Q is heat transfer rate, ΔT_m is the mean

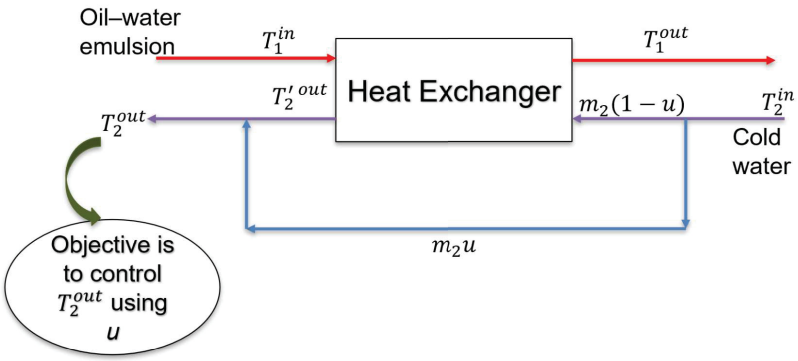

Figure 3.1: Bypass control of heat exchanger

temperature difference, and A is heat transfer area. In this work, the dynamic control problem of heat exchamger is formulated under the MPC framework. So, the objective function is given by,

$$obj = \sum_{t=0}^{t=t_p} (T_{st}(t) - T_2^{out}(t))^2 + \alpha \sum_{n=1}^{n=N} (u(n-1) - u(n))^2 \tag{3.4}$$

where, α is a weighing term, t_p is prediction horizon, and N is control horizon. The first term in the objective function indicates setpoint tracking, and the second term indicates controller effort.

3.2 Deterministic MPC for single HE

The Optimal Control Problem (OCP) of MPC is given by,

$$(OCP) \qquad \min_u \sum_{t=0}^{t=t_p} (T_{st}(t) - T_2^{out}(t))^2 + \alpha \sum_{n=1}^{n=N} (u^{opt,past}(n) - u(n))^2 \tag{3.5}$$

$$\text{s.t.} \quad \dot{T}(t) = f(T(t), u(n), \theta) \tag{3.6}$$

$$T(0) = T_0 \tag{3.7}$$

$$T_1^{in}(t) \leq T_2^{out}(t) \tag{3.8}$$

$$T_1^{out}(t) \leq T_2^{in}(t) \tag{3.9}$$

$$T_2^{out}(t) = u(n) T_2^{in}(t) + (1 - u(n)) T_2'^{out}(t) \tag{3.10}$$

Here, T(t) is the column vector and its elements are states at time t. Eq.3.8 and Eq.3.9 denotes Thermodynamics second law, this constraint ensures the flow of heat from hot fluid to cold fluid. Eq.3.6 denotes the heat exchanger model. Eq.3.10 denotes temperature of the mixed stream.

3.2.1 Dynamic model

The dynamic model of shell and tube heat exchanger used in the algorithm is given by following system of PDEs, and these PDEs denote energy conservation in a unit element represented by red rectangle of Figure 3.2.

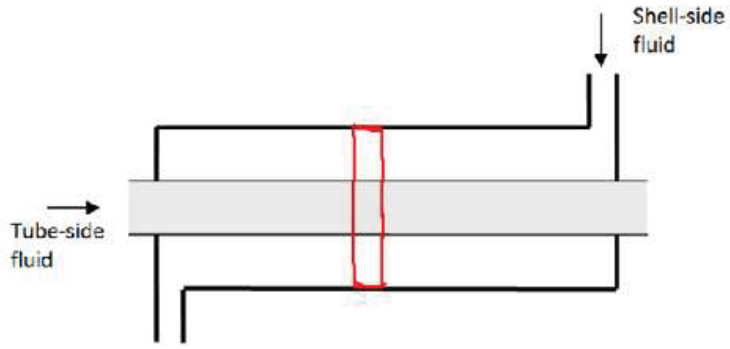

Figure 3.2: Shell and tube heat exchanger with unit element

t denotes time and x denotes position of the unit element. Hot stream flows through shell side, and cold through tube side. m_1 is the flow rate of hot fluid. If F_2 is the total flow rate of cold fluid, its flow rate through heat exchanger is given by,

$$m_2 = F_2(1-u) \tag{3.11}$$

M_1 and M_2 are the flow rates per unit area in heat exchanger of hot fluid and cold fluid respectively. The energy balance for the shell side can be modeled as,

$$\frac{\partial T_1(x,t)}{\partial t} = \frac{m_1}{M_1}\frac{\partial T_1(x,t)}{\partial x} + \frac{\pi d^{out} K^{out}}{M_1 C_{p_1}}[T^{wo}(x,t) - T_1(x,t)] \tag{3.12}$$

The first term in right hand side indicates energy accumulation in the unit element as stream passes through it. The second term in right hand side indicates convective heat transfer from outer wall to stream. The energy balance for the tube outer wall

can be modeled as,

$$\frac{\partial T^{wo}(x,t)}{\partial t} = \frac{2\lambda\pi}{M_w C_{p_w} \ln(\frac{r_2}{r_1})}[T^{wi}(x,t) - T^{wo}(x,t)] + \frac{\pi d^{out} K^{out}}{M_w C_{p_w}}[T_1(x,t) - T^{wo}(x,t)] \tag{3.13}$$

The first term in right hand side indicates conductive heat transfer from inner wall to outer wall. The second term indicates the convective heat transfer from shell side fluid to outer wall. The energy balance for the tube inner wall can be modeled as,

$$\frac{\partial T^{wi}(x,t)}{\partial t} = \frac{2\lambda\pi}{M_w C_{p_w} \ln(\frac{r_2}{r_1})}[T^{wo}(x,t) - T^{wi}(x,t)] + \frac{\pi d^{in} K^{in}}{M_w C_{p_w}}[T_2(x,t) - T^{wi}(x,t)] \tag{3.14}$$

The first term in right hand side indicates conductive heat transfer from outer wall to inner wall. The second term indicates the convective heat transfer from tube side fluid to inner wall. The energy balance for the tube side wall can be modeled as,

$$\frac{\partial T_2(x,t)}{\partial t} = \frac{m_2}{M_2}\frac{\partial T_2(x,t)}{\partial x} + \frac{\pi d^{in} K^{in}}{M_2 C_{p_2}}[T^{wi}(x,t) - T_2(x,t)] \tag{3.15}$$

The first term in right hand side indicates energy accumulation in unit element as stream passes through it. The second term in right hand side indicates convective heat transfer from inner wall to stream.

$$\frac{1}{K^{out}} = \frac{1}{K_1 m_1} + R^{out}(t) \tag{3.16}$$

K_1 represents heat transfer coefficient due flow of shell side fluid. R^{out} includes fouling resistance of outer wall which increases with time, and is given by,

$$R^{out}(t) = 4.35 \times 10^{-4}(1 - e^{(-5.767\times10^{-4})t}) \tag{3.17}$$

$$\frac{1}{K^{in}} = \frac{1}{K_2 m_2} + R^{in}(t) \tag{3.18}$$

K_2 represents heat transfer coefficient due flow of tube side fluid. R^{in} includes fouling resistance of inner wall which increases with time, and is given by,

$$R^{in}(t) = 0.0238 \times 10^{-4}(1 - e^{(-5.256\times10^{-6})t}) \tag{3.19}$$

The values of parameters used in above equations are specific to the case studies considered in this chapter.

3.2.2 Spatial Discretization

To model the heat exchanger, we convert these PDEs to ODEs by applying Finite difference method. Spatial discretization is done at points given by,
$x_{length} = [0, 0.005, 0.01, 0.05, 0.1, 0.2, 0.5, 0.7, 0.9, 0.95, 0.99, 0.995, 1]$
Assuming 0 indicates left end and 1 indicates right end of heat exchanger. At these discretization points, the partial derivatives are approximated as finite differences. The discretization points are closely spaced at both ends of heat exchanger, because the temperatures do not change significantly at centre of heat exchanger as compared to both ends. Let x_{len} denotes len^{th} element(discretization point) of x_{length}. The rate of change of temperature of Shell side fluid with respect to time at len^{th} discretization point is approximated as,

$$\frac{dT_1(len,t)}{dt} = \frac{m_1}{M_1}\frac{[T_1(len,t) - T_1(len-1,t)]}{[x_{len} - x_{len-1}]} + \frac{\pi d^{out} K^{out}}{M_1 C_{p_1}}[T^{wo}(len,t) - T_1(len,t)]$$
$$len = 2, 3, ..., 13, \quad \forall t \tag{3.20}$$

The rate of change of temperature of outer wall with respect to time at len^{th} discretization point is approximated as,

$$\frac{dT^{wo}(len,t)}{dt} = \frac{2\lambda\pi}{M_w C_{p_w} \ln(\frac{r_2}{r_1})}[T^{wi}(len,t) - T^{wo}(len,t)] + \frac{\pi d^{out} K^{out}}{M_w C_{p_w}}[T_1(len,t) - T^{wo}(len,t)]$$
$$len = 1, 2, 3, ..., 13, \quad \forall t \tag{3.21}$$

The rate of change of temperature of inner wall with respect to time at len^{th} discretization point is approximated as,

$$\frac{dT^{wi}(len,t)}{dt} = \frac{2\lambda\pi}{M_w C_{p_w} \ln(\frac{r_2}{r_1})}[T^{wo}(len,t) - T^{wi}(len,t)] + \frac{\pi d^{in} K^{in}}{M_w C_{p_w}}[T_2(len,t) - T^{wi}(len,t)]$$
$$len = 1,2,3,...,13, \quad \forall t \tag{3.22}$$

The rate of change of temperature of tube side fluid with respect to time at len^{th} discretization point is approximated as,

$$\frac{dT_2(len,t)}{dt} = \frac{m_2}{M_2}\frac{[T_2(len,t) - T_2(len+1,t)]}{[x_{len+1} - x_{len}]} + \frac{\pi d^{in} K^{in}}{M_2 C_{p_2}}[T^{wi}(len,t) - T_2(len,t)]$$
$$len = 1,2,3,...,12, \quad \forall t \tag{3.23}$$

These ODEs with boundary conditions completely represents the model used in the algorithm.

3.2.3 Objective function

The objective function is given by,

$$\min_u \sum_{t=0}^{t=t_p} (T_{st}(t) - T_2^{out}(t))^2 + \alpha \sum_{n=1}^{n=N} (u^{opt,past}(n) - u(n))^2 \tag{3.24}$$

Here, the prediction horizon t_p is divided in N (control horizon) intervals. In each interval, u is constant.

Figure 3.3: prediction horizon divided into n equal intervals

3.2.4 Results of single heat exchanger case

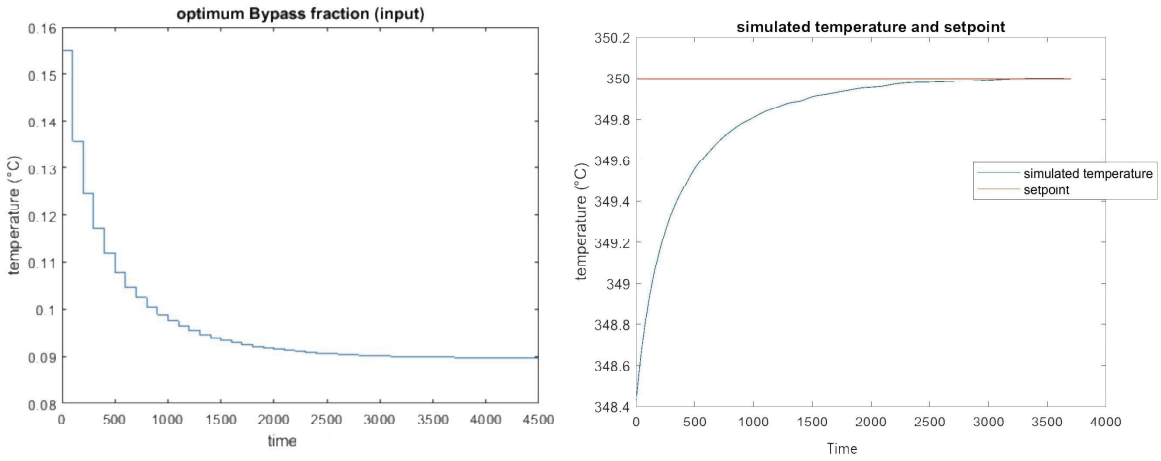

Figure 3.4: The plot on the left shows the plot for input over time, while the plot on the right shows the controlled variable(T_2^{out}) over time

Setpoint tracking:

The setpoint of out temperature of mixed stream is given as a step change at time step of $4,500$. The setpoint is changed from $350°c$ to $349°c$, and the graph trajectories of controlled variable and input are obtained as follows,

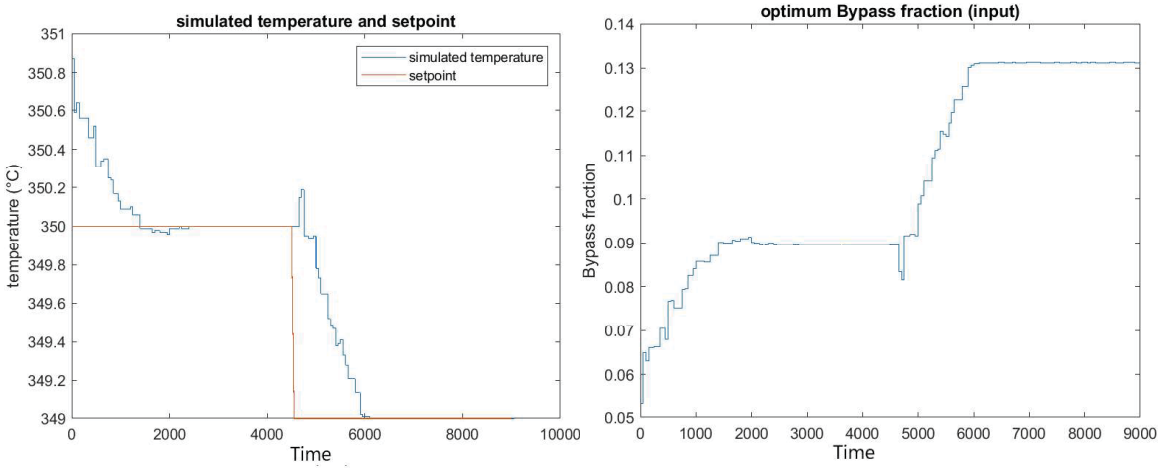

Figure 3.5: The plot on the left shows the plot for controlled variable (T_2^{out}) in step change in setpoint, while the plot on the right shows optimized input (u) step change in setpoint case

Disturbance rejection:

The step disturbance is introduced to the system at time step of 4000. The graphs

of output and input are as follows

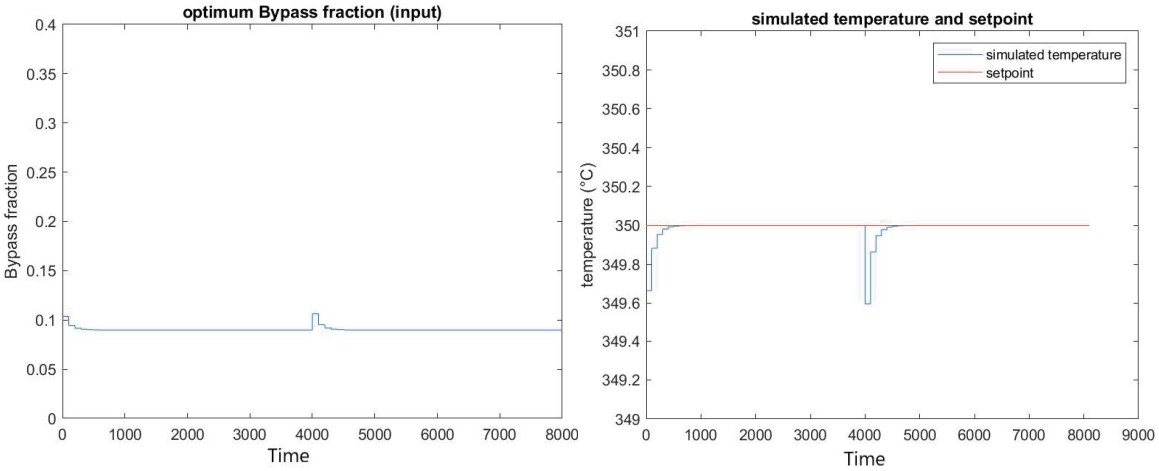

Figure 3.6: The plot on the left shows the plot optimized input (u) disturbance rejection case, while the plot on the right shows controlled variable (T_2^{out}) in case of disturbance rejection

3.3 Deterministic MPC For HEN

Until now, the MPC has been formulated for only the single HE case. The objective of this section is to extend the formulation to a HEN.

Consider the following HEN example as shown in Figure 3.7,

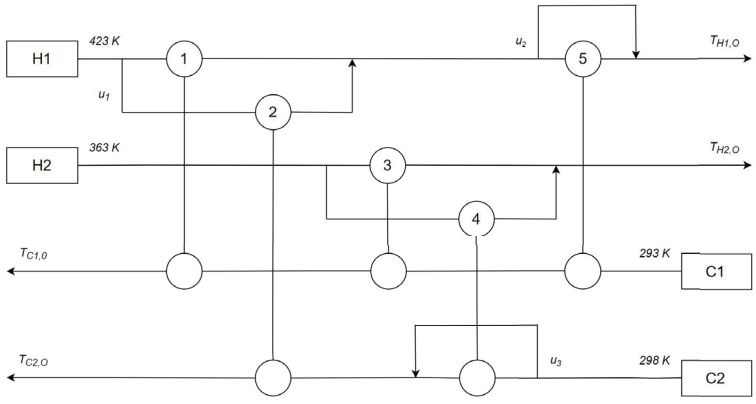

Figure 3.7: heat exchanger network

There are two hot streams H1 and H2, as well as two cold streams C1 and C2.

There are also five heat exchangers. u_1 is the bypass fraction of stream H1 around

heat exchanger 1. u_2 is the bypass fraction of stream H1 around heat exchanger 5. u_3 is the bypass fraction of stream C2 around heat exchanger 4. u_i is i^{th} element of vector u. The objective function includes setpoint tracking of out temperatures of streams H1 and C2, as well as controller effort terms. Let $T_{st,H1}$ be the setpoint of out temperature of H1 stream, and $T_{st,C2}$ be the setpoint of out temperature of C2 stream. The constraints in below OCP represent the heat exchanger model equations and energy balance equations. The Optimal Control Problem (OCP) of MPC is given by,

$$\begin{aligned}(OCP) \qquad \min_{u} \sum_{t=0}^{t=t_p} &((T_{st,H1}(t) - T_{H1}^{out}(t))^2 + (T_{st,C2}(t) - T_{C2}^{out}(t))^2) \\ &+ \sum_{i=1}^{i=3} \alpha_i \sum_{t=0}^{t=t_p} \left(u^{i,opt,past}(t) - u^i(t)\right)^2\end{aligned} \tag{3.25}$$

$$\text{s.t.} \quad \dot{T}(t) = f(T(t), u(n), \theta), \quad T(0) = T_0 \tag{3.26}$$

$$F_{H1}(1 - u_1(t))C_{p_{H1}}(423 - T_{H1,1}^{out}(t)) - m_{C1}C_{p_{C1}}(T_{C1}^{out}(t) - T_{C1,1}^{in}(t)) = 0 \tag{3.27}$$

$$F_{H1}u_1(t)C_{p_{H1}}(423 - T_{H1,2}^{out}(t)) - F_{C2}C_{p_{C2}}(T_{C1}^{out}(t) - T_{C1,2}^{in}(t)) = 0 \tag{3.28}$$

$$F_{H2}(1 - u_{H2}(t))C_{p_{H2}}(363 - T_{H2,3}^{out}(t)) - m_{C1}C_{p_{C1}}(T_{C1,3}^{out}(t) - T_{C1,3}^{in}(t)) = 0 \tag{3.29}$$

$$F_{H2}u_{H2}(t)C_{p_{H2}}(363 - T_{H2,4}^{out}(t)) - F_{C2}(1 - u_3(t))C_{p_{C2}}(T_{C2,4}^{out}(t) - 298) = 0 \tag{3.30}$$

$$F_{H1}(1 - u_2(t))C_{p_{H1}}(T_{H1,5}^{in}(t) - T_{H1,5}^{out}(t)) - m_{C1}C_{p_{C1}}(T_{C1,5}^{out}(t) - 293) = 0 \tag{3.31}$$

3.3.1 Results

In this section, the performance of the proposed control method is demonstrated by setpoint tracking, step change, and disturbance rejection cases. For this network, to make controlled variables converge to corresponding setpoints, the weights on percentage change of inputs (controller effort) have to be adjusted to an order of 10^{-20}. Even at such smaller weights, we can see from the below graphs that the optimal inputs do not vary much. The prediction horizon of 400 is divided into 4 control intervals. The controlled variables graphs show that setpoint is tracked efficiently, and inputs graphs show that the controller is sensitive to change in setpoint, and also disturbances.

Setpoint tracking:

The graphs of optimal input are given by figure 3.8, figure 3.9, and figure 3.10

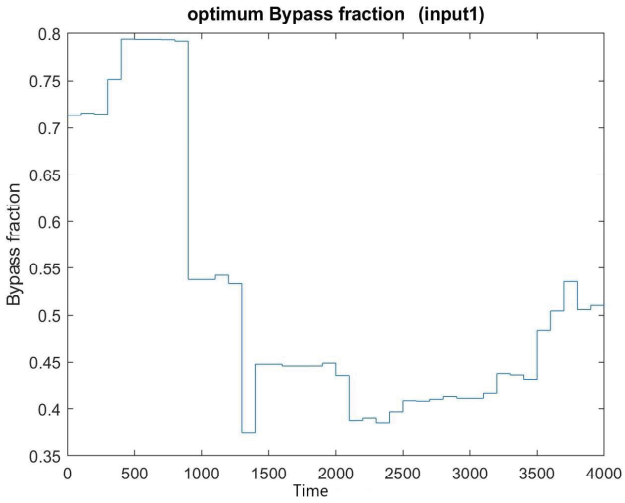

Figure 3.8: Optimized input (u_1)

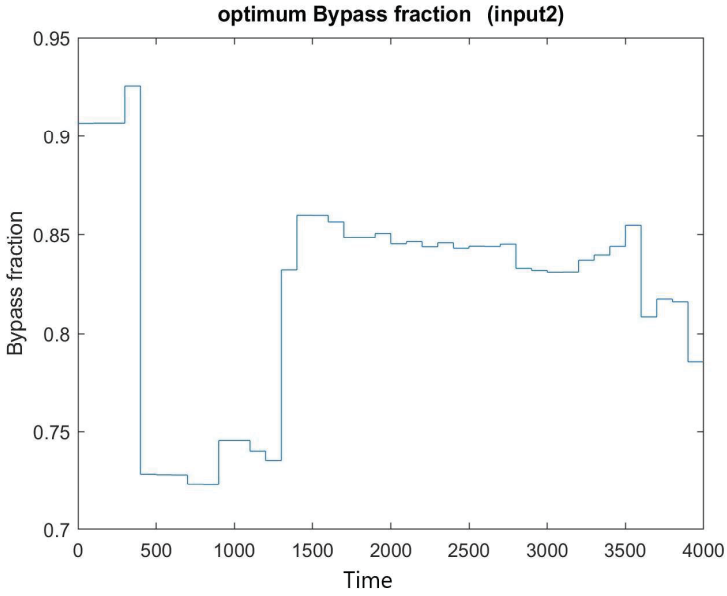

Figure 3.9: Optimized input (u_2)

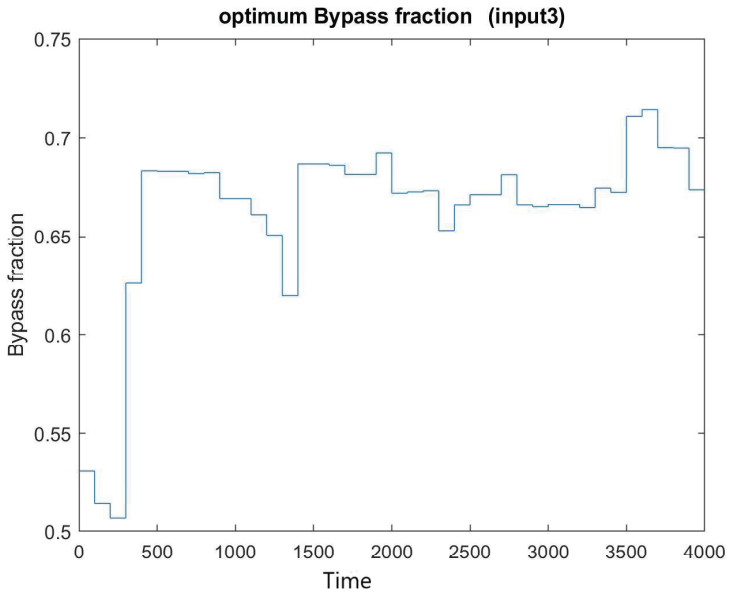

Figure 3.10: Optimized input (u_3)

The responses of controlled variables are given in Figure 3.11. These figures show that there is deviation of controlled variable from setpoint initially, and converges to setpoint as time passes. Figure 3.11 shows that (T_{C2}^{out}) is tracked better than (T_{H1}^{out}).

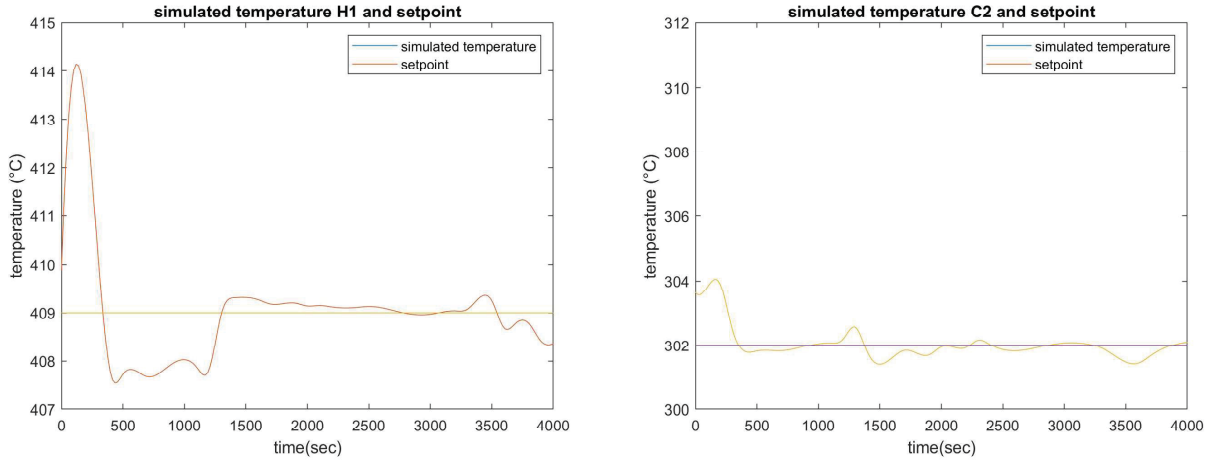

Figure 3.11: The plot on the left shows the plot controlled variable (T_{H1}^{out}), while the plot on the right shows controlled variable (T_{C2}^{out})

Step change:

The setpoint of out temperature of H1 stream has a step change at time step $7,200$. It is changed from $409°c$ to $410°c$. The setpoint of out temperature of C2 stream is given a step change at time step $7,200$, and it is changed from $302°c$ to $301°c$. The

graphs of optimal input in case of step change in setpoint are given in Figure 3.12, Figure 3.13,and Figure 3.14.

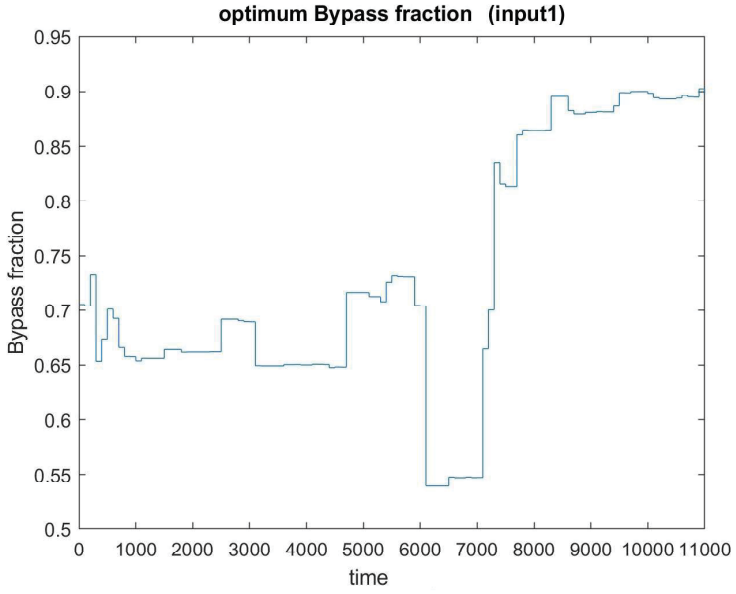

Figure 3.12: Optimized input (u_1) setpoint tracking case

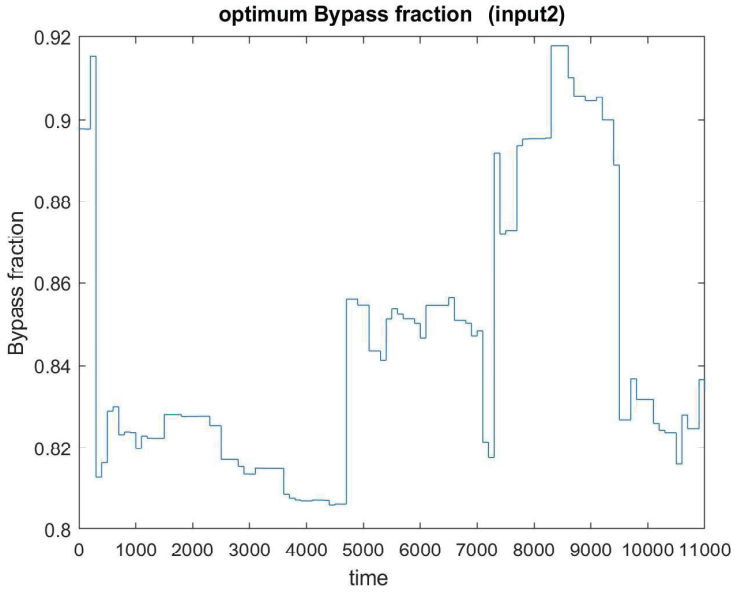

Figure 3.13: Optimized input (u_2) setpoint tracking case

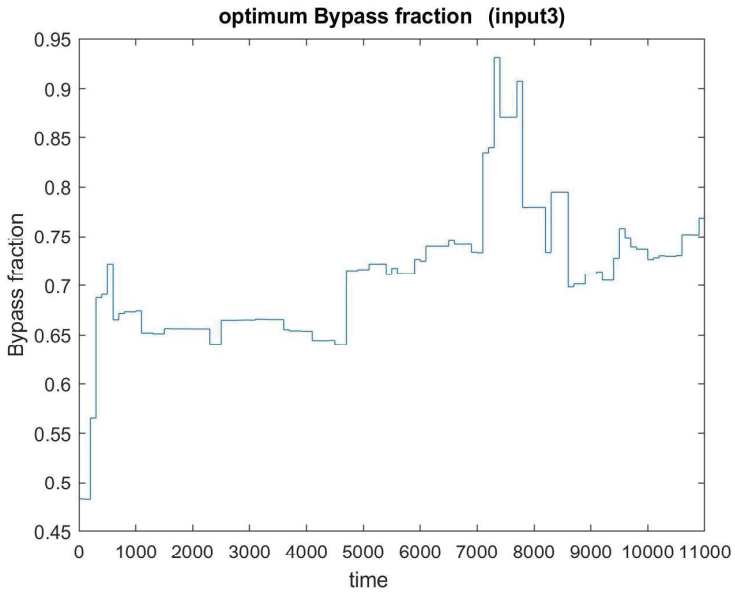

Figure 3.14: Optimized input (u_3) setpoint tracking case

The responses of controlled variables are given by figure 3.15. The same figure also shows the setpoint, from figure it is understood that controlled variable T_{H1}^{out} is tracked more closely than T_{C2}^{out}.

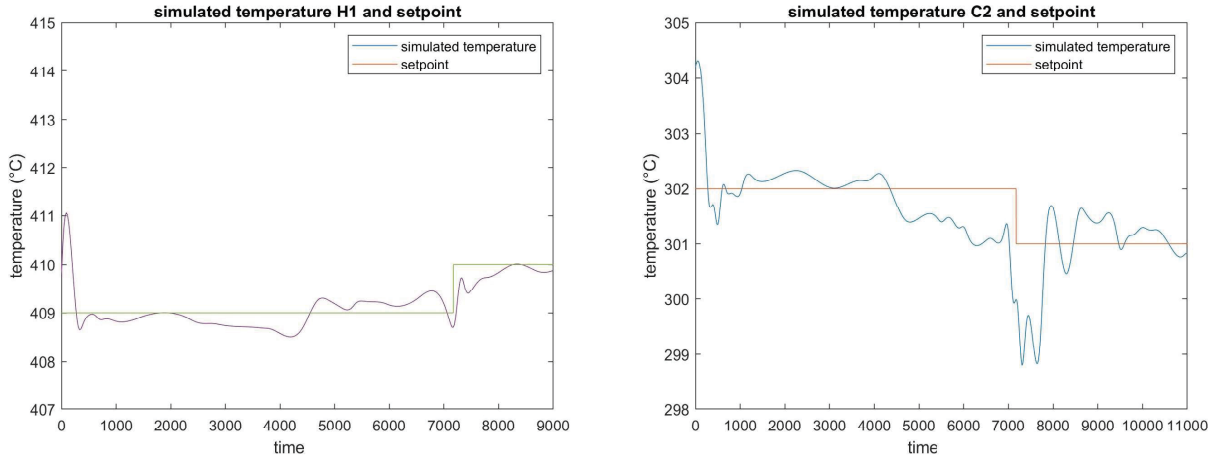

Figure 3.15: The plot on the left shows the plot controlled variable((T_{H1}^{out}), while the plot on the right shows controlled variable ((T_{C2}^{out}) with step change in setpoint

Disturbance rejection:

The step disturbance is introduced to system at time step of 800. The trajectories of optimal inputs u_1, u_2, and u_3 in the presence of disturbance rejection are given by Figure 3.16, Figure 3.17,and Figure 3.18.

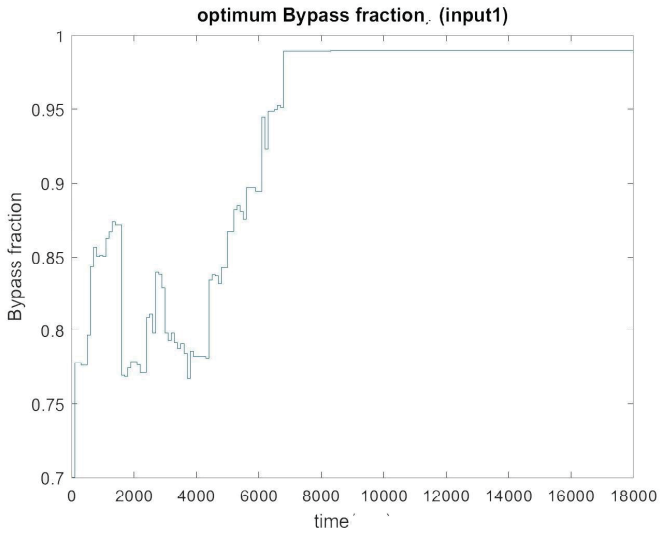

Figure 3.16: Optimized input (u_1) disturbance rejection case

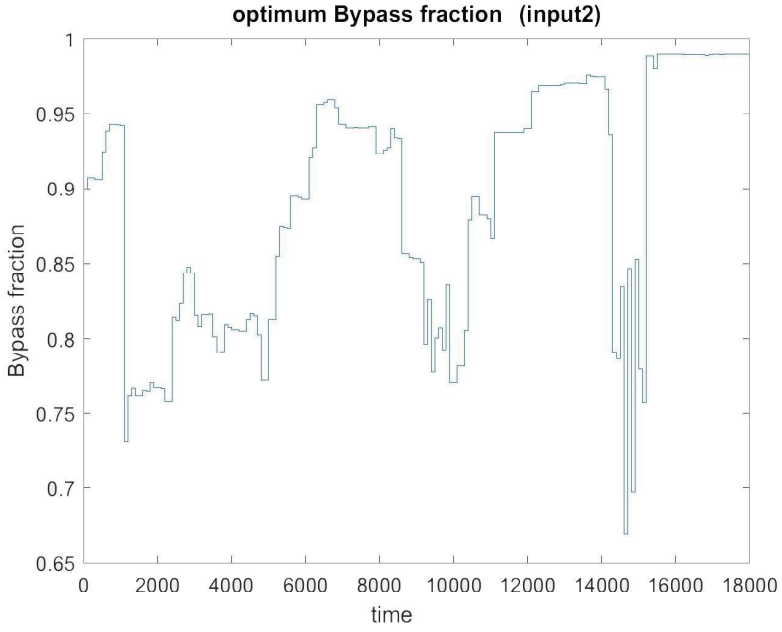

Figure 3.17: Optimized input (u_2) disturbance rejection case

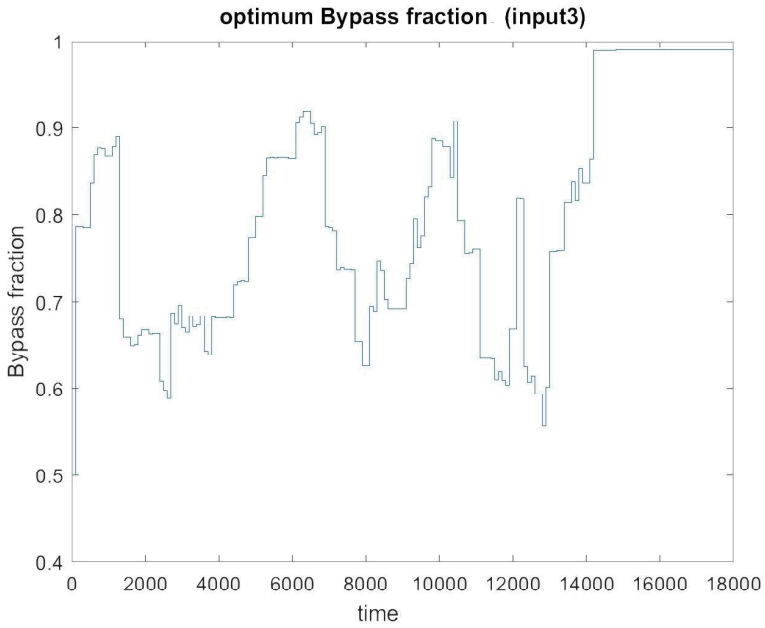

Figure 3.18: Optimized input (u_3) disturbance rejection case

Figures 3.16, 3.17,and 3.18 show that the input is constant after some time. This is because the effect of disturbance is mitigated gradually. The responses of controlled variables are given by Figure 3.19.

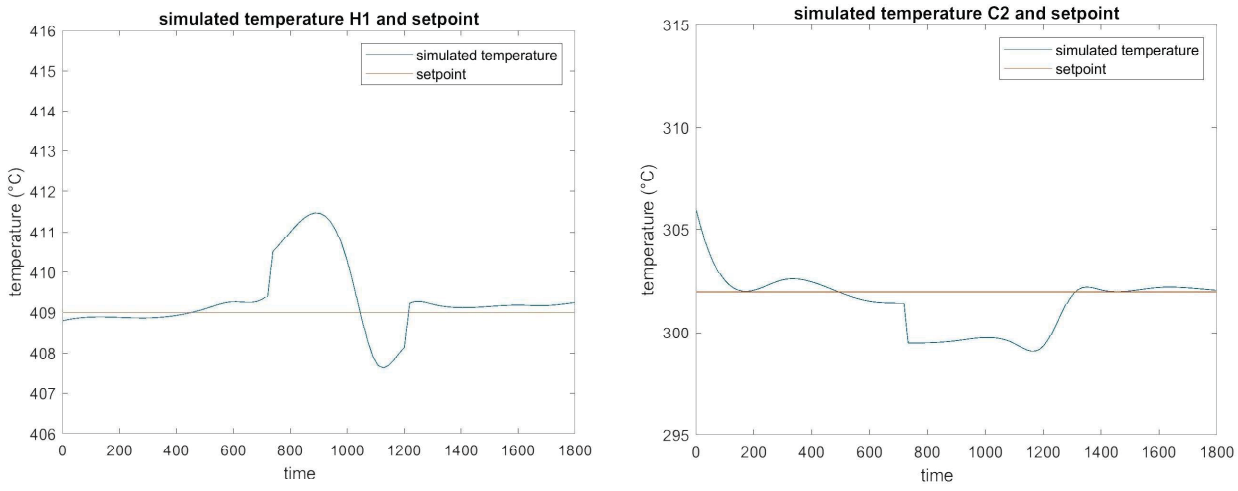

Figure 3.19: The plot on the left shows the plot controlled variable((T_{H1}^{out}), while the plot on the right shows controlled variable ((T_{C2}^{out}) in disturbance rejection case

3.4 MPC of single heat exchanger and HEN under uncertainty

From now, we will consider the uncertainty related to inlet temperature of hot streams. The state variables will be uncertainty dependent. The overall uncertain optimization problem is formulated as following:

$$(OCP) \qquad \min_{u} \int_{t=0}^{t=t_p} (T_{st}(t) - T_2^{out}(t,\zeta))^2 + \alpha \sum_{n=1}^{n=N} (u^{opt,past}(n) - u(n))^2 \tag{3.32}$$

$$\text{s.t.} \quad \dot{T}(t) = f(T(t,\zeta), u(n), \theta) \tag{3.33}$$

$$T(0) = T_0 \tag{3.34}$$

$$T_2^{out}(t,\zeta) = u(n)T_2^{in}(t) + (1-u(n))T_2'^{out}(t,\zeta) \tag{3.35}$$

$$T_1^{in}(t,\zeta) \leq T_2'^{out}(t,\zeta) \tag{3.36}$$

$$T_1^{out}(t,\zeta) \leq T_2^{in}(t,\zeta) \tag{3.37}$$

$$u_{min} \leq u(\zeta) \leq u_{max} \tag{3.38}$$

where, ζ represents the uncertainty. The above uncertain OCP is intractable because we assume that ζ belongs to a continuous compact set. So, the constraints in above OCP are infinite. This intractable OCP is made tractable by following the steps shown in Figure 3.20.

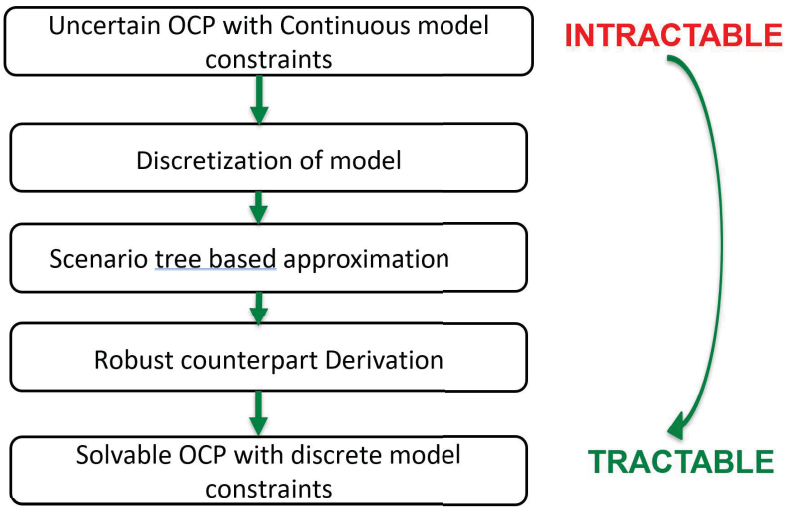

Figure 3.20: Steps to convert intractable problem to tractable

3.4.1 Discretization of ODEs

The orthogonal collocation technique is used to discretize the system of ODEs given in Section 3.2.2 into system of nonlinear equations. The model of the HEN is represented by these nonlinear equations. At each time instant, the prediction horizon t_p is divided into N (control horizon) intervals. The input is assumed to be constant in $n^{th}(n = 1, 2, ..., N)$ interval, and it is denoted by $u(n)$. Each n^{th} interval is divided into $K+1$ intervals using K collocation points. The state vector at $k^{th}(k = 1, 2, ..., K)$ collocation point, $len^{th}(len = 1, 2, ..., 13)$ spatial discretization point, and n^{th} interval is denoted by $T_{len,n,k}$.

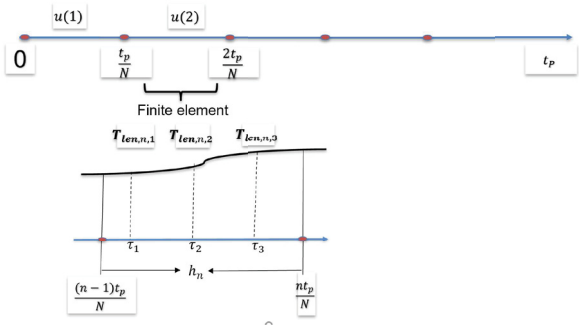

Figure 3.21: Polynomial approximation of state profile across finite element with 3 collocation points

The states in each finite element are approximated using Lagrange interpolation polynomials. They are given by,

$$t = t_{i-1} + h_i\tau \qquad \tau \in [0, 1] \tag{3.39}$$

$$T_{len}(t) = \sum_{k=0}^{k=K} T_{len,n,k} l_k(\tau) \tag{3.40}$$

$$l_k(\tau) = \prod_{j=0\neq k}^{j=K} \frac{\tau - \tau_j}{\tau_k - \tau_j} \tag{3.41}$$

The approximated derivative of states at these collocation points is equated with original ODEs, and the HEN model is thus given by,

$$\sum_{k=0}^{k=K} T_{1,len,n,k}\frac{dl_j(\tau_k)}{d\tau} = h_n[\frac{m_1}{M_1}\frac{[T_1(len,n,j)-T_1(len-1,n,j)]}{[x_{len}-x_{len-1}]}+\frac{\pi d^o K^o}{M_1 C_{p_1}}[T^{wo}_{len,n,j}-T_1(len,n,j)]]$$

$$len=1,2,3,...,13 \quad n=1,2,3,...,N \quad j=1,2,3,...,J \tag{3.42}$$

$$\sum_{k=0}^{k=K} T^{wo}_{len,n,k}\frac{dl_j(\tau_k)}{d\tau} = h_n[\frac{2\lambda\pi}{M^w C_{p_w}\ln(\frac{r_2}{r_1})}[T^{wi}_{len,n,j}-T^{wo}_{len,n,j}]+\frac{\pi d^o K^o}{M^w C_{p_w}}[T_{1,len,n,j}-T^{wo}_{len,n,j}]]$$

$$len=1,2,3,...,13 \quad n=1,2,3,...,N \quad j=1,2,3,...,J \tag{3.43}$$

$$\sum_{k=0}^{k=K} T^{wi}_{len,n,k}\frac{dl_j(\tau_k)}{d\tau} = h_n[\frac{2\lambda\pi}{M^w C_{p_w}\ln(\frac{r_2}{r_1})}[T^{wo}_{len,n,j}-T^{wi}_{len,n,j}]+\frac{\pi d^i K^i}{M^w C_{p_w}}[T_{2,len,n,j}-T^{wi}_{len,n,j}]]$$

$$len=1,2,3,...,13 \quad n=1,2,3,...,N \quad j=1,2,3,...,J \tag{3.44}$$

$$\sum_{k=0}^{k=K} T_{2,len,n,k}\frac{dl_j(\tau_k)}{d\tau} = h_n[\frac{m_2}{M_2}\frac{[T_2(len,n,j)-T_2(len+1,n,j)]}{[x_{len}-x_{len+1}]}+\frac{\pi d^i K^i}{M_2 C_{p_2}}[T^{wi}_{len,n,j}-T_2(len,n,j)]]$$

$$len=1,2,3,...,13 \quad n=1,2,3,...,N \quad j=1,2,3,...,J \tag{3.45}$$

3.4.2 Affine policy based method

In the Affine policy based method, the decision variable taken at the first instant is independent of the uncertainty. The decisions taken at the further stages are dependent of the uncertainty realized at the previous time instant. The decision variable or input (bypass fraction) is formulated as linear function of uncertainty.
The temperature of hot stream at inlet of heat exchanger is assumed as the linear function of uncertainty (disturbance). We further assume that uncertainty is constant

in a finite element and is denoted by ζ_n.

$$T_{1,n}^{in} = A\zeta_n + B(1-\zeta_n) \quad n = 1,2,3,...,N \tag{3.46}$$

$$\zeta_n \in [0,1] \quad n = 1,2,3,...,N \tag{3.47}$$

$$\boldsymbol{\zeta} \in \Xi = \{\boldsymbol{\zeta} : W \cdot \boldsymbol{\zeta} \geq \underline{\mathrm{h}}\} \tag{3.48}$$

$$\boldsymbol{\zeta} = [\zeta_1, \zeta_2, ..., \zeta_N]' \tag{3.49}$$

All states of the system and input are dependent on the primitive uncertainty.

Robust counterpart derivation

In Affine control policy, the decision variable or input (bypass fraction) is formulated as linear function of uncertainty.

$$u_n = \boldsymbol{u}^T \cdot [1, \zeta_1, \zeta_2, ..., \zeta_{n-1}]' \tag{3.50}$$

Consider the constraint,

$$u_n(s) \leq u_{max} \tag{3.51}$$

Apply linear decision rule,

$$\boldsymbol{u}^T \cdot [1, \zeta_1, \zeta_2, ..., \zeta_{n-1}]' \leq u_{max} \tag{3.52}$$

where $\boldsymbol{u}^T$ contains the affine rule parameters.

$$\boldsymbol{u}^T \cdot [1, \zeta_1, \zeta_2, ..., \zeta_{n-1}]' \leq u_{max} \tag{3.53}$$

To avoid change in dimension of $[1, \zeta_1, \zeta_2, ..., \zeta_{n-1}]'$ as n changes, the truncate operator is introduced:

$$\boldsymbol{u}^T \cdot P^n \cdot [1, \zeta_1, \zeta_2, ..., \zeta_{N-1}]' \leq u_{max} \tag{3.54}$$

P^n is a matrix and is function of n.
For example, if $N = 3, n = 2$,

$$P^n = \begin{bmatrix} 1 & 0 & 0 \\ 0 & 1 & 0 \\ 0 & 0 & 0 \end{bmatrix} \tag{3.55}$$

Derive the robust counterpart, and use the uncertainty set definition,

$$\{\max_{\boldsymbol{\zeta}, -W\cdot\boldsymbol{\zeta}\leq h} \boldsymbol{u}^T \cdot P^n \cdot \boldsymbol{\zeta}\} \leq u_{max} \tag{3.56}$$

Here, W and h are a matrix and a vector of known coefficients respectively. Using duality,

$$\{\min_{\wedge_n^{u,1}, \wedge_n^{u,1} \geq 0, -W\cdot\wedge_{\boldsymbol{n}}^{\boldsymbol{u,1}} \leq (\boldsymbol{u_n^T}\cdot P^n)} -\boldsymbol{h}\wedge_n^{u,1}\} \leq u_{max}, \quad n = 1, 2, ...N \tag{3.57}$$

Drop minimization operator,

$$\{\wedge_n^{u,1} \geq 0, -W^T\wedge_{\boldsymbol{n}}^{\boldsymbol{u,1}} = (\boldsymbol{u_n^T}\cdot P^n), -\boldsymbol{h}\wedge_n^{u,1} \leq u_{max}\}, \quad n = 1, 2, ...N \tag{3.58}$$

Thus, the constraint has become independent of uncertainty.
Similarly, the constraint $u_{min} \leq u_n(s)$ is replaced with,

$$\{\wedge_n^{u,2} \geq 0, -W^T\wedge_{\boldsymbol{n}}^{\boldsymbol{u,2}} = (-\boldsymbol{u_n^T}\cdot P^n), -\boldsymbol{h^T}\wedge_n^{u,2} \leq -u_{min}\}, \quad n = 1, 2, ...N \tag{3.59}$$

Optimization problem
The optimization problem is represented as:

$$(OCP) \qquad \min_{\mathbf{u}} \sum_{n=1}^{n=N}\sum_{k=1}^{k=K}(T_{2,n,k}^{out}(E(\zeta_n)) - T_{st,n,k})^2 + \alpha\sum_{n=1}^{n=N}(u^{opt,past}(n, E(\zeta_n)) - u(n, E(\zeta_n)))^2 \tag{3.60}$$

s.t.

$$\sum_{k=0}^{k=K} T_{1,len,n,k,s} \frac{dl_j(\tau_k)}{d\tau} = h_n[\frac{m_1}{M_1} \frac{[T_1(len,n,j,s) - T_1(len-1,n,j,s)]}{[x_{len} - x_{len-1}]} + \frac{\pi d^o K^o}{M_1 C_{p_1}} [T^{wo}_{len,n,j,s} - T_1(len,n,j,s)]] \tag{3.61}$$

$$len = 1,2,3,...,13 \quad n = 1,2,3,...,N \quad j = 1,2,3,...,J \quad \forall s$$

$$\sum_{k=0}^{k=K} T^{wo}_{len,n,k,s} \frac{dl_j(\tau_k)}{d\tau} = h_n[\frac{2\lambda\pi}{M^w C_{p_w} \ln(\frac{r_2}{r_1})} [T^{wi}_{len,n,j,s} - T^{wo}_{len,n,j,s}] + \frac{\pi d^o K^o}{M^w C_{p_w}} [T_{1,len,n,j,s} - T^{wo}_{len,n,j,s}]] \tag{3.62}$$

$$len = 1,2,3,...,13 \quad n = 1,2,3,...,N \quad j = 1,2,3,...,J \quad \forall s$$

$$\sum_{k=0}^{k=K} T^{wi}_{len,n,k,s} \frac{dl_j(\tau_k)}{d\tau} = h_n[\frac{2\lambda\pi}{M^w C_{p_w} \ln(\frac{r_2}{r_1})} [T^{wo}_{len,n,j,s} - T^{wi}_{len,n,j,s}] + \frac{\pi d^i K^i}{M^w C_{p_w}} [T_{2,len,n,j,s} - T^{wi}_{len,n,j,s}]] \tag{3.63}$$

$$len = 1,2,3,...,13 \quad n = 1,2,3,...,N \quad j = 1,2,3,...,J \quad \forall s$$

$$\sum_{k=0}^{k=K} T_{2,len,n,k,s} \frac{dl_j(\tau_k)}{d\tau} = h_n[\frac{m_2}{M_2} \frac{[T_2(len,n,j,s) - T_1(len+1,n,j,s)]}{[x_{len} - x_{len+1}]} + \frac{\pi d^i K^i}{M_2 C_{p_2}} [T^{wi}_{len,n,j,s} - T_2(len,n,j,s)]] \tag{3.64}$$

$$len = 1,2,3,...,13 \quad n = 1,2,3,...,N \quad j = 1,2,3,...,J \quad \forall s$$

$$m_2 = F_2(1-u) \tag{3.65}$$

$$T(0) = T_0 \tag{3.66}$$

$$T^{out}_{2,n,k,s} = u(n,s) T^{in}_{2,n,k,s} + (1 - u(n,s)) {T'_{2,n,k,s}}^{out} \tag{3.67}$$

$$T^{in}_{1,n,k,s} \leq {T'_{2,n,k,s}}^{out} \tag{3.68}$$

$$T^{out}_{1,n,k,s} \leq T^{in}_{2,n,k,s} \tag{3.69}$$

$$\{\wedge^{u,1}_n \geq 0, -W^T \wedge^{\boldsymbol{u,1}}_{\boldsymbol{n}} = (\boldsymbol{u^T_n} \cdot P^n), \boldsymbol{-h^T} \wedge^{u,1}_n \leq u_{max}\}, \quad n = 1, 2, ...N \tag{3.70}$$

$$\{\wedge^{u,2}_n \geq 0, -W^T \wedge^{\boldsymbol{u,2}}_{\boldsymbol{n}} = (-\boldsymbol{u^T_n} \cdot P^n), \boldsymbol{-h^T} \wedge^{u,2}_n \leq -u_{min}\}, \quad n = 1, 2, ...N \tag{3.71}$$

3.4.3 Results

The performance of the proposed control method is demonstrated using two case studies. First study is a simple heat exchanger, and second is a HEN. The optimization is done in GAMS 25.1.1, and overall MPC is implemented using MATLAB 2020a. The solvers used for optimization are DICOPT(MINLP) and CPLEX(MILP). The best solver for the specific case study is determined based on trial and error method.

Single HE:

The decision variable (bypass fraction of cold stream) is obtained by optimizing the uncertain OCP. Four scenarios of possible uncertainty are used in optimization to obtain the value of decision variable. The prediction horizon of 20 is divided into 2 finite elements. The scenarios used in optimization are four constant inlet temperature profiles of hot stream. The bypass fraction (the decision variable) obtained by optimization has constant value within each control interval.

Figure 3.22 gives the inlet temperature profiles of hot stream considered at different scenarios considered in the optimization. The four constant inlet temperatures of the hot stream are considered. These finite number of scenarios are assumed to model the uncertainty in inlet temperature of the hot stream. The probability of occurence of each of scenarios is assumed to be same.

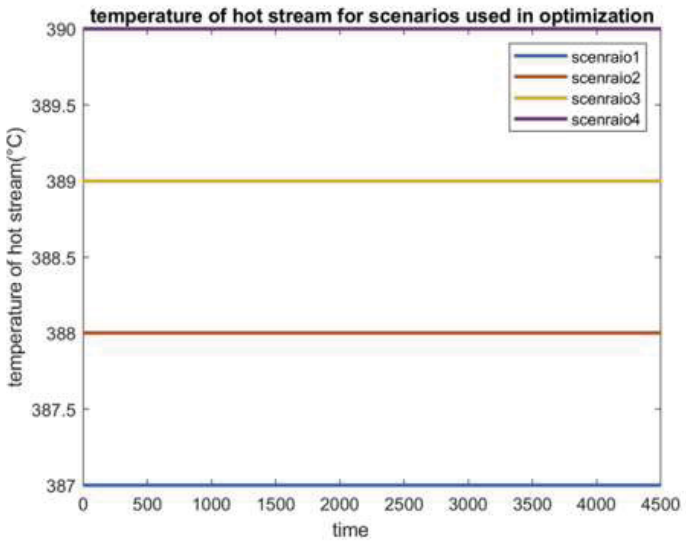

Figure 3.22: T_1^{in} considering 4 scenariors used in optimization

Figure 3.23 shows out temperature of mixed stream (controlled variable) $T_{2,n,k}^{out}$ considering the scenarios used in optimization. The figure shows that for the considered scenarios, the simulated controlled variable converges to setpoint for all the scenarios. To demonstrate the practicality of the proposed control method, four random scenarios of inlet temperature of hot stream are considered. The response of the corresponding controlled variable will be given later. To generate this plot, the values of decision variable i.e. affine rule parameters are used. These decision variables and the corresponding primitive uncertainty value of each scenario are used to calculate the input. They are calculated using affine rule, and these input values are used to calculate the values of all states under each scenario.

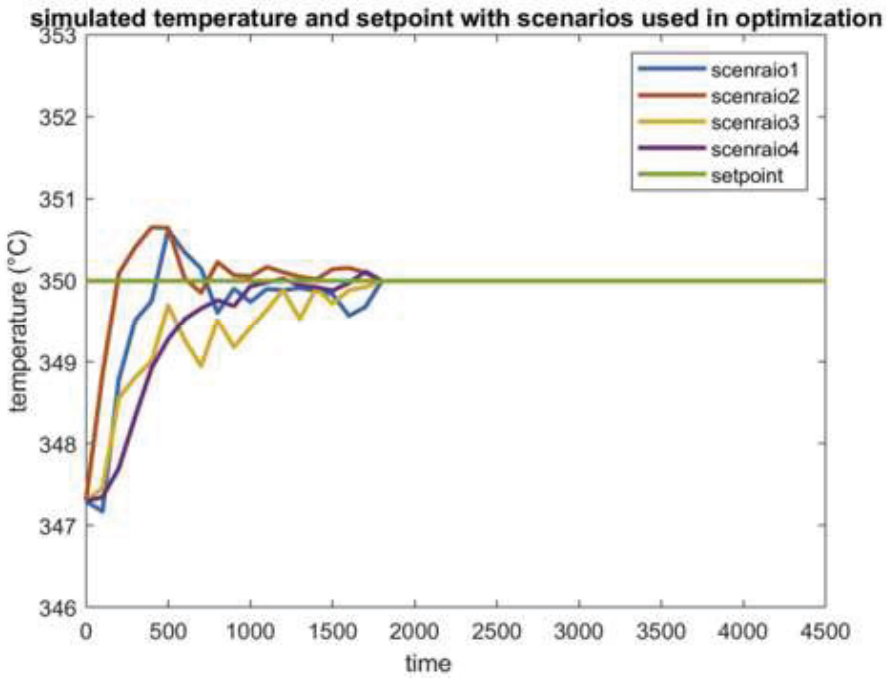

Figure 3.23: $T^{out}_{2,n,k}$ considering 4 scenarios used in optimization

Figure 3.24 gives the trajectory of the optimal bypass fraction (manipulated variable) u_n. These profiles are obtained by using optimised affine rule parameter values and uncertainty values in each scenario.

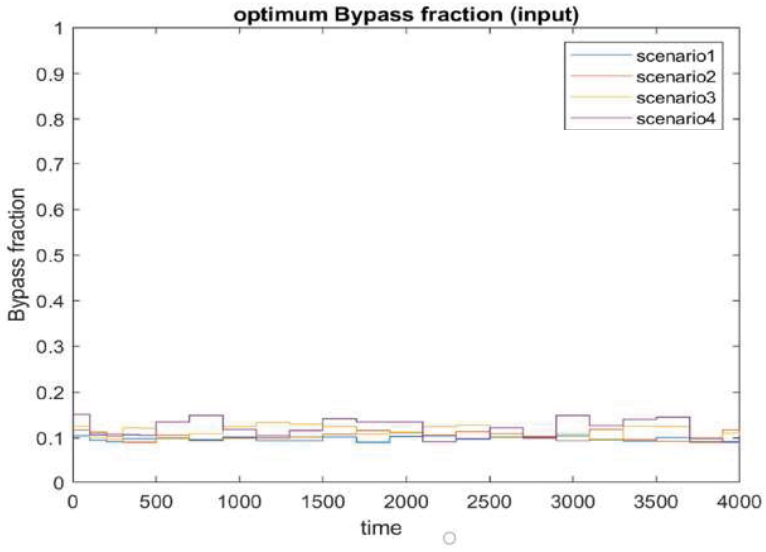

Figure 3.24: u_n for 4 scenarios used in optimization

To test the performance of the optimization, the average value of optimal input

is given to the system. Four random scenarios of inlet temperature of hot stream are considered. The controlled variable is simulated using average optimal input and these random scenarios of inlet temperature of hot stream. Figure 3.25 gives the inlet temperature profiles of hot stream under the random scenarios.

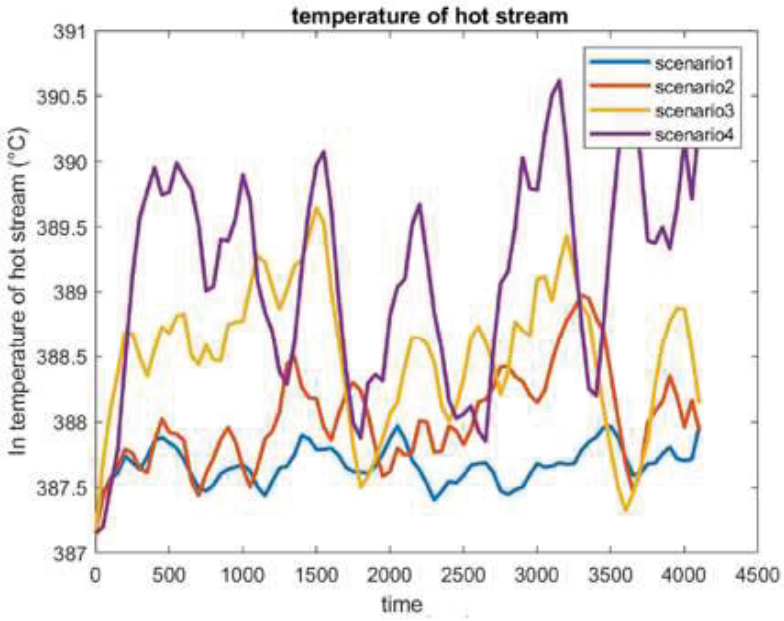

Figure 3.25: T_1^{in} considering 4 random scenariors

Figure 3.26 shows out temperature of mixed stream (controlled variable) $T_{2,n,k}^{out}$. This is the plot generated using random scenarios. As expected, the controlled variable does not converge to the setpoint efficiently. The figure shows that the controlled variable fluctuates around the setpoint. This is because there is always a random disturbance in the inlet temperature. For all the scenarios the controlled variable is generated using corresponding random inlet temperature of hot stream and the average value of the decision variable. The results demonstrate that the proposed control method is effective in the presence of uncertainty as the deviation of controlled variable from setpoint is constant or not increasing as time passes.

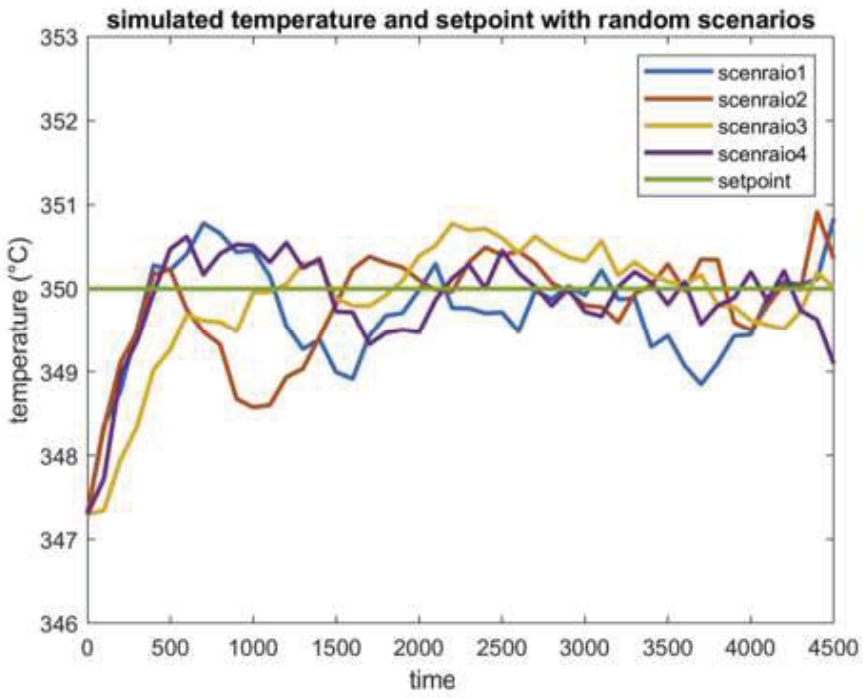

Figure 3.26: $T^{out}_{2,n,k}$ considering 4 random scenariors

The controlled variable profiles are generated using deterministic inputs for the testing scenarios. The corresponding response is given by figure 3.27, which shows the controlled variable deviates from the setpoint as time passes if using deterministic inputs.

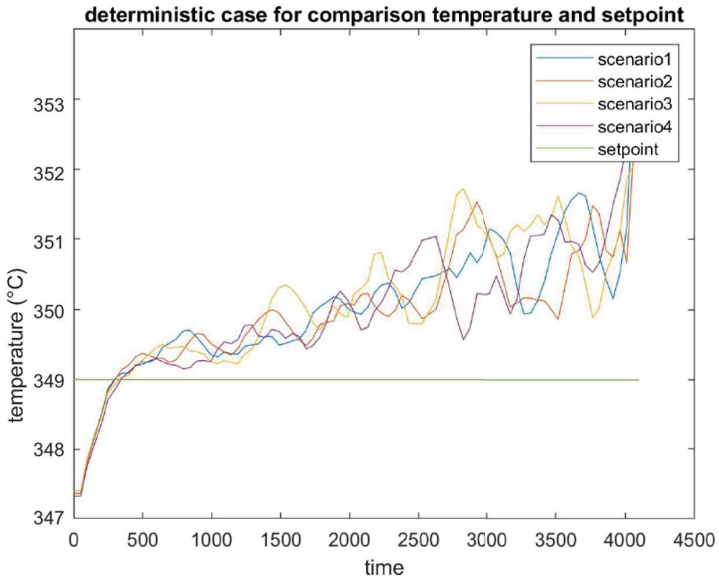

Figure 3.27: $T^{out}_{2,n,k}$ using the deterministic input considering 4 scenariors

The following table gives the values of objective function, MSE between the controlled variable and setpoint using bypass fraction from deterministic optimization, and MSE using bypass fraction from uncertain optimization.

objective function	7.49×10^5
MSE using uncertain input	2.85×10^5
MSE using deterministic input	4.52×10^6

Table 3.1: Results of uncertain MPC for single HE

HEN:

The HEN considered for second case study is given by Figure 3.7. This HEN is adopted from [1]. For the considered HEN, four constant scenarios of possible uncertainty are used in the optimization to obtain the value of the decision variable. The prediction horizon of 40 is divided into 2 finite elements. For this case study, we consider disturbances in H1 stream, and the controlled variable is out temperature of C2 stream. In deterministic MPC, the out temperature of H1 stream is also considered as the controlled variable. Here, only out temperature of C2 is taken as controlled variable to reduce the computational load of the optimization. The objective function is also modified accordingly. The decision variables include all the three bypass fractions as that of deterministic case. The OCP with uncertainty is solved in receding horizon approach to implement the MPC. The single HE dynamic model is extended i.e. considering all the five heat exchangers as given in figure 3.7. The constraints for the connection between the heat exchangers i.e. series and parallel arrangements of heat exchangers are also included in the formulation.

Figure 3.28 shows the inlet temperature profiles of hot stream considered at different scenarios used in the optimization. The scenarios used in optimization are different constant inlet temperatures of hot stream with respect to time. These four scenarios are assumed to be sufficient to model uncertainty in inlet temperature of hot stream.

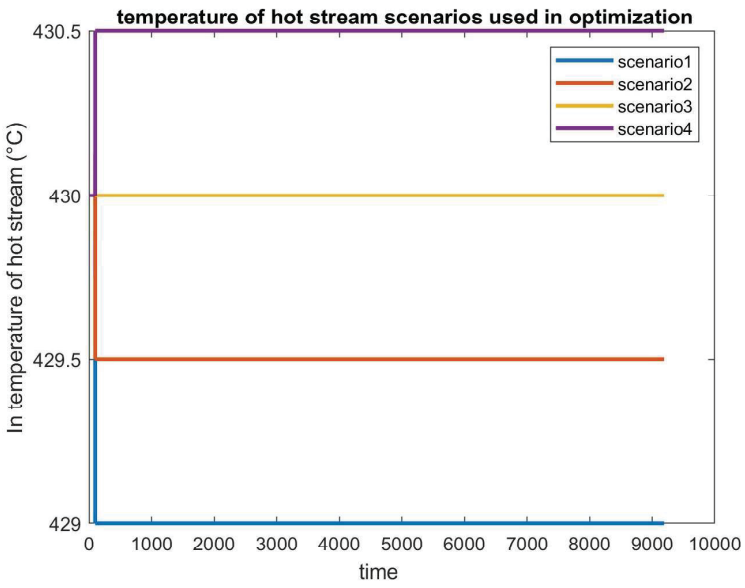

Figure 3.28: T_{H1}^{in} considering 4 scenariors used in optimization

Figure 3.29 gives the out temperature of mixed stream (controlled variable) $T_{C2,n,k}^{out}$ considering step change in setpoint and under the scenarios used in optimization. Figure 3.29 shows that for the considered scenarios, the controlled variable effectively tracks the setpoint using the average value optimal input.

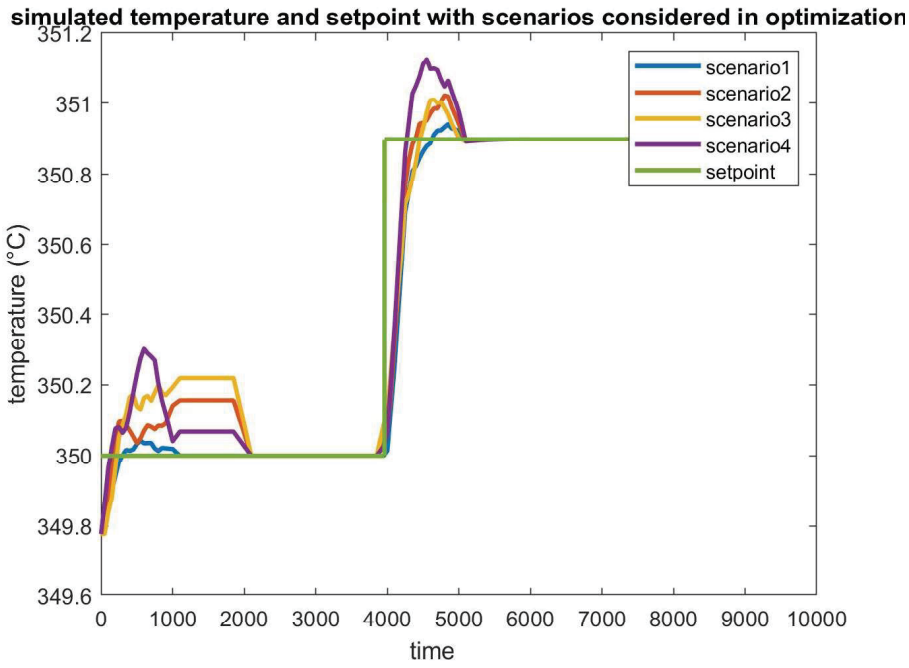

Figure 3.29: $T^{out}_{C2,n,k}$ considering 4 scenarios used in optimization

Figures 3.30, 3.31, and 3.32 show the optimal bypass fraction (manipulated variables) u_1, u_2, u_3, with a step change in the setpoint.

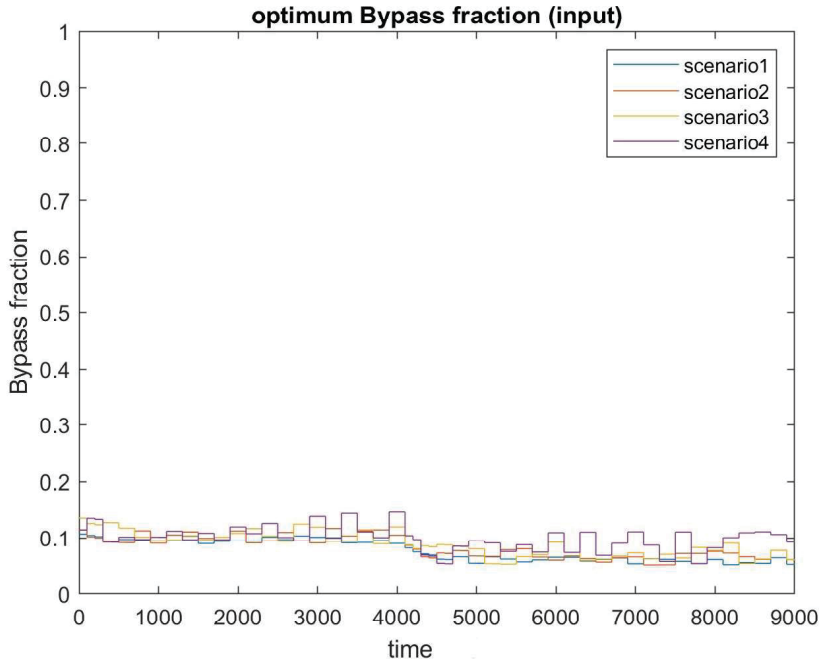

Figure 3.30: u_1 for four scenarios used in optimization

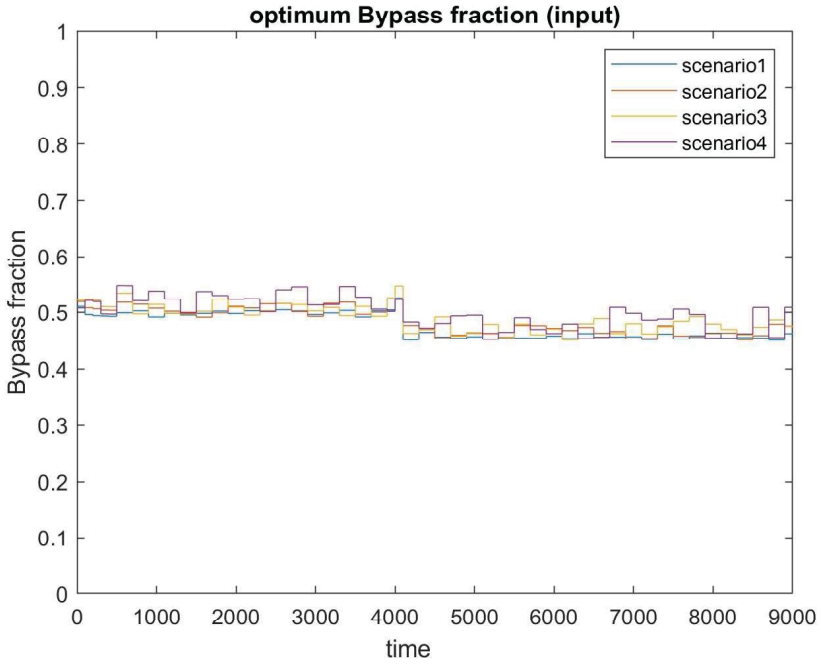

Figure 3.31: u_2 considering four random scenariors

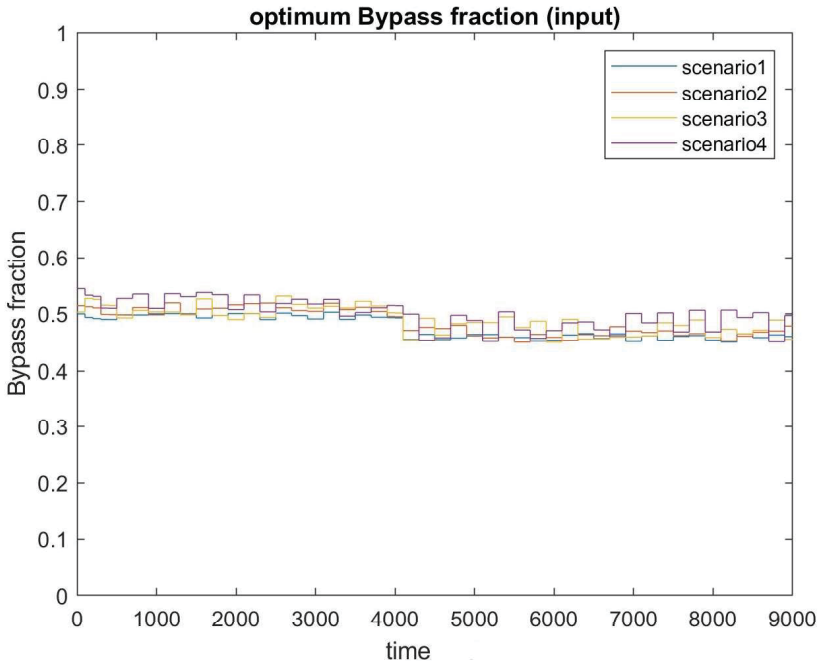

Figure 3.32: u_3 considering four scenarios used in optimization

To test the performance of the optimization, the average value of optimal input is given to the system. Four random scenarios of inlet temperature of hot stream are

considered. The controlled variable is simulated using average optimal input under the random scenarios of inlet temperature of hot stream.

For the network, a step change in setpoint is considered. The response of controlled variable is also generated under these random scenarios. The graph is given by Figure 3.34. It shows that proposed control method under uncertainty is effective as the controlled variable does not deviate significantly in comparison with that of using deterministic input. The response of controlled variable using deterministic input is given by Figure 3.35. The MSE between controlled variable and setpoint is also calulated for both uncertain optimization and deterministic optimizaion, and the values are given in Table 3.2. These values show that there is significant reduction in MSE using uncertain optimization. In Figure 3.34, the fluctuation of the controlled variable around the setpoint is expected as there is always a random disturbance in inlet temperature of hot stream as the random scenarios are considered.

Figure 3.33 gives the inlet temperature profiles of hot stream considered in random scenarios in step change in setpoint case.

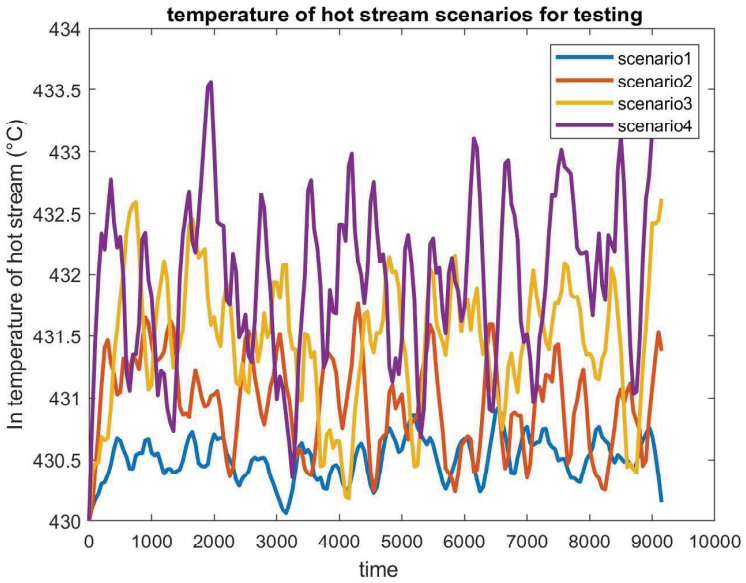

Figure 3.33: T_{H1}^{in} considering 4 random scenariors

Figure 3.34 gives the plot for out temperature of mixed stream (controlled variable) $T_{C2,n,k}^{out}$ considering step change in setpoint and under the four random scenarios,

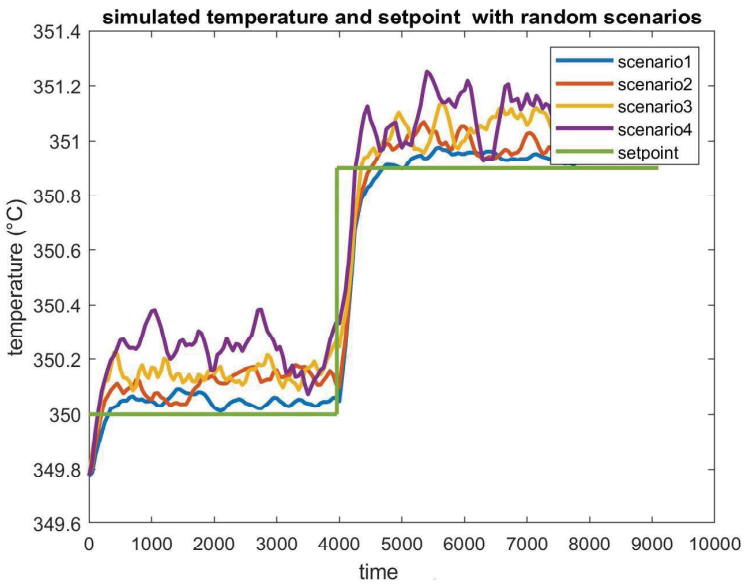

Figure 3.34: $T^{out}_{C2,n,k}$ considering 4 random scenariors

For the step change in setpoint, the controlled variable profiles are generated using deterministic inputs. The corresponding graph is given by Figure 3.35, which shows the controlled variable deviates from the setpoint as time passes if using deterministic inputs.

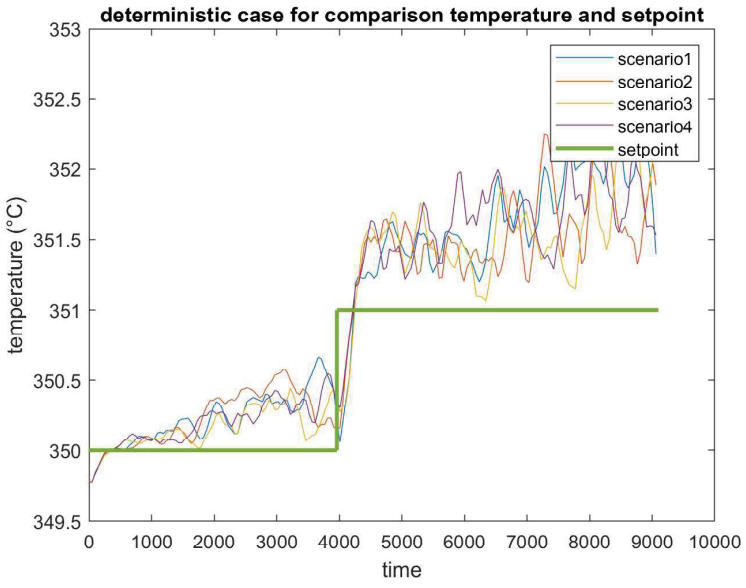

Figure 3.35: $T^{out}_{C2,n,k}$ using the deterministic input considering 4 scenariors

Objective function	8.44×10^6
MSE using uncertain input	9.50×10^5
MSE using deterministic input	5.82×10^7

Table 3.2: Results of uncertain MPC for HEN

3.5 Conclusion

In this work, the MPC of HEN is implemented considering disturbances in inlet temperature of hot stream. The uncertain OCP is intractable initially, and is made tractable first by discretizing heat exchanger model. Then, some of the constraints are approximated by scenario tree based approximation and rest of the constraints are modified by deriving their robust counterparts. Finally we arrive at solvable or tractable OCP with discrete model constraints.

Orthogonal collocation technique is used for discretization of the model. The tractable OCP is solved in receding horizon manner. At each sampling time, the decision varaiables i.e. affine rule coefficients are obtained for entire prediction horizon. Only the values of decision variables at $n = 1$ (first control interval) are used, and then we update the initial values of all states. Thus the initial values of all states are updated at each sampling instant. Using uncertain MPC, the MSE between controlled variable and setpoint is reduced by order of 1 from deterministic MPC.

Chapter 4

Integrated optimal cleaning and control problem

4.1 Introduction

Fouling is the accumulation or deposition of unwanted solid material on a surface. Fouling on heat exchanger surface offers extra resistance to heat transfer, and it increases the pressure drop, operational costs and the environmental impact on the process. Fouling is the most evident in the preheat train (PHT) of the crude distillation unit (CDU), which processes all the crude oil that comes into the refinery under extreme conditions, such as high temperature, varying range of composition and high amounts of contaminants.

Generally, periodical cleaning and control of the flowrate distribution in the HEN are used to mitigate the effects of fouling and restore the performance of the units. In the literature, the optimal cleaning schedule problem is formulated as MILP or MINLP problem, and the optimalm control problem is formulated as NLP problem. These two problems have been solved independently or sequentially. As in principle both problems affect each other, in the present work, these two problems are formulated and solved simultaneously. The objective function to be minimized here is the extra cost that is incurred because of fouling.
The decision variables are:

1. Binary variables which indicate whether a heat exchanger in HEN is being cleaned or not within a time period.

2. The mass flowrate distribution.

The constraints considered here are:

1. The heat transfer dynamics
2. Fouling resistance dynamics
3. Pressure drop model
4. Network constraints
5. Scheduling and operational constraints
6. Disjunctions

In this chapter, first, the deterministic problem is formulated. Later, the uncertainty in inlet temperature of cold stream is introduced, and uncertain optimization problem is formulated.

4.2 Heat exhanger model, fouling dynamics, and additional constraints

The heat exchanger considered here is a shell and tube type, which is a concentric double pipe (outer is shell, inner is tube). The shell-side fluid is hot stream, and tube-side fluid is cold stream. The cross-section of the heat exchanger is shown in Figure 4.1(a), and the temperatures used in modelling heat transfer and resistance dynamics is shown in Figure 4.1(b).

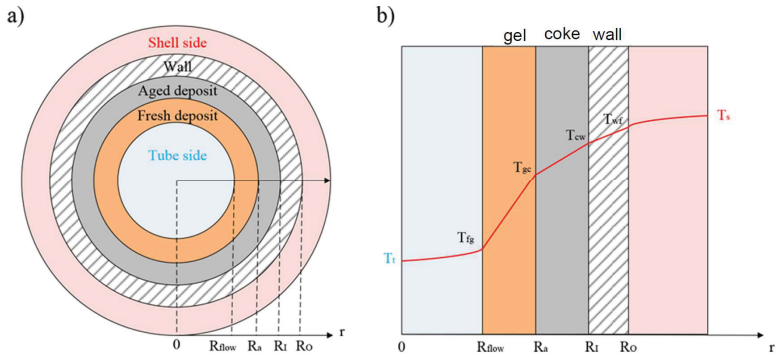

Figure 4.1: Multiple layer representation for the heat transfer between the shell-side fluid and the tube-side fluid [20]

Heat transfer dynamics

The following constraints are used to model the heat transfer dynamics. The model of heat exchanger considered here is axially lumped and radially distribured model. Counter-current flow is assumed.

$$m_t = F(1-u) \tag{4.1}$$

$$NTU = \frac{UA}{C_{P_t} m_t} \tag{4.2}$$

$$R_c = \frac{C_{P_t} m_t}{C_{P_s} m_s} \tag{4.3}$$

$$P = 2\Bigg\{1 + R_c + (1+R_c^2)^{0.5}\left[\frac{1+exp(-NTU(1+R_c^2)^{0.5})}{1-exp(-NTU(1+R_c^2)^{0.5})}\right]\Bigg\}^{-1} \tag{4.4}$$

$$Q = P(C_{P_t} m_t)(T_s^{in} - T_t^{in}) \tag{4.5}$$

$$T_t^{out} = T_t^{in} + P(T_s^{in} - T_t^{in}) \tag{4.6}$$

$$T_s^{out} = T_s^{in} - PR_c(T_s^{in} - T_t^{in}) \tag{4.7}$$

$$\tag{4.8}$$

Fouling resistance dynamics

The following constraints give fouling resistance and mass fraction of fresh gel dynamics.

$$T_{fg} = T_t + \frac{U}{h_t}\left[\frac{R_o}{R_{flow}}\right] \tag{4.9}$$

$$T_f = T_t + 0.55(T_{fg} - T_t) \tag{4.10}$$

$$T_{gc} = T_{fg} + \frac{U}{\lambda_g / R_o} \ln\big(\frac{R_I - \delta_c}{R_{flow}}\big)(T_s - T_t) \tag{4.11}$$

$$\frac{dR_f}{dt} = \alpha Pr^{-0.33} Re^{-0.66} exp\left[-\frac{E_f}{RT_f}\right] - \gamma\tau_w \tag{4.12}$$

$$\frac{dx_g}{dt} = -k_a^0 exp\left[-\frac{E_a}{RT_{gc}}\right] x_g \tag{4.13}$$

$$x_g = \frac{[2R_I - (\delta_T + \delta_c)]\delta_g \rho_g}{[2R_I - (\delta_T + \delta_c)]\delta_g \rho_g + [2R_I - \delta_c]\delta_c \rho_c} \tag{4.14}$$

$$R_{f,c} = \frac{R_o}{\lambda_c} \ln\left[\frac{R_I}{R_I - \delta_c}\right] \tag{4.15}$$

$$R_{f,g} = \frac{R_o}{\lambda_g} \ln\left[\frac{R_I - \delta_C}{R_I - \delta_c - \delta_g}\right] \tag{4.16}$$

$$\frac{1}{U} = \frac{1}{U_c} + R_f \tag{4.17}$$

where, U_c is the Overall heat transfer coefficient when there is no fouling. Eq. 4.12 is Ebert Panchal model [20]. The Ebert Panchal model is used to describe the fouling deposition rate in terms of rate of change in the thermal fouling resistance. The first term of the model gives deposition as a product of chemical reaction interms of activation energy. The second term indicates that the rate of deposit removal is proportional to wall shear stress. To solve the optimization problem, the differential equations given by 4.12 and 4.13 are discretized using finite difference method. The corresponding algebraic equations are given by,

$$\frac{R_f(t) - R_f(t-1)}{Time(t) - Time(t-1)} = \alpha Pr^{-0.33} Re^{-0.66} exp\Big[- \frac{E_f}{RT_f(t-1)}\Big] - \gamma\tau_w \qquad t = 2, 3, ..., length(Time) \tag{4.18}$$

$$\frac{x_g(t) - x_g(t-1)}{Time(t) - Time(t-1)} = -k_a^0 exp\Big[- \frac{E_a}{RT_{gc}(t-1)}\Big] x_g(t-1) \qquad t = 2, 3, ..., length(Time) \tag{4.19}$$

Pressure drop model:

The pressure drop constraint is needed to make sure that the branch pairs have same pressure drop. This ensures a safe industrial operation.

$$\Delta P = \frac{G_t^2}{2\rho_t}\Big[\frac{1.5}{N_p} + \frac{fL}{2R_{flow}} + 4\Big] N_p \tag{4.20}$$

Network constraints:

These constraints represent mass balance and energy balance.

$$\sum_{i \in Nodes | (i,j,k) \in Arcs} (m_{t,i,j,k} - m_{t,j,i,k}) = 0 \qquad \forall t \in Time, j \in \{Mx \cup Sp \cup HEX\}, k \in Fluids \tag{4.21}$$

$$\sum_{i \in Nodes | (i,j,k) \in Arcs} (C_{p_k} T_{t,i,j,k} m_{t,i,j,k} - C_{p_k} T_{t,j,i,k} m_{t,j,i,k}) = 0 \quad \forall t \in Time, j \in \{Mx \cup Sp \cup HEX\}, k \in Fluids \tag{4.22}$$

Scheduling and operational constraints:

These constraints represent that consecutive cleaning that should not be done. maximum number of simultaneous cleaning actions, maximum number of cleaning per exchanger, minimum number of operating exchangers, minimum CIT so that the furnace can be ignited, maximum furnace duty, and same pressure drop for the branch pairs

$$y_{t+1,i} \leq 1 - y_{t,i}, \quad \forall t \in Time \backslash \{n_t\}, i \in HEX \tag{4.23}$$

$$\sum_{i \in HEX} y_{t,i} \leq N_T^{max}, \quad \forall t \in Time \tag{4.24}$$

$$\sum_{t \in Time} y_{t,i} \leq N_U^{max}, \quad \forall i \in HEX \tag{4.25}$$

$$\sum_{i \in HEX_{sub} \subseteq HEX} (1 - y_{t,i}) \geq N_{Op}^{min}, \quad \forall t \in Time \tag{4.26}$$

The following constraints represent operational or safety constraints,

$$CIT_t = T_{t,i,j,k} \geq CIT^{min}, \quad \forall t \in Time, (i,j,k) \in Arcs | (i,j,k) = "tofurnace" \tag{4.27}$$

$$Q_{f,t} = FC_{p_k}(COT - T_{t,i,j,k}) \leq Q_f^{max}, \quad \forall t \in Time, (i,j,k) \in Arcs | (i,j,k) = "tofurnace" \tag{4.28}$$

$$\sum_{i \in Branch_{1,b} \subseteq HEX} \Delta P_{t,i} = \sum_{i \in Branch_{2,b} \subseteq HEX} \Delta P_{t,i}, \quad \forall t \in Time, b \in Branchpairs \tag{4.29}$$

Disjunctions:

These constraints represent that flowrates, NTU, and resistance and massfraction of fresh gel are zero during the cleaning.

$$0 \leq m_{t,Sp\_k,HE,k,i} \leq M(1 - y_{t,i}), \quad \forall t \in Time, i \in HEX, k \in \{tubeside, shellside\} \tag{4.30}$$

$$0 \leq s_{t,i,l} \leq My_{t,i}, \quad \forall t \in Time, i \in HEX, l \in \{NTU, R_{f,g}, x_g\} \tag{4.31}$$

$$0 \leq NTU_{t,i} \leq M(1 - y_{t,i}), \qquad \forall t \in Time, i \in HEX \tag{4.32}$$

$$0 \leq R_{f,g_{t,i}} \leq (1 - y_{t,i}), \qquad \forall t \in Time, i \in HEX \tag{4.33}$$

$$y_{t,i} \leq x_{g_{t,i}} \leq 1, \qquad \forall t \in Time, i \in HEX \tag{4.34}$$

4.3 Objective function

The objective function is the additional cost compared to the cost of operating the HEN for the entire horizon under cleaned conditions. The objective function is given as,

$$\begin{aligned} F(m, y) = P_{kg} \int_0^{t_f} (m^{clean}_{production} - m_{production,t})\, dt \\ + P_{fuel} \int_0^{t_f} \frac{(Q_f - Q_f^{clean})}{\eta}\, dt \\ + P_{CO_2} m_{CO_2} \int_0^{t_f} \frac{(Q_f - Q_f^{clean})}{\eta}\, dt \\ + \sum_{i \in HEX} \sum_{t \in TIME} P_{cl} y_{t,i} \end{aligned} \tag{4.35}$$

4.4 Results

Single HE

The optimization problem is solved in GAMS. As an initial step, a single heat exchanger is considered, and the time span of one year is divided into 13 intervals. All the temperatures, bypass fraction, cleaning decision variable are assumed to be constant within each interval. The NLP solver used is IPOPT and MILP solver used is CPLEX. The patterns in the graphs of input and furnace duty represent cleaning actions. After each cleaning all the conditions are assumed to be ideal, and hence the variables take values in repeated patterns. The optimization problem formulated

is a MINLP problem. The bypass fraction decision variables are continuous and the cleaning scheduling variables are binary decision variables. The MINLP problem is solved in several steps. First, we fix the values of binary decision variables, and obtain the optimal values of bypass fraction. Next, these bypass fraction values are given as initial values to the solver, and the entire optimization problem is solved. Both binary cleaning scheduling variables and bypass fraction optimal values are obtained. The optimal cleaning schedule is given by Figure 4.2. The green color indicates that the cleaning action is performed in that interval.

	Period 1	Period 2	Period 3	Period 4	Period 5	Period 6	Period 7	Period 8	Period 9	Period 10	Period 11	Period 12
HE 1												

Figure 4.2: Optimal cleaning schedule for single HE

The optimal bypass fraction is given by Figure 4.3,

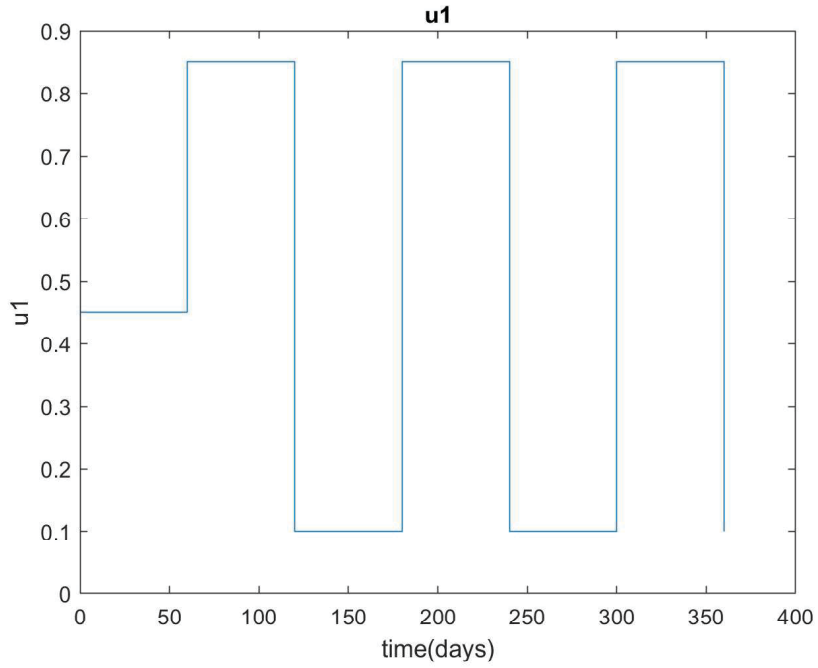

Figure 4.3: The optimal bypass fraction

The engergy consumed in furnace (Q_f) is given by Figure 4.4. The figure also shows that minimum furnace duty required to meet the target out temperatures of

cold stream. This minimum furnace duty is seen in the ideal conditions.The value of objective function is 18.88×10^5\$.

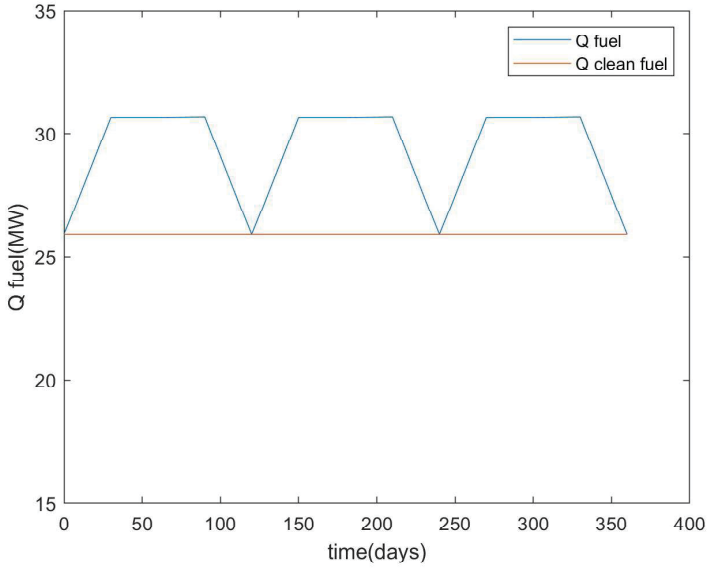

Figure 4.4: Furnace duty

The mixed stream temperature (CIT) is given by Figure 4.5 ,

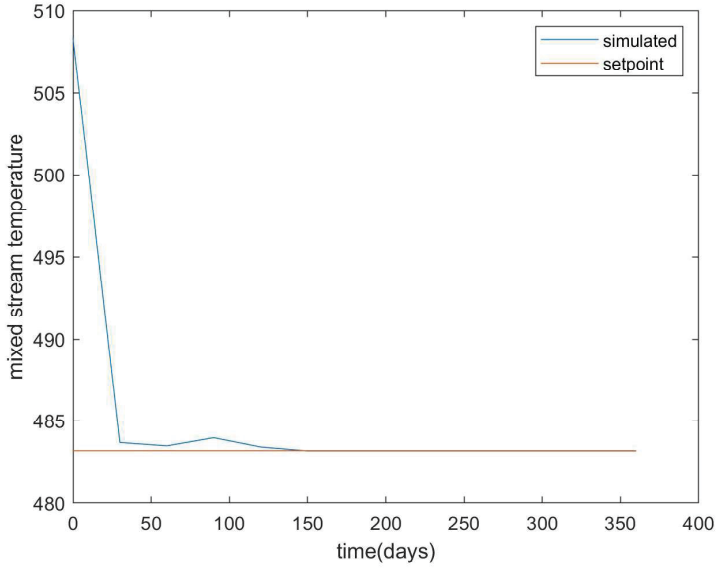

Figure 4.5: Mixed stream temperature

2 Parallel HE

For the second case study, two heat exchangers in parallel are considered. The decision variables are bypass fraction of both hot stream and cold stream, and cleaning schedule. For the network, the heat exchanger model is updated to include the connections between the exchangers. The optimal value of objective function is 20.85. $\times 10^5$\$. The optimal cleaning schedule is given by Figure 4.6,

	Period 1	Period 2	Period 3	Period 4	Period 5	Period 6	Period 7	Period 8	Period 9	Period 10	Period 11	Period 12
HE 1							■					
HE 2				■						■		

Figure 4.6: optimal cleaning schedule for 2HE

The optimal bypass fraction of cold stream through HE 2 is given by Figure 4.7,

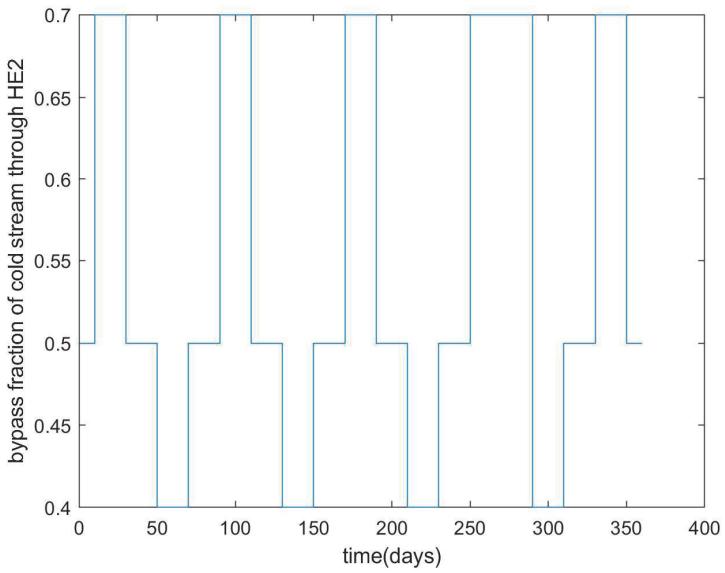

Figure 4.7: The optimal bypass fraction of cold stream through HE 2

The optimal bypass fraction of hot stream through HE 2 is given by Figure 4.8,

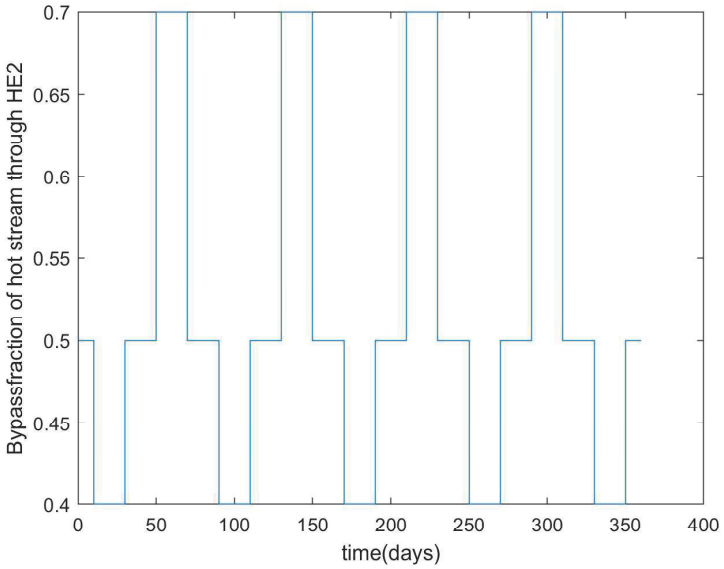

Figure 4.8: The optimal bypass fraction of hot stream through HE 2

The energy consumed in furnace (Q_f) is given by Figure 4.9,

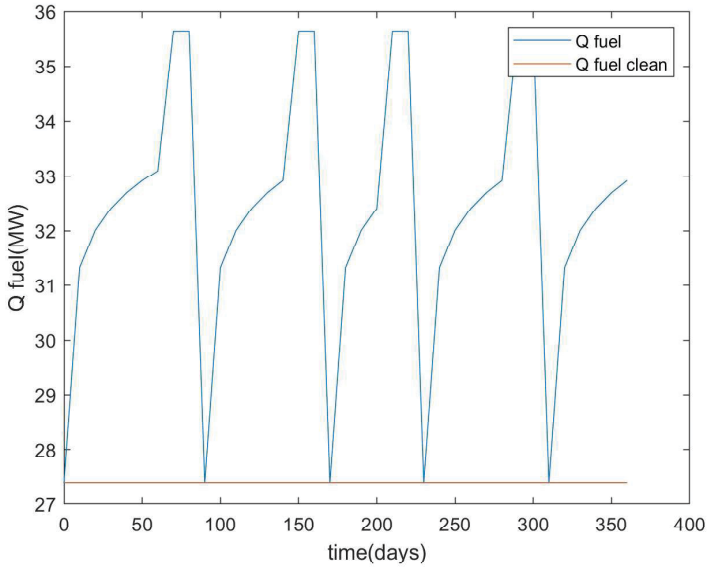

Figure 4.9: Furnace duty

The mixed stream temperature (CIT) is given by Figure 4.10 ,

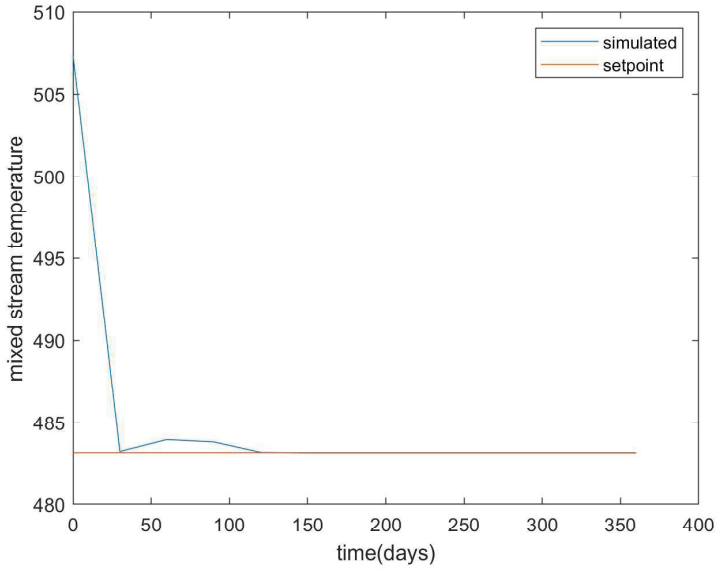

Figure 4.10: mixed stream temperature

4.5 Integrated problem under uncertainty

So far, we have not considered disturbances in inlet temperatures of streams. However, it is common that the inlet temperatures of cold stream (crude oil) is uncertain in the preheat train (PHT) of the crude distillation unit (CDU). So, from now on, we assume that inlet temperatures of cold stream are uncertain, and then formulate and solve the problem of Integration of Optimal cleaning scheduling and control of HENs undergoing fouling. Let the uncertainty in inlet temperature of cold stream be denoted by ζ. The overall uncertain optimization model shows the variables that depend on uncertainty, and it is given as,

$$
\begin{aligned}
(OCP) \qquad \min_{u(\zeta),y} F(m,y,\zeta) = P_{kg} \int_0^{t_f} (m^{clean}_{production} - m_{production,t}(\zeta))\, dt \\
+P_{fuel} \int_0^{t_f} \frac{(Q_f(\zeta) - Q_f^{clean})}{\eta}\, dt \\
+P_{CO_2} m_{CO_2} \int_0^{t_f} \frac{(Q_f(\zeta) - Q_f^{clean})}{\eta}\, dt \\
+ \sum_{i \in HEX} \sum_{t \in TIME} P_{cl} y_{t,i}
\end{aligned}
\tag{4.36}
$$

$$\text{s.t.} \quad m_t(\zeta) = F(1 - u(\zeta)) \tag{4.37}$$

$$NTU(\zeta) = \frac{UA}{C_{P_t} m_t(\zeta)} \tag{4.38}$$

$$R_c(\zeta) = \frac{C_{P_t} m_t(\zeta)}{C_{P_s} m_s} \tag{4.39}$$

$$P(\zeta) = 2\Bigg\{1 + R_c(\zeta) + (1 + R_c^2(\zeta))^{0.5} \left[\frac{1 + exp(-NTU(\zeta)(1 + R_c^2(\zeta))^{0.5})}{1 - exp(-NTU(\zeta)(1 + R_c^2(\zeta))^{0.5})}\right]\Bigg\}^{-1} \tag{4.40}$$

$$Q(\zeta) = P(\zeta)(C_{P_t} m_t(\zeta))(T_s^{in} - T_t^{in}(\zeta)) \tag{4.41}$$

$$T_t^{out}(\zeta) = T_t^{in}(\zeta) + P(\zeta)(T_s^{in}(\zeta) - T_t^{in}) \tag{4.42}$$

$$T_s^{out}(\zeta) = T_s^{in} - P(\zeta) R_c(\zeta)(T_s^{in} - T_t^{in}(\zeta)) \tag{4.43}$$

$$T_{fg}(\zeta) = T_t(\zeta) + \frac{U}{h_t}\left[\frac{R_o}{R_{flow}}\right] \tag{4.44}$$

$$T_f(\zeta) = T_t(\zeta) + 0.55(T_{fg}(\zeta) - T_t(\zeta)) \tag{4.45}$$

$$T_{gc}(\zeta) = T_{fg}(\zeta) + \frac{U}{\lambda_g / R_o} \ln\big(\frac{R_I - \delta_c}{R_{flow}}\big)(T_s(\zeta) - T_t(\zeta)) \tag{4.46}$$

$$\frac{R_f(t,\zeta) - R_f(t-1,\zeta)}{Time(t) - Time(t-1)} = \alpha Pr^{-0.33} Re^{-0.66} exp\left[-\frac{E_f}{RT_f(t-1,\zeta)}\right] - \gamma\tau_w \qquad t = 2, 3, ..., length(Time) \tag{4.47}$$

$$\frac{x_g(t,\zeta) - x_g(t-1,\zeta)}{Time(t) - Time(t-1)} = -k_a^0 exp\left[-\frac{E_a}{RT_{gc}(t-1,\zeta)}\right] x_g(t-1,\zeta) \qquad t = 2, 3, ..., length(Time) \tag{4.48}$$

$$x_g(\zeta) = \frac{[2R_I - (\delta_T(\zeta) + \delta_c(\zeta))]\delta_g \rho_g}{[2R_I - (\delta_T(\zeta) + \delta_c(\zeta))]\delta_g \rho_g + [2R_I - \delta_c(\zeta)]\delta_c \rho_c} \tag{4.49}$$

$$R_{f,c}(\zeta) = \frac{R_o}{\lambda_c} \ln\left[\frac{R_I}{R_I - \delta_c(\zeta)}\right] \tag{4.50}$$

$$R_{f,g}(\zeta) = \frac{R_o}{\lambda_g} \ln\left[\frac{R_I - \delta_C(\zeta)}{R_I - \delta_c(\zeta) - \delta_g}\right] \tag{4.51}$$

$$\frac{1}{U(\zeta)} = \frac{1}{U_c} + R_f(\zeta) \tag{4.52}$$

$$\Delta P = \frac{G_t^2}{2\rho_t}\left[\frac{1.5}{N_p} + \frac{fL}{2R_{flow}} + 4\right]N_p \tag{4.53}$$

$$\sum_{i \in Nodes|(i,j,k) \in Arcs} (m_{t,i,j,k}(\zeta) - m_{t,j,i,k}(\zeta)) = 0$$
$$\forall t \in Time, j \in \{Mx \cup Sp \cup HEX\}, k \in Fluids \tag{4.54}$$

$$\sum_{i \in Nodes|(i,j,k) \in Arcs} (C_{p_k} T_{t,i,j,k}(\zeta) m_{t,i,j,k}(\zeta) - C_{p_k} T_{t,j,i,k}(\zeta) m_{t,j,i,k}(\zeta)) = 0$$
$$\forall t \in Time, j \in \{Mx \cup Sp \cup HEX\}, k \in Fluids \tag{4.55}$$

$$y_{t+1,i} \leq 1 - y_{t,i}, \quad \forall t \in Time \backslash \{n_t\}, i \in HEX \tag{4.56}$$

$$\sum_{i \in HEX} y_{t,i} \leq N_T^{max}, \quad \forall t \in Time \tag{4.57}$$

$$\sum_{t \in Time} y_{t,i} \leq N_U^{max}, \quad \forall i \in HEX \tag{4.58}$$

$$\sum_{i \in HEX_{sub} \subseteq HEX} (1 - y_{t,i}) \geq N_{Op}^{min}, \quad \forall t \in Time \tag{4.59}$$

$$CIT_t(\zeta) = T_{t,i,j,k}(\zeta) \geq CIT^{min}, \quad \forall t \in Time, (i,j,k) = "to furnace" \tag{4.60}$$

$$Q_{f,t}(\zeta) = FC_{p_k}(COT - T_{t,i,j,k}(\zeta)) \leq Q_f^{max}, \quad \forall t \in Time, (i,j,k) = "to furnace" \tag{4.61}$$

$$\sum_{i \in Branch_{1,b} \subseteq HEX} \Delta P_{t,i} = \sum_{i \in Branch_{2,b} \subseteq HEX} \Delta P_{t,i}, \quad \forall t \in Time, b \in Branchpairs \tag{4.62}$$

$$0 \leq m_{t,Sp\_k,HE,k,i}(\zeta) \leq M(1 - y_{t,i}), \quad \forall t \in Time, i \in HEX, k \in \{tubeside, shellside\} \tag{4.63}$$

$$0 \leq s_{t,i,l} \leq M y_{t,i}, \quad \forall t \in Time, i \in HEX, l \in \{NTU, R_{f,g}, x_g\} \tag{4.64}$$

$$0 \leq NTU_{t,i} \leq M(1 - y_{t,i}), \qquad \forall t \in Time, i \in HEX \tag{4.65}$$

$$0 \leq R_{f,g_{t,i}} \leq M(1 - y_{t,i}), \qquad \forall t \in Time, i \in HEX \tag{4.66}$$

$$y_{t,i} \leq x_{g_{t,i}}(\zeta) \leq 1, \qquad \forall t \in Time, i \in HEX \tag{4.67}$$

4.5.1 Tractable problem formulation

We consider that the primitive uncerainty belongs to a compact set i.e. $\zeta \in [0, 1]$. The inlet temperature of cold stream is given as, $T_t^{in} = A\zeta + B(1 - \zeta)$. Here, A and B are upper and lower bounds of T_t^{in}. So, as ζ is continuous variable, the above uncertain optimization problem is not tractable.

To convert it to a tractable problem, we assume that the bypass fraction is affine function of unceratinty i.e. $u(\zeta, t, i) = u^0 + u^1\zeta(t, i), i \in HEX, t \in Time$. In the integrated problem, the time of one year is divided into N intervals, indexed by t, and denoted by set $Time$.

The equality constraints in the above uncertain optimization problem are functions of primitive uncertainty, so in the tractable problem formulation, they are modelled using scenarios of possible primitive uncertainty. The possible scenarios of primitive uncertainty are given by the set S and indexed by s.

Let any inequality constraint in the above uncertain optimization problem be denoted by $G(\zeta, y, u(\zeta), x(\zeta)) \leq 0$. Here, $y, u(\zeta)$, and $x(\zeta)$ denote scheduling variable, input or manipulated variable, and state variable respectively. Each constraint in the original set of inequality constraints under uncertainty, $G(\zeta, y, u(\zeta), x(\zeta)) \leq 0$, is formulated by first linearizing it with respect to uncertainty using first-order Taylor series, followed by applying the duality technique to obtain the finite tractable counterpart. The formulation is given as,

$$G \simeq G^* + (\zeta - \zeta^*)G_{\zeta^*} \tag{4.68}$$

Here, G_{ζ^*} is implicit derivative of G at ζ^*, and $G^* = G(\zeta^*, y, u(\zeta^*), x(\zeta^*))$.

Robust counterpart of $G^* + (\zeta - \zeta^*)G_{\zeta^*} \geq 0$ is given as,

$$[-G^* + \zeta^* G_{\zeta^*}] - \min_{\zeta} \zeta(G_{\zeta^*}) \leq 0. \tag{4.69a}$$

$$\implies [-G^* + \zeta^* G_{\zeta^*}] + \max_{\zeta}(-\zeta(G_{\zeta^*})) \leq 0. \tag{4.69b}$$

By including the initial assumption that uncertainty belongs to a compact set i.e. $A\zeta \leq b$, we apply duality as follows,

$$[-G^* + \zeta^* G_{\zeta^*}] + \min_{\lambda} b^T\lambda \geq 0 \tag{4.70a}$$

$$s.t. \quad A^T\lambda = -G_{\zeta^*} \tag{4.70b}$$

$$\lambda \geq 0 \tag{4.70c}$$

Drop the min operator,

$$[-G^* + \zeta^* G_{\zeta^*}] + b^T\lambda \geq 0 \tag{4.71a}$$

$$s.t. \quad A^T\lambda = -G_{\zeta^*} \tag{4.71b}$$

$$\lambda \geq 0 \tag{4.71c}$$

For example, consider the constraint represented by the Eq.4.60, we derive the formulation as follows,

$$CIT(\zeta^*) + (\zeta - \zeta^*)\Delta_\zeta CIT(\zeta^*) - CIT^{min} \geq 0 \tag{4.72a}$$

$$[-CIT(\zeta^*) + \zeta^*\Delta_\zeta CIT(\zeta^*)] - \min_\zeta \zeta(\Delta_\zeta CIT(\zeta^*)) + CIT^{min} \leq 0 \tag{4.72b}$$

$$\implies [-CIT(\zeta^*) + \zeta^*\Delta_\zeta CIT(\zeta^*) + CIT^{min}] + \max_\zeta \zeta(-\Delta_\zeta CIT(\zeta^*)) \leq 0 \tag{4.72c}$$

$$\implies [-CIT(\zeta^*) + \zeta^*\Delta_\zeta CIT(\zeta^*) + CIT^{min}] + \min_\lambda b^T\lambda \geq 0 \tag{4.72d}$$

$$s.t. \quad A^T\lambda = -\Delta_\zeta CIT(\zeta^*) \tag{4.72e}$$

$$\lambda \geq 0 \tag{4.72f}$$

$$\implies [-CIT(\zeta^*) + \zeta^*\Delta_\zeta CIT(\zeta^*) + CIT^{min}] + b^T\lambda \geq 0 \tag{4.72g}$$

$$s.t. \quad A^T\lambda = -\Delta_\zeta CIT(\zeta^*) \tag{4.72h}$$

$$\lambda \geq 0 \tag{4.72i}$$

Now consider $\Delta_\zeta CIT(\zeta^*)$. As an example, we show how to simplify this for a single HE as follows,

$$CIT = (1-u)T_t^{out} + uT_t^{in}, \quad u = u^0 + u^1\zeta. \tag{4.73a}$$

$$\implies \Delta_\zeta CIT(\zeta^*) = (1 - u^0 - u^1(\zeta^*))T_{t\zeta^*}^{out} + (-u^1)T_t^{out} + (A-B)((1-u^0-u^1(\zeta^*)) + T_t^{in}(-u^1) \tag{4.73b}$$

The objective function is evaluated at a nominal uncertainty denoted by (ζ^*).

The overall optimization problem formulation is given as,

$$
\begin{aligned}
(OCP) \qquad \min_{\mathbf{u},y} F(\mathbf{u},y) = P_{kg} \sum_{0}^{t_f} (m^{clean}_{production} - m_{production,t}(\zeta^*)) \\
+P_{fuel} \sum_{0}^{t_f} \frac{(Q_f(\zeta^*) - Q_f^{clean})}{\eta} \\
+P_{CO_2} m_{CO_2} \sum_{0}^{t_f} \frac{(Q_f(\zeta^*) - Q_f^{clean})}{\eta} \\
+ \sum_{i \in HEX} \sum_{t \in TIME} P_{cl} y_{t,i}
\end{aligned}
\tag{4.74}
$$

$$
\text{s.t.} \quad m(s,t,i,k) = F(k)(1 - u(s,t,i,k)) \qquad s \in S, i \in HEX, t \in Time, k \in Fluids \tag{4.75}
$$

$$
m\_t(s,t,i) = m(s,t,i,cold) \qquad s \in S, i \in HEX, t \in Time \tag{4.76}
$$

$$
m\_s(s,t,i) = m(s,t,i,hot) \qquad s \in S, i \in HEX, t \in Time \tag{4.77}
$$

$$
NTU(s,t,i) = \frac{U(s,t,i)A}{C_{P_t} m\_t(s,t,i)} \qquad s \in S, i \in HEX, t \in Time \tag{4.78}
$$

$$
R_c(s,t,i) = \frac{C_{P_t} m\_t(s,t,i)}{C_{P_s} m\_s(s,t,i)} \qquad s \in S, i \in HEX, t \in Time \tag{4.79}
$$

$$
P(s,t,i) = 2 \left\{ 1 + R_c(s,t,i) + (1 + R_c^2(s,t,i))^{0.5} \left[\frac{1 + exp(-NTU(s,t,i)(1 + R_c^2(s,t,i))^{0.5})}{1 - exp(-NTU(s,t,i)(1 + R_c^2(s,t,i))^{0.5})} \right] \right\}^{-1} \tag{4.80}
$$

$$
Q(s,t,i) = P(s,t,i)(C_{P_t} m\_t(s,t,i))(T_s^{in} - T_t^{in}(s)) \qquad s \in S, i \in HEX, t \in Time \tag{4.81}
$$

$$
T_t^{out}(s,t,i) = T_t^{in}(s) + P(s,t,i)(T_s^{in} - T_t^{in}(s)) \qquad s \in S, i \in HEX, t \in Time \tag{4.82}
$$

$$
T_s^{out}(s,t,i) = T_s^{in} - P(s,t,i) R_c(s,t,i)(T_s^{in} - T_t^{in}(s)) \qquad s \in S, i \in HEX, t \in Time \tag{4.83}
$$

$$
T_{fg}(s,t,i) = T_t(s,t,i) + \frac{U}{h_t} \left[\frac{R_o}{R_{flow}} \right] \qquad s \in S, i \in HEX, t \in Time \tag{4.84}
$$

$$
T_f(s,t,i) = T_t(s,t,i) + 0.55(T_{fg}(s,t,i) - T_t(s,t,i)) \qquad s \in S, i \in HEX, t \in Time \tag{4.85}
$$

$$T_{gc}(s,t,i) = T_{fg}(s,t,i) + \frac{U}{\lambda_g/R_o}\ln\big(\frac{R_I-\delta_c}{R_{flow}}\big)(T_s(s,t,i) - T_t(s,t,i)) \qquad s \in S, i \in HEX, t \in Time \tag{4.86}$$

$$\frac{R_f(s,t,i) - R_f(s,t-1,i)}{Time(t) - Time(t-1)} = \alpha Pr^{-0.33} Re^{-0.66} exp\bigg[-\frac{E_f}{RT_f(s,t-1,i)}\bigg] - \gamma\tau_w \qquad s \in S, i \in HEX, t \in Time \tag{4.87}$$

$$\frac{x_g(s,t,i) - x_g((s,t-1,i)}{Time(t) - Time(t-1)} = -k_a^0 exp\bigg[-\frac{E_a}{RT_{gc}((s,t-1,i)}\bigg] x_g((s,t-1,i) \qquad s \in S, i \in HEX, t \in Time \tag{4.88}$$

$$x_g(s,t,i) = \frac{[2R_I - (\delta_T(s,t,i) + \delta_c(s,t,i))]\delta_g\rho_g}{[2R_I - (\delta_T(s,t,i) + \delta_c(s,t,i))]\delta_g\rho_g + [2R_I - \delta_c(s,t,i)]\delta_c\rho_c} \tag{4.89}$$

$$R_{f,c}(s,t,i) = \frac{R_o}{\lambda_c}\ln\bigg[\frac{R_I}{R_I - \delta_c(s,t,i)}\bigg] \qquad s \in S, i \in HEX, t \in Time \tag{4.90}$$

$$R_{f,g}(s,t,i) = \frac{R_o}{\lambda_g}\ln\bigg[\frac{R_I - \delta_C(s,t,i)}{R_I - \delta_c(s,t,i) - \delta_g}\bigg] \qquad s \in S, i \in HEX, t \in Time \tag{4.91}$$

$$\frac{1}{U(s,t,i)} = \frac{1}{U_c} + R_f(s,t,i) \qquad s \in S, i \in HEX, t \in Time \tag{4.92}$$

$$\Delta P = \frac{G_t^2}{2\rho_t}\bigg[\frac{1.5}{N_p} + \frac{fL}{2R_{flow}} + 4\bigg]N_p \tag{4.93}$$

$$\sum_{i \in Nodes | (i,j,k) \in Arcs} (m_{t,i,j,k}(s) - m_{t,j,i,k}(s)) = 0 \qquad \forall t \in Time, j \in \{Mx \cup Sp \cup HEX\}, k \in Fluids, s \in S. \tag{4.94}$$

$$\sum_{i \in Nodes | (i,j,k) \in Arcs} (C_{p_k} T_{t,i,j,k}(\zeta) m_{t,i,j,k}(\zeta) - C_{p_k} T_{t,j,i,k}(\zeta) m_{t,j,i,k}(\zeta)) = 0 \qquad \forall t \in Time, j \in \{Mx \cup Sp \cup HEX\}, k \in Fluids, s \in S \tag{4.95}$$

$$y_{t+1,i} \leq 1 - y_{t,i}, \quad \forall t \in Time \backslash \{n_t\}, i \in HEX \tag{4.96}$$

$$\sum_{i \in HEX} y_{t,i} \leq N_T^{max}, \quad \forall t \in Time \tag{4.97}$$

$$\sum_{t \in Time} y_{t,i} \leq N_U^{max}, \quad \forall i \in HEX \tag{4.98}$$

$$\sum_{i \in HEX_{sub} \subseteq HEX} (1 - y_{t,i}) \geq N_{Op}^{min}, \quad \forall t \in Time \tag{4.99}$$

$$[-CIT(\zeta^*) + \zeta^* \Delta_\zeta CIT(\zeta^*) + CIT^{min}] + b^T \lambda \geq 0 \tag{4.100a}$$

$$s.t. \quad A^T \lambda = -\Delta_\zeta CIT(\zeta^*) \tag{4.100b}$$

$$\lambda \geq 0 \tag{4.100c}$$

$$[-CIT(\zeta^*) + \zeta^* \Delta_\zeta CIT(\zeta^*) + CIT^{min}] + b^T \lambda_{CIT} \geq 0 \tag{4.101a}$$

$$s.t. \quad A^T \lambda_{CIT} = -\Delta_\zeta CIT(\zeta^*) \tag{4.101b}$$

$$\lambda_{CIT} \geq 0 \tag{4.101c}$$

$$[Q_{f,t}(\zeta^*) + \zeta^* \Delta_\zeta (-Q_{f,t}(\zeta^*)) + (-Q_f^{max})] + b^T \lambda_{Q_f} \geq 0 \tag{4.102a}$$

$$s.t. \quad A^T \lambda_{Q_f} = \Delta_\zeta Q_{f,t}(\zeta^*) \tag{4.102b}$$

$$\lambda_{Q_f} \geq 0 \tag{4.102c}$$

$$[m_{t,Sp\_k,HE,k,i}(\zeta^*) + \zeta^* \Delta_\zeta (-m_{t,Sp\_k,HE,k,i}(\zeta^*)) + (-M(1 - y_{t,i}))] + b^T \lambda_m \geq 0 \tag{4.103a}$$

$$s.t. \quad A^T \lambda_m = \Delta_\zeta (-m_{t,Sp\_k,HE,k,i}(\zeta^*)) \tag{4.103b}$$

$$\lambda_m \geq 0 \tag{4.103c}$$

$$[NTU_{t,i}(\zeta^*) + \zeta^* \Delta_\zeta(-NTU_{t,i}(\zeta^*)) + (-M(1-y_{t,i}))] + b^T \lambda_{NTU} \geq 0 \tag{4.104a}$$

$$s.t. \quad A^T \lambda_{NTU} = \Delta_\zeta(-NTU_{t,i}(\zeta^*)) \tag{4.104b}$$

$$\lambda_{NTU} \geq 0 \tag{4.104c}$$

$$[R_{f,g_{t,i}}(\zeta^*) + \zeta^* \Delta_\zeta(-R_{f,g_{t,i}}(\zeta^*)) + (-M(1-y_{t,i}))] + b^T \lambda_{R_f} \geq 0 \tag{4.105a}$$

$$s.t. \quad A^T \lambda_{R_f} = \Delta_\zeta(-R_{f,g_{t,i}}(\zeta^*)) \tag{4.105b}$$

$$\lambda_{R_f} \geq 0 \tag{4.105c}$$

$$[x_{g_{t,i}}(\zeta^*) + \zeta^* \Delta_\zeta(-x_{g_{t,i}}(\zeta^*)) + 1] + b^T \lambda_{x_g} \geq 0 \tag{4.106a}$$

$$s.t. \quad A^T \lambda_{x_g} = \Delta_\zeta(-x_{g_{t,i}}(\zeta^*)) \tag{4.106b}$$

$$\lambda_{x_g} \geq 0 \tag{4.106c}$$

$$[-x_{g_{t,i}}(\zeta^*) + \zeta^* \Delta_\zeta(x_{g_{t,i}}(\zeta^*)) - y_{t,i}] + b^T \lambda'_{x_g} \geq 0 \tag{4.107a}$$

$$s.t. \quad A^T \lambda'_{x_g} = \Delta_\zeta(x_{g_{t,i}}(\zeta^*)) \tag{4.107b}$$

$$\lambda'_{x_g} \geq 0 \tag{4.107c}$$

4.5.2 Results

Single heat exchanger

The following are the results for uncertain case of single HE. Here the decision variables include optimal cleaning schedule and bypass fraction of cold stream. Three scenarios of possible uncertainty are considered i.e. $\zeta = 0, \zeta = 0.5$ and $\zeta = 1$. The graph of bypass fraction of cold stream is given by Figure 4.11,

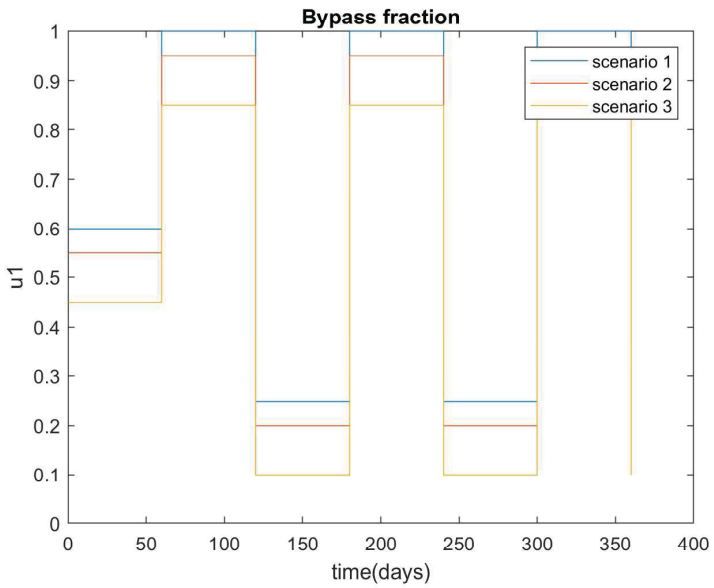

Figure 4.11: The optimal bypass fraction of cold stream

The input for each scenario is calculated by using affine rule decision variables and the corresponding value of uncertainty. Affine rule is used to calculate these input values. For each scenario, the values of all states are obtained by using corresponding input values. Furnace duty is the energy consumed in the furnace. This indicates the extra energy needed to bring the out temperatures of cold stream to the set targets. This variable indicates the efficiency of heat transfer. So the minimum furnace duty is achieved in ideal conditions i.e. no fouling resistance and having maximum heat transfer. The energy consumed in furnace (Q_f) is given by Figure 4.12,

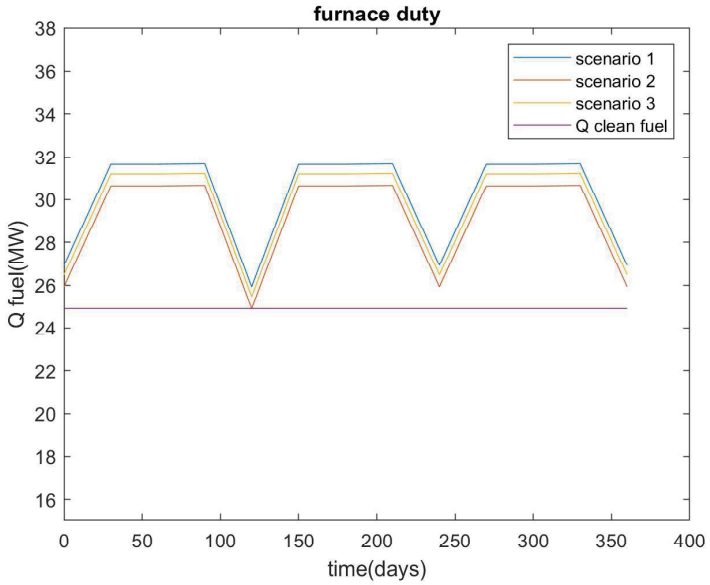

Figure 4.12: Furnace duty

The mixed stream temperature (CIT) is given by Figure 4.13. The figure shows CIT or controlled variable for all scenarios. It shows that the controlled variable tracks the setpoint effectively.

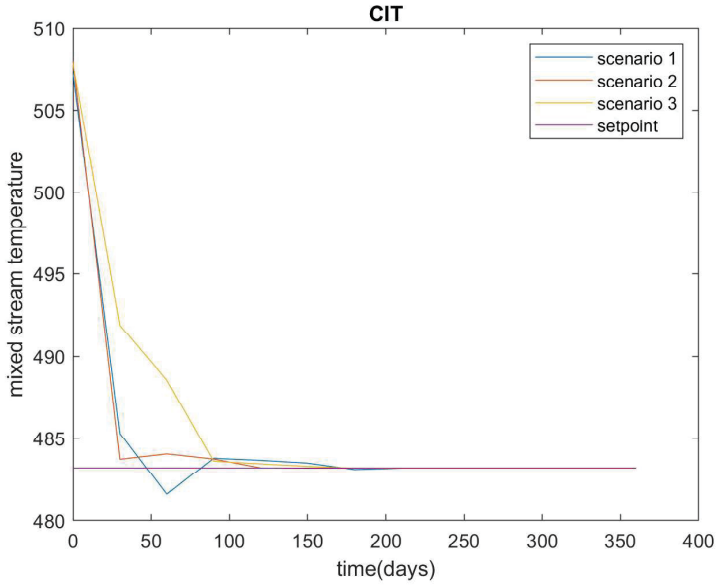

Figure 4.13: Mixed stream temperature

The optimal cleaning schedule is given by Figure 4.14.

	Period 1	Period 2	Period 3	Period 4	Period 5	Period 6	Period 7	Period 8	Period 9	Period 10	Period 11	Period 12
HE 1												

Figure 4.14: Optimal cleaning schedule for 1HE

Figure 4.15 demonstrates the advantage of proposed uncertain optimization over deterministic optimization. Considering the same scenarios of disturbances in inlet temperature of cold stream, the controlled variable or CIT is simulated using deterministic optimal input. The plot shows that using deterministic optimal bypass fraction, the controlled variable does not converge to the setpoint.

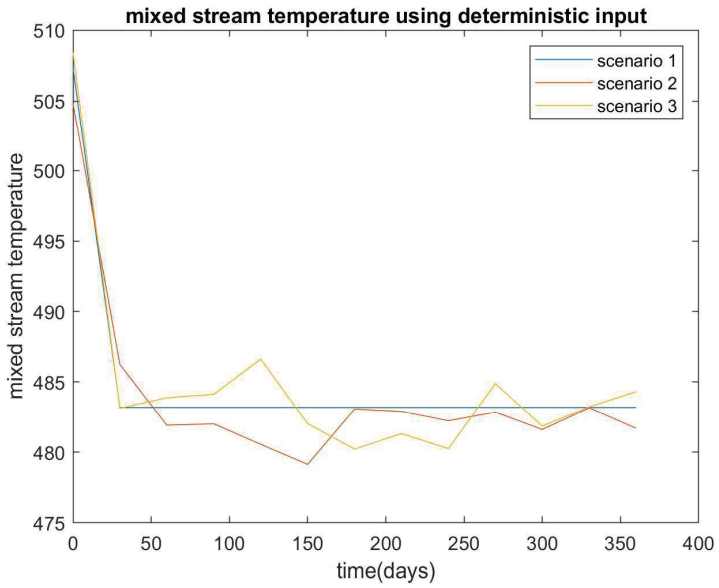

Figure 4.15: CIT using deterministic input

Table 4.1 gives the mean and the variance of objective function, and these values are calculated using 100 random scenarios of possible uncertainty. The table also gives MSE between the controlled variable and setpoint using bypass fraction from deterministic optimization, and it gives MSE using bypass fraction from uncertain optimization.

2 Parallel HEN

2 Parallel HEN is considered for the second case study. The HEN is described using following Figure 4.16.

mean	12.52×10^5\$
variance	0.18×10^2\$
MSE using uncertain input	8.85×10^3
MSE using deterministic input	9.25×10^4

Table 4.1: Results of uncertain integrated problem for single HE

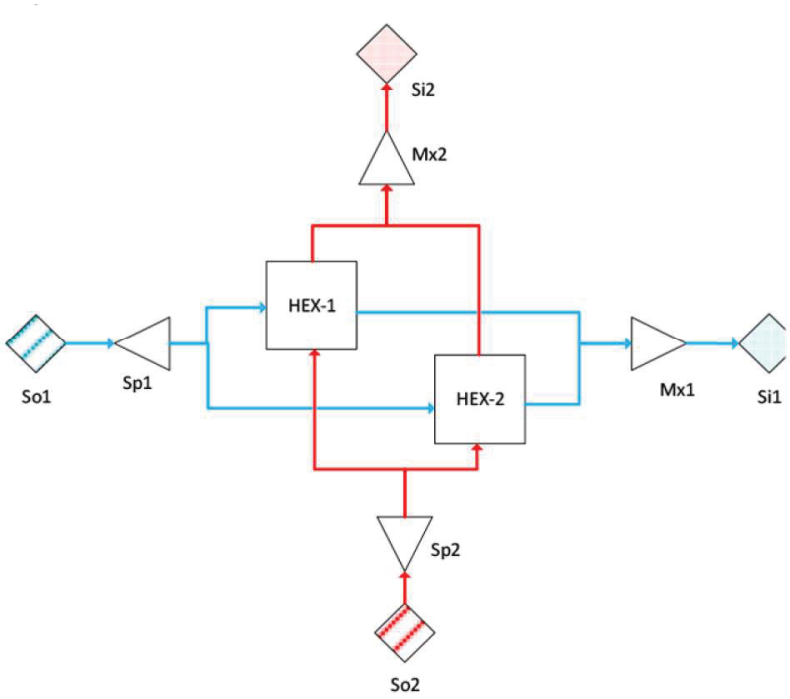

Figure 4.16: 2 parallel HEN

The decision variables include byapss fraction of both hot stream and cold stream, as well as the cleaning scheduling variable. The following are results for uncertain problem of the 2 parallel HEN cases. The optimal cleaning schedule is given by Figure 4.17,

	Period 1	Period 2	Period 3	Period 4	Period 5	Period 6	Period 7	Period 8	Period 9	Period 10	Period 11	Period 12
HE 1												
HE 2												

Figure 4.17: Optimal cleaning schedule for 2HE

The optimal bypass fraction of cold stream through heat exchanger - 2 is given

by Figure 4.18,

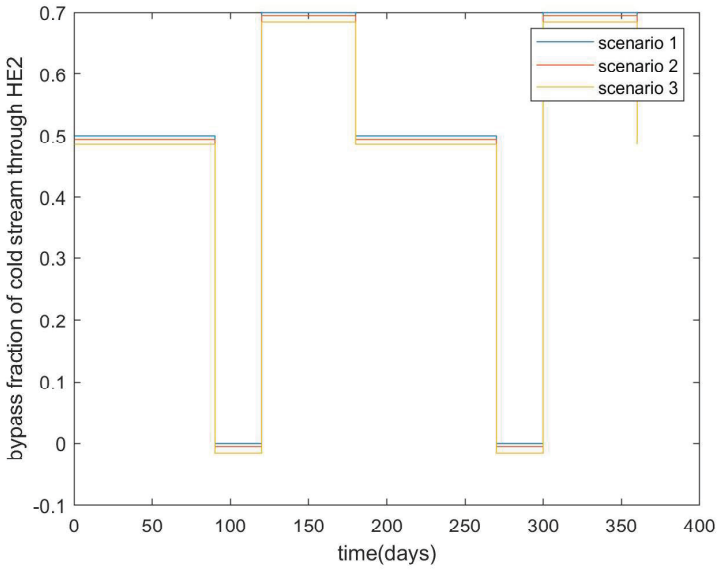

Figure 4.18: The optimal bypass fraction of cold stream through HE 2

For this case study, two bypass fractions are considered as decision variables, the hot stream bypass fraction and cold stream bypass fraction. Both values are given according to heat exchanger 2. Subtracting these values from 1 gives the bypass fractionn values through heat exchanger-1. The optimal bypass fraction of hot stream through heat exchanger - 2 is given by Figure 4.19,

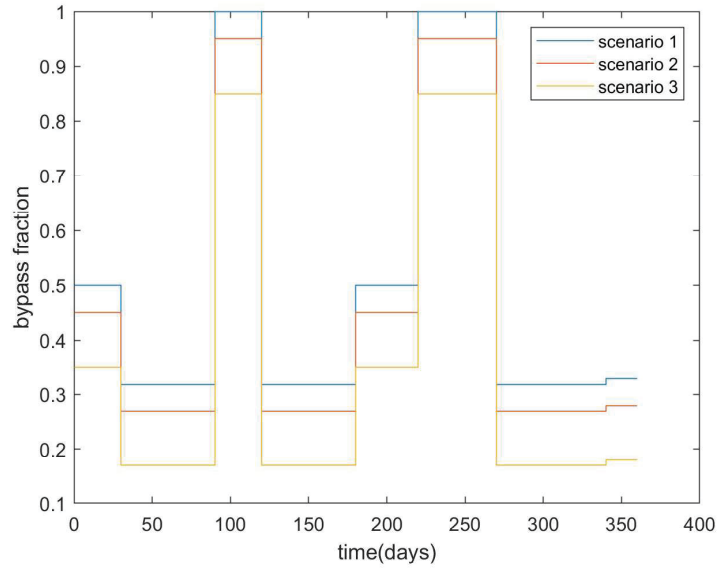

Figure 4.19: The optimal bypass fraction of hot stream through HE 2

The energy consumed in furnace (Q_f) is given by Figure 4.20,

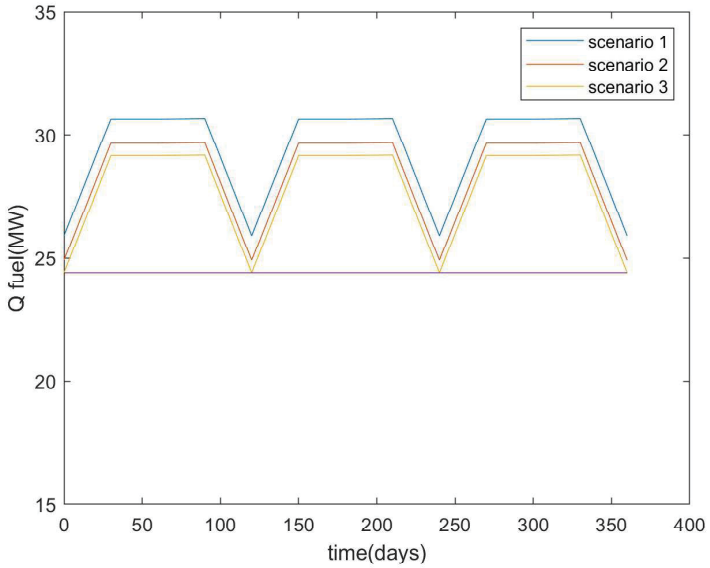

Figure 4.20: Furnace duty

The graph of mixed stream (controlled variable) is given by Figure 4.21,

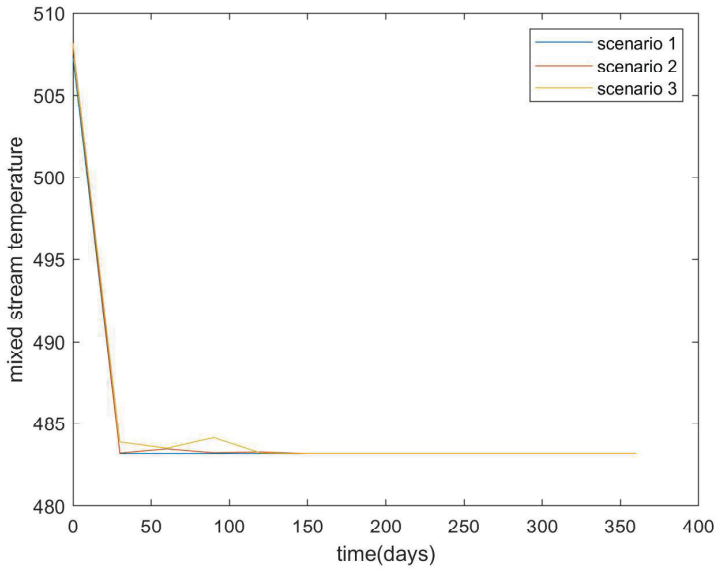

Figure 4.21: Mixed stream temperature (controlled variable)

For a comparison, the mixed stream temperature is simulated for the same scenarios using the deterministic input. Figure 4.22 shows that using the deterministic

input the controlled variable (mixed stream temperature) is not converging to the setpoint.

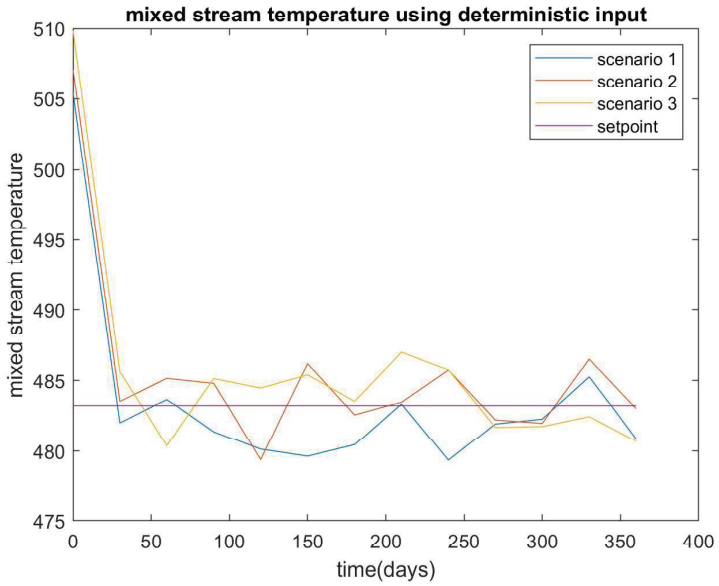

Figure 4.22: Mixed stream temperature (controlled variable) using deterministic input for different scenarios of uncertainty

The following table gives the mean and the variance of objective function, which are calculated using 100 random scenarios of possible uncertainty. The table also gives MSE between the controlled variable and setpoint using bypass fraction from deterministic optimization, and it also gives MSE using bypass fraction from uncertain optimization.

mean	14.2881×10^5\$
variance	0.07×10^2\$
MSE using uncertain input	7.66×10^3
MSE using deterministic input	8.52×10^4

Table 4.2: Results of uncertain integrated problem for 2HE parallel

The mean value of the objective function (additional operational and cleaning cost as compared to no fouling case) is calculated as 14.2881×10^5\$ and has the variance of 0.07×10^2\$. These values are calculated using 100 random scenarios of possible uncertainty.

4.5.3 Industrial preheat train for a crude oil distillation column

To demonstrate a more practical application of the proposed optimization, the industrial preheat train for a crude oil distillation column in a refinery plant is considered as the third case study. The following HEN is a grid diagram of the preheat train considered.

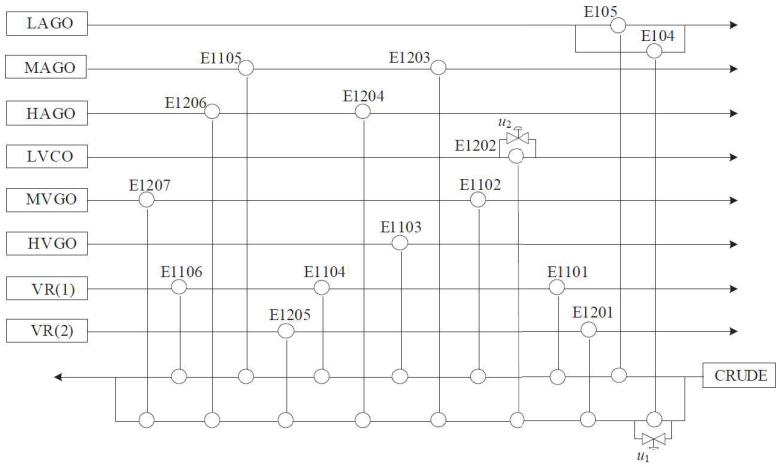

Figure 4.23: Grid diagram of the preheat train for a crude oil distillation column

The decision variables include four bypass fractions, two split fractions and the optimal cleaning schedule. The bypass fraction is considered an affine function of uncertainty, and split fraction and optimal cleaning schedule are considered as independent of uncertainty.

The optimization problem is solved in pyomo. The time period of one year is divided into 12 intervals. The overall optimization problem has 5276 constraints and 3663 variables in which 195 are binary variables.

The mean value of objective function (additional operational and cleaning cost as compared to no fouling case) is 18.81×10^6 and has the variance of 0.28×10^2. These values are calculated using 100 random scenarios of possible uncertainty.

The industrial PHT is relevant to this integrated problem. The crude heated in PHT is contaminated by a variety of minerals and salts. These contaminants are formed as unwanted deposits on heat exchanger surfaces. They offer extra resistance against the heat transfer. The considered PHT has 15 heat exchangers and 9 streams including the crude. So, for such an complex system, to decrease the computational load on the

solver, the optimization problem is solved in a few steps. First, the cleaning scheduling variables values are fixed, and the bypass fraction optimal values are obtained. Using these as initial values, the overall optimization problem is solved. Figure 4.24 gives the optimal cleaning schedule

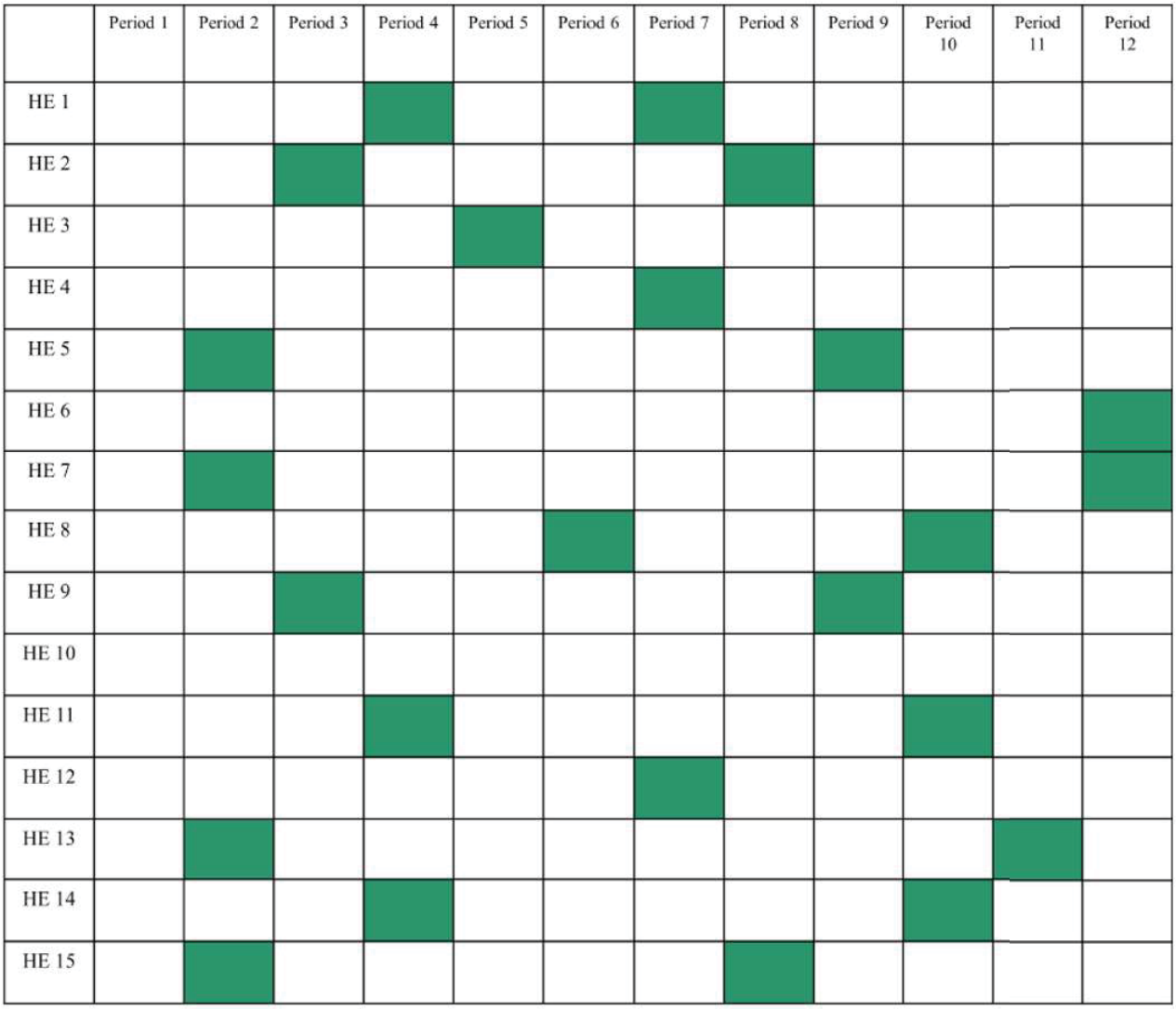

Figure 4.24: optimal cleaning schedule for PHT

The optimal bypass fraction of u_1 is shown by Figure 4.25, the optimal bypass fraction of u_2 by Figure 4.26, the optimal bypass fraction of u_3 by Figure 4.27, and the optimal bypass fraction of u_4 by Figure 4.28.

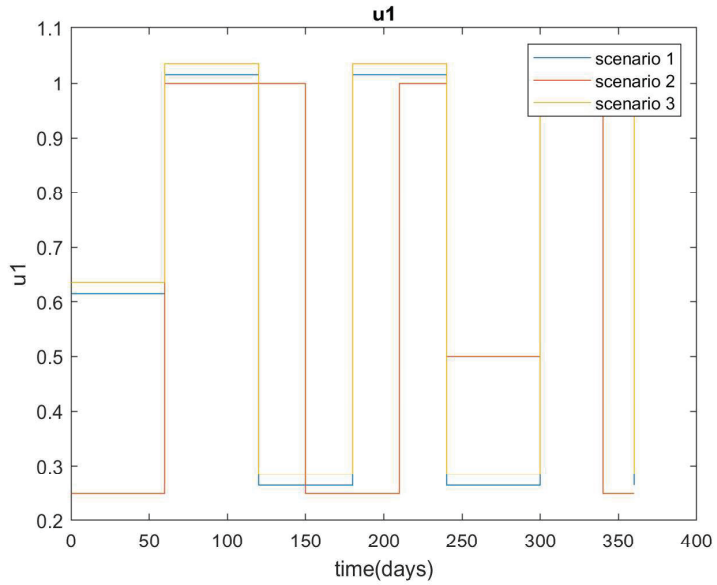

Figure 4.25: Bypass fraction 1

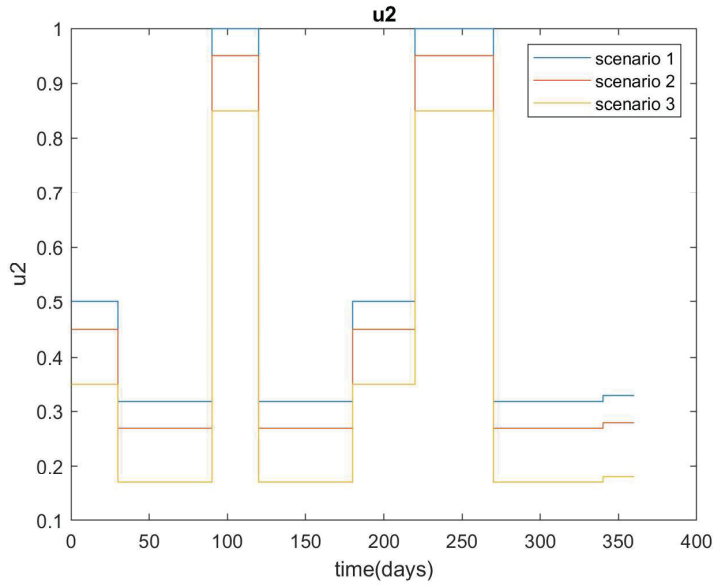

Figure 4.26: Bypass fraction 2

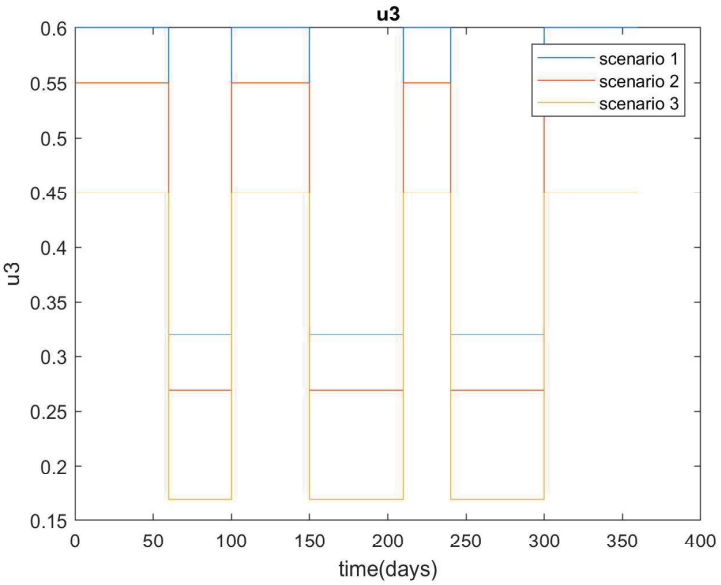

Figure 4.27: Bypass fraction 3

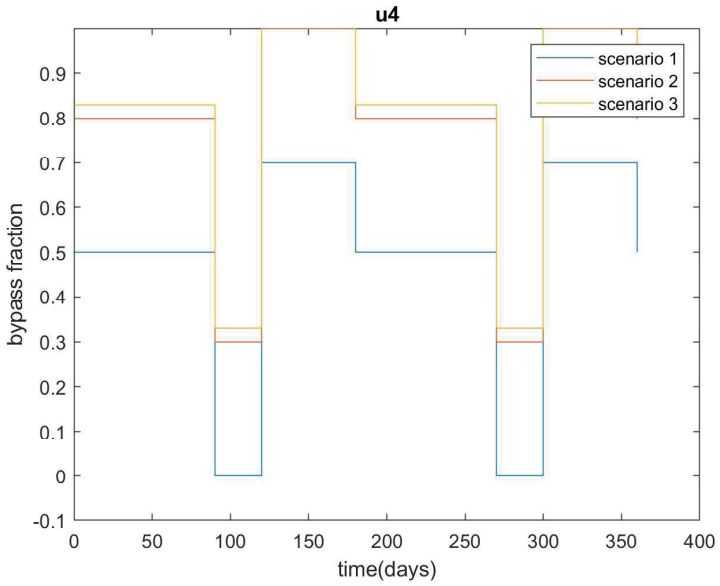

Figure 4.28: Bypass fraction 4

For each scenario, these bypass fraction values are calculated using optimized affine rule parameters and values of uncertainty of the corresponding scenario. The affine rule parameters are obtained for all four bypass fractions. The graph of mixed stream(controlled variable) is given by Figure 4.29 ,

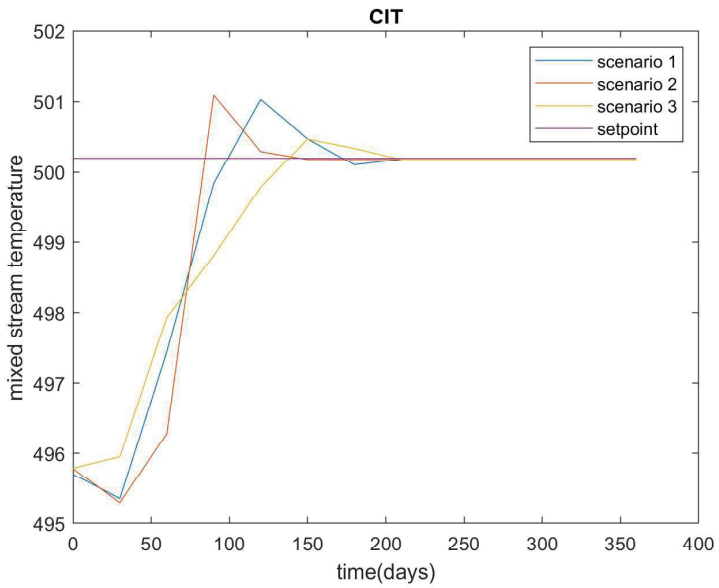

Figure 4.29: Mixed stream temperature (controlled variable)

For comparison, the mixed stream temperature is simulated for the same scenarios using deterministic input. Figure 4.30 shows that using deterministic input the controlled variable (mixed stream temperature) is not converging to setpoint.

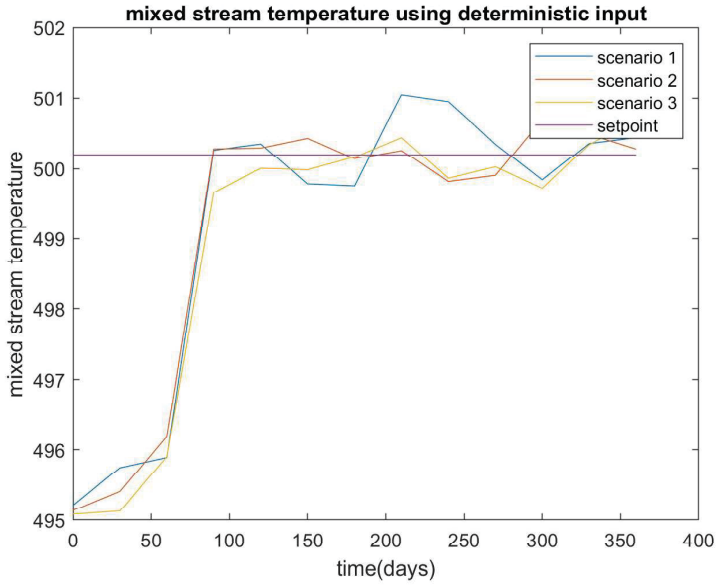

Figure 4.30: Mixed stream temperature (controlled variable) using deterministic input for different scenarios of uncertainty

The energy consumed in furnace (Q_f) is given by Figure 4.31,

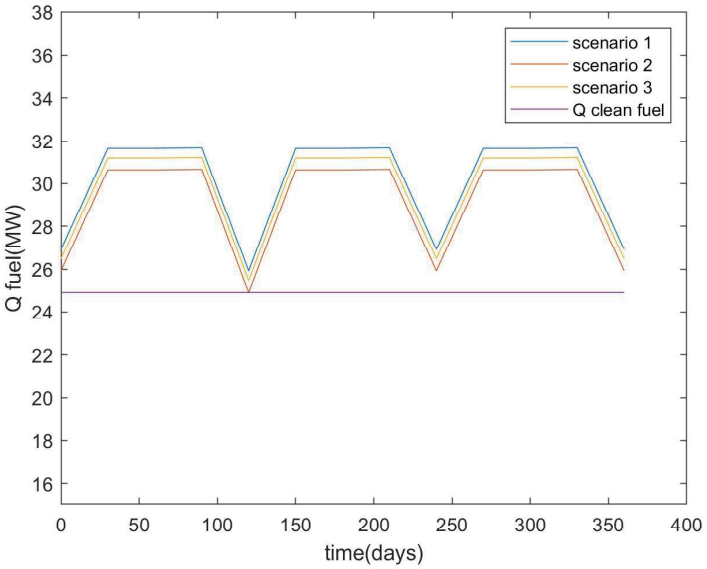

Figure 4.31: Furnace duty

The following table gives the mean and the variance of objective function, which are calculated using 100 random scenarios of possible uncertainty. The table also gives MSE between the controlled variable and setpoint using bypass fraction from deterministic optimization, and it also provides MSE using bypass fraction from uncertain optimization.

mean	16.21×10^5\$
variance	0.31×10^2\$
MSE using uncertain input	8.76×10^3
MSE using deterministic input	9.65×10^4

Table 4.3: Results of uncertain integrated problem for PHT

4.6 Conclusion

In this work, to mitigate the negative effects of fouling resistance on heat transfer, the integrated problem of optimal cleaning and bypass control is considered. The objective function represents additional cost occurred because of fouling as compared to ideal cleaned case.The disturbances in inlet temperature of cold stream are also

considered. The uncertain OCP is made tractable by using affine rule policy and scenario based approximations. The OCP is solved for an time horizon of one year and the values of decision variables are obtained for the entire year.

As both the optimization variables i.e. optimal cleaning and bypass control are solved simultaneously, the considered timescale is in days. If treated independently, generally, the values of cleaning variables are obtained in a time scale of months, and values of bypass fraction are obtained in a time scale of minutes. As the cleaning scheduling variables are not sensitive to disturbances in the inlet temperature of cold stream, they are formulated as independent of uncertainty whereas bypass fraction is formulated as affine function of uncertainty.

An axially lumped but radially distributed HEN model is considered as it is suitable for integrated problem. One of the case studies includes PHT of crude oil. Fouling is more evident in PHT of crude oil because of the presence of impurities in the crude. With the uncertain optimization formulation, the MSE between controlled variable and setpint is reduced by of tenfold as compared with deterministic optimization. The mean value of objective function is reduced by 44% approximately.

Chapter 5

Conclusions and prospective work

5.1 Conclusions

In chapter 3 of the thesis the bypass control of HEN is implemented under the MPC framework. First, the control problem is formulated and solved in deterministic framework. The performance of deterministic control is demonstrated using various case studies including setpoint change and disturbance rejection. Later, the uncertainty in inlet temperature of hot stream is introduced. The initial uncertain problem formulated is not tractable. The steps to convert intractable problem to tractable one is given in this chapter. These steps include affine rule policy methods and scenario tree approximations. Then, the tractable OCP is solved in a receding horizon manner. The first principles dynamic HEN model is considered initially, which is later discretized using orthogonal collocation as given in section 3.4.1.

The uncertain MPC is demonstrated using two case studies. First one is a simple single HE and second one is a HEN. The responses of decision variables and controlled variables are given in section 3.4.3. The performance of uncertain optimization is demonstrated using testing scenarios of inlet temperature of hot stream. For a comparison, the controlled variable is also simulated using deterministic optimization input values. The results show that MSE between controlled variable and setpoint is reduced by tenfold using uncertain optimization decision variable as compared to deterministic optimization decision variables.

In chapter 4, to mitigate the negative effects of fouling the optimal cleaning scheduling problem and bypass control problem are formulated simultaneously. The model

of HEN considered is different from that of chapter 3. Here, a axially lumped model and radially distributed model of HEN is considered. A model like this is sufficient to capture the fouling resistance dynamics without increasing the computational load significantly. The integrated problem formulated is a MINLP problem. It has binary optimal cleaning scheduling decision variables, and continuous bypass fraction decision variable. For the integrated problem, the time scale considered is in days, and the optimization problem is solved for a time period of one year. The uncertainty in OCP is dealt by deriving robust counterparts and scenario tree based approximations. The objective function represents the additional operational costs because of fouling. For 2HE case study, the value of objective function is reduced by 40% using the uncertain optimization as compared to deterministic optimization. In section 4.5.2, the performance of the proposed integrated optimization problem is demonstrated by using various cases including a PHT case study. This is because fouling is very much evident in PHT of crude as crude oil is contaminated with variety of impurities.

5.2 Prospective work

The work done in this thesis can be extended by considering more than one source of primitive uncertainty. The disturbance in flowrates of streams or in inlet temperatures of multiple streams can be considered. The formulation of the problem can be made more practical by considering these uncertainties. To decrease the computational load because of multiple uncertainties considered, a simple but effective model of HEN can be considered.

Another approach for the future work could be formulating a real time optimization. This could be done by linearizing constraints of the OCP or relaxing some of the constraints. Liearization of the model can be done around a steady state operating point of the system. Such a linearized model could be used for practical real time applications of the proposed control methods as industrial processes do not deviate much from the steady state operating points. The use of commercial licenses of the solver could also help for this.

References

1. Lin Sun, Xinlang Zha, Xionglin Luo, Coordination between bypass control and economic optimization for heat exchanger network,Energy.

2. Ehlinger, Victoria Mesbah, Ali. (2017). Model Predictive Control of Chemical Processes: A Tutorial. 10.1016/B978-0-08-101095-2.00009-6.

3. Luo, Xiong-Lin Xia, Chekui Sun, Lin. (2013). Margin design, online optimization, and control approach of a heat exchanger network with bypasses. Computers Chemical Engineering. 53. 102–121. 10.1016/j.compchemeng.2013.02.002.

4. Mohankumar, Yashas Li, Zukui Huang, Biao. (2019). Steam allocation and production optimization in SAGD reservoir under steam-to-oil ratio uncertainty. Journal of Petroleum Science and Engineering. 183. 106456. 10.1016/j.petrol.2019.106456.

5. Wang, Yi-Fei Chen, Qun. (2015). A direct optimal control strategy of variable speed pumps in heat exchanger networks and experimental validations.

6. Skorospeshkin MV, Sukhodoev MS, Skorospeshkin VN. An adaptive control system for a shell-and-tube heat exchanger. J Phys Conf 2016;803:2e6.

7. Delatore, Fabio Jaime, José Leonardi, Fabrizio Novazzi, Luís. (2010). Multivariable Optimal Control of a Heat Exchanger Network (HEN) With Bypasses.. 10.2316/P.2010.697-062.

8. Lozano Santamaria, Federico Macchietto, Sandro. (2019). Integration of Optimal Cleaning Scheduling and Control of Heat Exchanger Networks Under Fouling: MPCC Solution. Computers Chemical Engineering. 126. 10.1016/j.compchemeng.2019.04.012.

9. Coletti, F.; Joshi, H. M.; Macchietto, S.; Hewitt, G. F. Introduction. In Crude Oil Fouling; 2015; Chapter 1, pp 122.

10. Georgiadis, M. C.; Rotstein, G. E.; Macchietto, S. Optimal Design and Operation of Heat Exchangers under Milk Fouling. AIChE J. 1998, 44 (9), 2099.

11. Cho, Y. I.; Fridman, A. F.; Lee, S. H.; Kim, W. T. Physical Water Treatment for Fouling Prevention in Heat Exchangers. Adv. Heat Transfer 2004, 38, 1.

12. Coletti, F.; Macchietto, S. Refinery Pre-Heat Train Network Simulation Undergoing Fouling: Assessment of Energy Efficiency and Carbon Emissions. Heat Transfer Eng. 2011, 32 (34), 228.

13. Andras Prekopa. Stochastic programming, volume 324. Springer Science Business Media, 2013.

14. Boyaci, C., Uztürk, D., Konukman, A., Akman, U., “Dynamics and optimal

control of flexible heat-exchanger networks", Computers Chemical Engineering., 20, 775-780 (1996).
15. Nisenfeld, A.E., "Applying control computers to an integrated plant",Chem. Eng. Prog., 69, 45-48 (1973).
16. Beautyman, A.C., Cornish, A.R.H., "The design of flexible heat exchanger networks", In: Proc. of First U.K. National Heat Transfer Conference 1, Leeds, 547-565 (1984).
17. Calandranis, J., Stephanopoulos, G., "A structural approach to the design of control systems in heat exchanger networks", Computers and Chemical Engineering, 12 (7), 651-669 (1988).
18. McMillam, G. K.; Toarmina, C. M. AdVanced Temperature Measurement and Control; Instrument Society for Measurement and Control: Research Triangle Park, N.C., 1995.
19. Riggs, J. B.; Karim, M. N. Chemical and Bio-Process Control; Ferret Publishing: Austin, TX, 2007.
20. Lozano Santamaria, Federico Macchietto, Sandro. (2018). Integration of Optimal Cleaning Scheduling and Control of Heat Exchanger Networks Undergoing Fouling: Model and Formulation. Industrial Engineering Chemistry Research. 57. 10.1021/acs.iecr.8b01701.
21. Diaby, A. L.; Luong, L.; Yousef, A.; Addai Mensah, J. A Review of Optimal Scheduling Cleaning of Refinery Crude Preheat Trains Subject to Fouling and Ageing. Appl. Mech. Mater. 2011, 148149,643.
22. Lanchas-Fuentes, L.; Dias-Bejarano, E.; Coletti, F.; Macchietto,S. Management of Cleaning Types and Schedules in Refinery Heat Exchangers. Presented at the 12th International Conference on Heat Transfer, Fluid Mechanics and Thermodynamics (HEFAT2016), Costa del Sol, Spain, 2016.
23. Rodriguez, C.; Smith, R. Optimization of Operating Conditions for Mitigating Fouling in Heat Exchanger Networks. Chem. Eng. Res.Des. 2007, 85 (6), 839.
24. Smaïli, F.; Vassiliadis, V. S.; Wilson, D. I. Mitigation of Fouling in Refinery Heat Exchanger Networks by OptimalManagement of Cleaning. Energy Fuels 2001, 15 (5), 1038.
25. Assis, B. C. G.; Lemos, J. C.; Liporace, F. S.; Oliveira, S. G.; Queiroz, E. M.; Pessoa, F. L. P.; Costa, A. L. H. Dynamic Optimization of the Flow Rate Distribution in Heat Exchanger Networks for Fouling Mitigation. Ind. Eng. Chem. Res. 2015, 54

(25), 6497.
26. de Silva, R. L.; Costa, L. H.; Queiroz, E. M. Stream Flow Rate Optimization for Fouling Mitigation in the Presence of Thermohydraulic Channeling. In Proceedings of International Conference on Heat Exchanger Fouling and Cleaning; Malayeri, M., Muller-Steinhagen, H., Walkinson, A., Eds.; PP Publico Publications: Essen, Germany, 2015; pp 384391.
27. Liu, L.; Fan, J.; Chen, P.; Du, J.; Yang, F. Synthesis of Heat Exchanger Networks Considering Fouling, Aging, and Cleaning. Ind. Eng. Chem. Res. 2015, 54 (1), 296.
28. Nie, Y.; Biegler, L. T.; Villa, C. M.; Wassick, J. M. Discrete Time Formulation for the Integration of Scheduling and Dynamic Optimization. Ind. Eng. Chem. Res. 2015, 54 (16), 4303.
29. Zhuge, J.; Ierapetritou, M. G. Integration of Scheduling and Control for Batch Processes Using Multi-Parametric Model Predictive Control. AIChE J. 2014, 60 (9), 3169.
30. Edgar, T. F.; Himmelblau, D. M.; Lasdon, L. S. Integrated Planning, Scheduling, and Control in the Process Industries. In Optimization of Chemical Processes; McGrawHill: New York, 2001; pp 549582.
31. Biegler, L. T. Nonlinear Programming: Concepts, Algorithms, and Applications to Chemical Processes; Society for Industrial and Applied Mathematics (SIAM) and Mathematical Optimization Society: Philadelphia, PA, 2010.
32. Bassett, M. H.; Pekny, J. F.; Reklaitis, G. V. Decomposition Techniques for the Solution of Large-Scale Scheduling Problems. AIChE J. 1996, 42 (12), 3373.
33. Floudas, C. A.; Lin, X. Continuous-Time versus Discrete-Time Approaches for Scheduling of Chemical Processes: A Review. Comput. Chem. Eng. 2004, 28 (11), 2109.
34.Pinto, J. M.; Grossmann, I. E. Assignment and Sequencing Models for Theschedluling of Process Systems. Ann. Oper. Res. 1998, 81, 433.
35. Sundaramoorthy, A.; Maravelias, C. T. Computational Study of Network-Based Mixed-Integer Programming Approaches for Chemical Production Scheduling. Ind. Eng. Chem. Res. 2011, 50 (9), 5023.
36. Wang CF, Luo XL. Overdesign for control and its application in tube and shell heat exchanger design. Pertrleum Refin Eng 2004;34(2):21e4.
37. Lee K, Kim M, Ha MY, Min JK. Investigation of heat-exchanger-sizing methods using genetic, pattern search, and simulated annealing algorithms and the effect of

entropy generation. J Mech Sci Technol 2018;32(2):915e28.
38. Andres T, Julian PR, Juan VC. Maximum power point tracking panels by using improved pattern search methods. Energies 2017;10(9):1316e30.
39. Mohankumar, Y.. "Steam allocation optimization and control for SAGD process." (2020).
40. Giuseppe C Cala ore and Laurent El Ghaoui. Optimization models. Cambridge university press, 2014.
41. Aharon Ben-Tal, Alexander Goryashko, Elana Guslitzer, and Arkadi Nemirovski. Adjustable robust solutions of uncertain linear programs. Mathematical Programming, 99(2):351376, 2004.